IRE Transactions on AUDIO

Volume AU-8 NOVEMBER-DECEMBER, 1960 Number 6

Published Bi-Monthly

TABLE OF CONTENTS

PUBLISHED BY THE

Professional Group on Audio

IRE TRANSACTIONS® ON AUDIO

Published by The Institute of Radio Engineers, Inc., for the Professional Group on Audio at 1 East 79th Street, New York 21, N.Y. Responsibility for the contests rests upon the authors, and not upon the IRE, the Group, or its members. Individual copies of this issue and all available back issues may be purchased at the following prices: IRE members (one copy) $2.25, libraries and colleges $3.25, all others $4.50.

The Editor's Corner

STATUS OF AN AUDIO PROJECT

In a past report we emphasized that an objective evaluation of the present situation might well yield a recommendation for further study. We noted that lack of time had allowed only a very rudimentary investigation of preliminary outlines of the program, and that heretofore only a nonrigorous analysis was presented. Accordingly, during the present period, we considered it worthwhile to clear up several issues that obscured the key problems.

Before undertaking this approach, we also had in mind that a preliminary feasibility study might prove enlightening, and could save considerable unproductive effort in the long run. Such a study might encompass a literature survey, a certain amount of experimental work, and also a search of the marketplace. Past experience in this regard has shown that a survey of this nature may prove invaluable as an aid to orientation.

It might be well to mention that the problems, by their very nature, are formidable, and their solution requires a high degree of ingenuity in devising a new appoach. We believe that we are on the right track, and will continue to explore every avenue diligently.

(The above is a generalized report which fits almost any situation. We are reproducing it as an aid to harassed engineers who don't have anything to report but still have to hand one in anyway. This may be called hi-fi writing because it makes a pleasant sound, and soothes the savage boss.)

—MARVIN CAMRAS, *Editor*

PGA News

NATIONAL OFFICERS OF THE PGA, 1960–1961

Hugh S. Knowles (A'25–F'41) was born on September 23, 1904, in Hynes, Iowa. He received the B.A. degree from Columbia University, New York, N. Y., in 1928, did graduate work at the University of Chicago, Ill., from 1930–1933, and lectured in graduate physics at the University of Chicago in 1934–1935.

He was Chief Engineer of Jensen Manufacturing Company, Chicago, Ill., from 1931 to 1950, and Vice President from 1940 to 1950. A consulting engineer since 1936, he has been President and Director of Research of Industrial Research Products, Inc., Franklin Park, Ill., since 1946, and President of Knowles Electronics, Franklin Park, since 1954.

H. S. KNOWLES
Chairman, 1959–1960

He was Chairman of the IRE Chicago Section from 1934–1935, and has been chairman and member of many committees, including Electroacoustics, Editorial Review, Annual Review, Standards, and Board of Editors. He has been active in the Acoustical Society of America (President, 1945–1947), the Electronic Industries Association, American Standards Association, National Research Council, American Institute of Physics, International Electrotechnical Commission, International Standards Organization, and R&D Board Chairman on Acoustics for the Secretary of Defense.

Mr. Knowles holds numerous patents in acoustics and electronics and is the author of technical articles and papers, including sections on acoustics, loudspeakers, telephone receivers, and microphones in the "Engineering Hand-Book" (1936 and 1951), and sections on loudspeakers and room acoustics in Henny's "Radio Engineering Handbook" (1941, 1951, and 1959).

Peter C. Goldmark (A'36–M'38–F'43) was born in Budapest, Hungary, on December 2, 1906. He studied at the University of Berlin, Germany, and the University of Vienna, Austria, receiving the Ph.D. degree in physics from the latter.

In 1936, he joined the Columbia Broadcasting System, Inc., as Chief Television Engineer, later becoming Director of the Research and Development Division. The first practical color television system was developed under his direction in the CBS Laboratories, and on August 27, 1940, the first color broadcast in history was made from the CBS Television transmitter in New York.

P. C. GOLDMARK
Vice Chairman, 1960–1961

During World War II, CBS Laboratories, under Dr. Goldmark, was responsible for many military developments in the field of electronic countermeasures and reconnaissance. After the war, he and his associates developed the long-playing record in the CBS Laboratories.

In 1954 he became President of CBS Laboratories and Vice President of CBS, Inc.

Dr. Goldmark is a Fellow of the AIEE, the SMPTE, the Audio Engineering Society, and the British Television Society. In 1945 he was awarded the Television Broadcasters Association medal for his color television pioneering work, and in 1946 the IRE awarded him the Morris Liebman Memorial Prize for electronic research. In 1960 he was given the PGA Achievement Award. He is also a Visiting Professor for Medical Electronics at the University of Pennsylvania Medical School, Philadelphia, Pa.

Robert W. Benson (M'52) was born on January 21, 1924 in Grand Island, Neb. He received the B.S.E.E., M.S.E.E., and Ph.D. degrees in 1948, 1949, and 1951, respectively, from Washington University, St. Louis, Mo.

He worked as a research assistant at Central Institute for the Deaf, St. Louis, Mo., from 1948 until 1951, when he was made a research associate. From 1951 to 1954 he worked on various audio research programs relating to speech and hearing and, in addition, was Assistant Professor of Electrical Engineering at Washington University. In 1954 he joined Armour Research Foundation, Chicago, Ill., as supervisor of the Acoustics Section. He has conducted programs relating to atmospheric sound propagation, electroacoustic transducer design and calibration, and experiments in ultrasonics. From 1956 to 1960 he was Assistant Director of the Physics Research Division, but remained active in the research programs in acoustics. In October, 1960, he became Professor of Electrical Engineering at Vanderbilt University, Nashville, Tenn.

Dr. Benson is a Fellow of the Acoustical Society of America and a member of Sigma Xi. He is a former Chairman of the IRE St. Louis Section, a member of the Committee on Hearing and Bio-Acoustics of NRC, a member of the Editorial Board of *Noise Control*, a consultant to the American Academy of Ophthamology and Otolaryngology, and Program Chairman of the Chicago Section of PGA.

R. W. Benson
Administrative Committee, 1960–1963

Michel Copel (M'53–SM'57) was born in Paris, France, on March 20, 1916. He received the B.S. and E.E. degrees in 1935 and 1937, respectively, from the Conservatoire National des Arts et Metiers, Paris. He also attended New York University, New York, N. Y.

From 1942 to 1946 he was engaged in the design and development of military loudspeaker equipment as Chief Design Engineer of University Loudspeakers, Inc., White Plains, N. Y. From 1946 to 1948 he was Senior Engineer at Dictograph Products, Inc., Jamaica, N. Y. Since 1948 he has been engaged in investigations, developments and evaluations of audio communication equipment at the Naval Materiel Laboratory, Brooklyn, N. Y., where he has written many technical reports on his work. He holds the position of Supervising Electronic Scientist (Electroacoustic).

Mr. Copel is a member of the Acoustical Society of America. He has served on the IRE Electroacoustic Committee and the American Standards Association Committee Z24W22 on Loudspeaker Measurements. He is presently serving on the IRE Audio and Electroacoustic Committee 30, as Chairman of Subcommittee 30.6 on Microphone Measurements, and as Chairman of the PGA Ways and Means Committee. As East Coast Regional Program Chairman, he organized the Audio Sessions of the 1955 and 1956 IRE National Conventions.

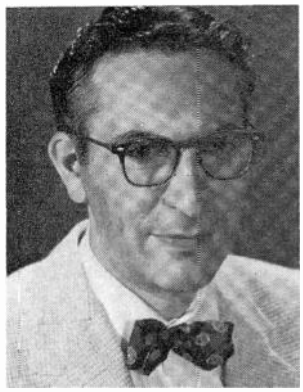

M. Copel
Administrative Committee, 1960–1963

Cont'd on next page

Cyril M. Harris (SM'50) was born in Detroit, Mich., on June 20, 1917. He received the B.A. degree in mathematics in 1938 from the University of California, Berkeley, Calif., and the M.A. and Ph.D. degrees in physics in 1940 and 1945, respectively, from the Massachusetts Institute of Technology, Cambridge, Mass.

From 1945 to 1951 he was Research Engineer at the Bell Telephone Laboratories. In 1951, he was Scientific Consultant, ONR, in the U. S. Embassy, London, England. From 1951 to 1952 he was Visiting Fulbright Lecturer at the University of Delft, The Netherlands. Since 1952 he has been Associate Professor of Electrical Engineering at Columbia University, New York, N. Y.

C. M. HARRIS
Administrative Committee, 1960–1963

PGA AWARDS FOR 1959

The Awards Committee of the Professional Group on Audio is proud to announce the following awards for the year 1959.

IRE-PGA Achievement Award (Two awards were presented this year.)

Alexander B. Bereskin

Peter C. Goldmark

To honor a member of the PGA, who, over a period of years, has made outstanding contributions to audio technology documented by papers in IRE publications. Certificates and $200 have been presented in each case.

IRE-PGA Senior Award

Hugh K. Dunn—For the paper "Absolute Amplitudes and Spectra of Certain Musical Instruments and Orchestras," by L. J. Sivian, H. K. Dunn, and S. D. White, which was revised to its present form by Mr. Dunn and published in IRE TRANSACTIONS ON AUDIO, vol. AU-7, pp. 47–75; May–June, 1959. A certificate and $100 award have been presented.

IRE-PGA Award

James S. Aagard—For the paper "Improved Method for the Measurement of Nonlinear Audio Distortion," which appeared in IRE TRANSACTIONS ON AUDIO, vol. AU-6, pp. 121–130; November–December, 1958. A certificate and cash award were presented.

Alexander B. Bereskin (A'41–M'44–SM'46–F'58) was born in San Francisco, Calif., on November 15, 1912. He received the E.E. degree and the M.S. degree in engineering in 1935 and 1941, respectively, from the University of Cincinnati, Ohio.

A. B. BERESKIN
Achievement Award, 1959

From 1936 to 1939 he was affiliated with the Commonwealth Manufacturing Corporation and the Cincinnati Gas and Electric Company. He is presently Professor of Electrical Engineering at the University of Cincinnati.

He has published work on vacuum-tube and transistor audio power amplifiers, low-level transistor audio amplifiers, video amplifiers, regulated power supplies, and power factor meters. He has also done work in the fields of special RC oscillators, frequency selective amplifiers, low-jitter multivibrators, special stabilized power supplies, and transistor pulse amplifiers.

Mr. Bereskin is a member of the AIEE, Sigma Xi, Eta Kappa Nu, and Tau Beta Pi. He is past National Chairman of the PGA and past *Editor* of the IRE TRANSACTIONS ON AUDIO. He is a member of the Education Committee, past Chairman of the Region IV Subcommittee of the Education Committee, past member of the Professional Groups and the Sections Committees, and past Institute Representative at the University of Cincinnati. He is past Chairman, Vice Chairman, and Treasurer of the Cincinnati Section.

P. C. GOLDMARK
Achievement Award, 1959

(For biography, see page 190 of this issue.)

(Cont'd on next page)

Hugh K. Dunn was born in Shawneetown, Ill., on October 31, 1897. He received the B.A. degree in 1918 from Miami University, Oxford, Ohio, and the Ph.D. degree in 1925 from California Institute of Technology, Pasadena.

H. K. DUNN
Senior Award, 1959

He has been with Bell Telephone Laboratories, New York, N. Y., since 1925. For a number of years, he was engaged in statistical studies of amplitudes and spectra in music and speech, and the characteristics of telephone instruments and circuits in terms of real speech. He took part in the early work on the sound spectrograph, and during World War II he worked on an acoustic torpedo. After the war he returned to speech studies, including development of the transmission-line analog of the vocal tract, showing how it leads to prediction of vowel formant positions. He has recently been concerned with improvement of the artificial larynx.

Dr. Dunn is a Fellow of the Acoustical Society of America and the AAAS, and a member of the American Physical Society, Phi Beta Kappa, and Sigma Xi.

James S. Aagard (S'48–A'53–M'57) was born on July 20, 1930, in Lake Forest, Ill. He attended Northwestern University, Evanston, Ill., on the cooperative program, working with Shure Brothers, Inc., and received the B.S.E.E. degree in 1953. He continued at Northwestern to receive the M.S. and Ph.D. degrees in 1955 and 1957, respectively, and is now an Assistant Professor of Electrical Engineering.

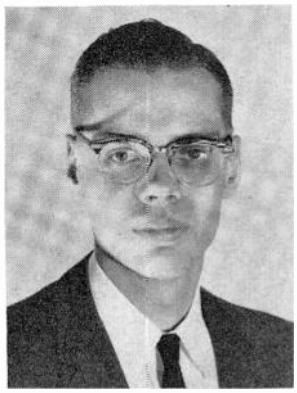

J. S. AAGARD
PGA Award, 1959

Dr. Aagard is a member of the Audio Engineering Society, the Chicago Acoustical and Audio Group, Tau Beta Pi, Eta Kappa Nu, and Sigma Xi. He has been a member of the board of directors of the National Electronics Conference since 1958.

Transistor Power Amplifiers With Negative Output Impedance*

WERNER STEIGER†, SENIOR MEMBER, IRE

Summary—The response of electromechanical transducers can often be greatly improved by proper electrical termination that compensates for their coil impedance.

The results of a detailed analysis are presented for two practical transistor amplifier configurations which produce negative output impedance.

A push-pull power amplifier, based on this analysis, uses the bias stabilizing elements of the output stage to obtain the necessary positive current feedback. The three-stage circuit delivers, without a transformer, 12 watts into 8 ohms or 8 watts into 16 ohms. The output impedance is adjustable from plus 1 ohm to either minus 7 or minus 14 ohms.

This amplifier has been used successfully in an all-transistor stereophonic high-fidelity system.

List of Symbols

a = position of damping control
Bl = magnetic flux density × length of wire
C_m, L_m, R_m = components of Z_m
d = mechanical damping
E = induced voltage, EMF
F = force
i = amplifier input current
I = transducer current
k = stiffness
L_e, R_e = components of Z_e
M = mass
r = input impedance of first transistor
$r_b = g_b^{-1}$ = external base resistor of first stage
$r_e = g_e^{-1}$ = external emitter resistor of first stage
$r_n = g_n^{-1}$, $r_s = g_s^{-1}$ = negative feedback divider
$R = G^{-1}$ = output impedance of amplifier without feedbacks
u = amplifier input voltage
v = velocity of moving coil
$Y_{in} = Z_{in}^{-1}$ = input admittance of amplifier
Y_t = transfer admittance
Z_e = electrical impedance of transducer (blocked)
$Z_m = Y_m^{-1}$ = motional impedance of transducer
Z_{out} = output impedance of amplifier
$Z_p = Y_p^{-1}$ = positive feedback impedance
Z_t = transfer impedance
Z_{tm} = over-all transfer impedance (to motion)
β = short-circuit current gain from base of first stage to output of last stage
β_1 = current gain of input stage
γ = over-all current gain of amplifier
λ = positive feedback ratio
ν = voltage gain of amplifier
ν_0 = open-circuit voltage gain
ν_m = over-all voltage gain (to motion)
σ = negative feedback ratio
ϕ, ψ = auxiliary amplifier parameters.

* Received by the PGA, May 2, 1960.
† Hughes Semiconductor Div., Newport Beach, Calif.

I. Introduction

THE improvement of loudspeaker performance by negative driver impedance and motional feedback has been dealt with in several articles.[1–5] Proper speaker damping results in extended low-frequency and better transient response, and in reduced nonlinear distortion. This may allow the use of less expensive speakers and smaller enclosures in high-quality systems. However, transistor amplifiers apparently have not yet found use in this manner. Therefore, it is the purpose of this paper to present the analyses of two transistor amplifier configurations with negative output impedance, and to describe a practical transformerless power amplifier with good performance and stability.

The electrical equivalent circuit of the moving-coil arrangement in Fig. 1 gives immediate insight into the amplifier requirements. The fact that the force in the mechanical system is coupled to current in the electrical system ($F = BlI$) and the voltage in the electrical system is coupled to velocity in the mechanical system ($E = Blv$) leads to the force-current mass-capacitance analogy.

Many electromechanical transducers can be described adequately by such series connections of an electrical impedance Z_e with a motional impedance Z_m, the electrical picture of the mechanical part. The problem is, of course, not restricted to sound reproduction; it is the same wherever good transient response of transducers (such as recorders, machines, meters, etc.) is important.

[1] J. De Boer and G. Schenkel, "Electromechanical feedback," *J. Acoust. Soc. Am.*, vol. 20, pp. 641–647; September, 1948.
[2] R. Tanner, "Improving loudspeaker response with motional feedback," *Electronics*, vol. 24, pp. 142–144; March, 1951.
[3] W. Clements, "A new approach to loudspeaker damping," *Audio Engrg.*, vol. 35, pp. 20–23, August, 1951; vol. 36, pp. 20–21, May, 1952.
[4] U. Childs, "Loudspeaker damping with dynamic negative feedback," *Audio Engrg.*, vol. 36, pp. 11–13, February; pp. 21–23, May, 1952.
[5] R. E. Werner, "Loudspeakers and negative impedances," IRE Trans. on Audio, vol. AU-6, pp. 83–89; July–August, 1958. See also, *J. Acoust. Soc. Am.*, vol. 29, pp. 335–340; March, 1957.

Since Z_m is usually strongly frequency-dependent, a flat amplifier response will not provide a constant mechanical output. Negative feedback of E (motional feedback) is a possibility; but this can be done only if the transducer features an independent second winding which makes the EMF accessible.

An elegant alternative is the use of an amplifier with negative output impedance. v_m in Fig. 2 is the true overall gain desired to be constant. Point B is not available for feedback. But if we make

$$Z_{out} = -Z_e,$$

point A becomes equivalent to B, so that

$$v_m = v_0,$$

over which control can be exercised.

The output impedance can be made negative by positive current feedback. For stabilization and reduction of distortion, a negative feedback that assists the impedance decrease has to be chosen: negative voltage feedback.

II. Amplifier Configurations and Their Analyses

There is some freedom as to the feedback connections at the input of the amplifier. Since the current measuring resistor for the positive feedback should be small in the interest of little power loss, this feedback has to be introduced in series with the input. The four possibilities reduce, therefore, to two practical configurations; configuration I has series voltage feedback (Fig. 3), and configuration II, parallel voltage feedback (Fig. 4).

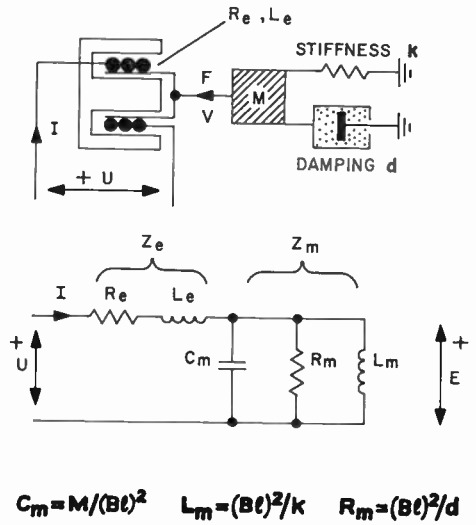

Fig. 1—Moving-coil transducer and equivalent circuit.

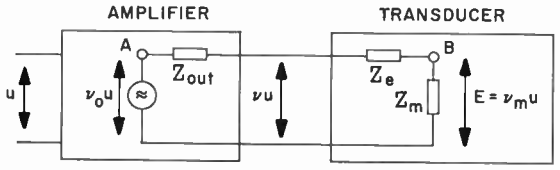

Fig. 2—Amplifier and transducer.

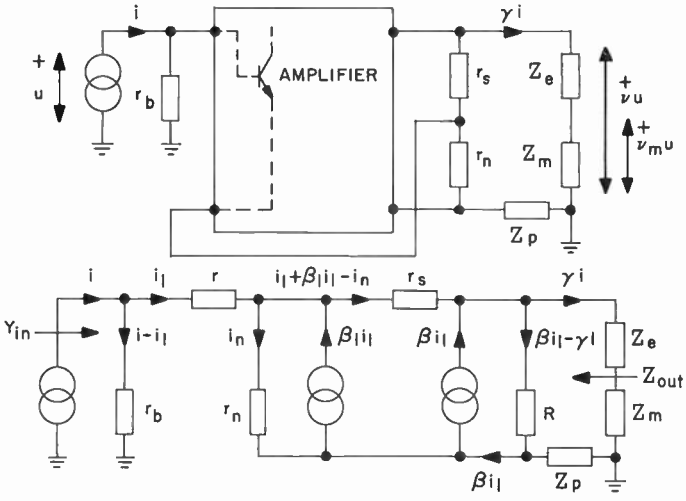

CONDITIONS:

$$\beta \gg \beta_1, 1$$
$$r_s + r_n \gg Z_e + Z_m + Z_p, R$$

CIRCUIT EQUATIONS:

$$i_1 r + i_n r_n - \gamma i Z_p - (i - i_1) r_b = 0$$
$$(i_1 + \beta_1 i_1 - i_n) r_s + \gamma i (Z_e + Z_m + Z_p) - i_n r_n = 0$$
$$\gamma i (Z_e + Z_m + Z_p) - (\beta i_1 - \gamma i) R = 0$$

Fig. 3—Amplifier configuration I.

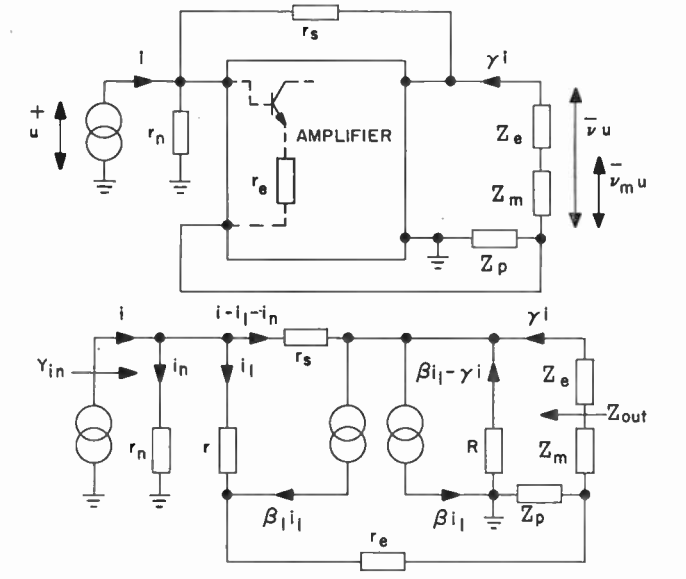

CONDITIONS:

$$\beta \gg \beta_1, 1$$
$$r_s + r_n \gg Z_e + Z_m + Z_p, R$$

CIRCUIT EQUATIONS:

$$i_1 r + (\beta_1 + 1) i_1 r_e - \gamma i Z_p - i_n r_n = 0$$
$$(i - i_1 - i_n) r_s - \gamma i (Z_e + Z_m + Z_p) - i_n r_n = 0$$
$$\gamma i (Z_e + Z_m + Z_p) - (\beta i_1 - \gamma i) R = 0$$

Fig. 4—Amplifier configuration II.

The results of a detailed analysis for these two amplifier configurations are presented in Table I.

For infinite gain or no negative feedback, these expressions reduce to the ones given in Table II.

Table III shows the relationships that hold in the case of special interest, ideal transducer damping.

TABLE I
ANALYSIS OF NEGATIVE IMPEDANCE AMPLIFIERS

	Configuration I	Configuration II
g_b	g_b	$g_n + g_s$
g_s	$g_n + g_s$	g_s
ψ	$[r + r_b + (\beta_1 + 1)r_e]G/\beta$	
ϕ	$[r + (\beta_1 + 1)r_e](G + \lambda Y_p)/\beta$	
σ	$r_n(r_s + r_n)^{-1}$	
λ	$Z_p(Z_s + Z_m + Z_p)^{-1}$	
γ	$r_b\left[Z_p\left(\frac{\sigma+\psi}{\lambda} - 1\right) + \psi R\right]^{-1}$	
ν	$(1 - \lambda)(\phi + \sigma - \lambda)^{-1}$	$(1 - \lambda)(\phi - \lambda)^{-1}$
Z_t	$r_b(1 - \lambda)[\sigma - \lambda + \psi(1 + \lambda R Y_p)]^{-1}$	
Y_t	$\lambda Y_p(\phi + \sigma - \lambda)^{-1}$	$\lambda Y_p(\phi - \lambda)^{-1}$
Y_{in}	$g_b + \frac{G + \lambda Y_p}{\beta(\phi + \sigma - \lambda)}$	$g_b + \frac{G + \lambda Y_p + \beta\sigma g_b}{\beta(\phi - \lambda)}$
Z_{out}	$Z_p + (\psi R - Z_p)(\sigma + \psi)^{-1}$	

TABLE II
NEGATIVE IMPEDANCE AMPLIFIERS WITH $\beta = \infty$ OR $\sigma = 0$

	$\beta = \infty$		$\sigma = 0$
	I	II	I and II
γ	$\lambda Y_p r_b(\sigma - \lambda)^{-1}$		$r_b\left[Z_p\left(\frac{\Psi}{\lambda} - 1\right) + \Psi R\right]^{-1}$
ν	$(1 - \lambda)(\sigma - \lambda)^{-1}$	$(\lambda - 1)/\lambda$	$(1 - \lambda)(\phi - \lambda)^{-1}$
Z_t	$r_b(1 - \lambda)(\sigma - \lambda)^{-1}$		$r_b(1 - \lambda)[\Psi(1 + \lambda R Y_p) - \lambda]^{-1}$
Y_t	$\lambda Y_p(\sigma - \lambda)^{-1}$	$-Y_p$	$\lambda Y_p(\phi - \lambda)^{-1}$
Y_{in}	g_b	$-g_b\left(\frac{\sigma}{\lambda} - 1\right)$	$g_b + \frac{G + \lambda Y_p}{\beta(\phi - \lambda)}$
Z_{out}	$-Z_p\left(\frac{1}{\sigma} - 1\right)$		$R - Z_p\left(\frac{1}{\Psi} - 1\right)$

TABLE III
NEGATIVE IMPEDANCE AMPLIFIERS FOR IDEAL DAMPING

	I and II	$\sigma = 0$	$\beta = \infty$
Z_{out}	$-Z_s$	$-Z_s$	$-Z_s$
Z_p	$\frac{Z_s(\sigma + \Psi) + \Psi R}{1 - \sigma - \Psi}$	$\frac{\Psi}{1 - \Psi}(R + Z_s)$	$Z_s\frac{r_n}{r_s}$
σ	$\frac{Z_p - \Psi R}{Z_s + Z_p} - \Psi$	0	$\frac{Z_p}{Z_s + Z_p}$
Ψ	Ψ	$Z_p(R + Z_s + Z_p)^{-1}$	0
β_{min}	$\frac{r + r_b + (\beta_1 + 1)r_e}{Z_p}\left(1 + \frac{Z_s + Z_p}{R}\right)$		—
γ	$r_b Y_m(\sigma + \Psi)^{-1}$	$r_b Y_m/\Psi$	$r_b Y_m/\sigma$
Z_{tm}	$r_b(\sigma + \Psi)^{-1}$	r_b/Ψ	r_b/σ

III. A Transistor Power Amplifier

Based on the analysis of configuration I, the power amplifier shown in Fig. 5 was designed and built. It delivers about 12 watts into a resistive load of 8 ohms or 8 watts into 16 ohms, and has an output impedance adjustable from approximately plus 1 ohm to either minus 7 or minus 14 ohms. The components are listed in Table IV and the construction is illustrated in Figs. 6 and 7. A reason for the choice of this configuration is that the input impedance (refer to Table II) is positive and, for high over-all current gain, becomes independent of load and output impedance.

The outside measurements of the amplifier are 3 by 5 by 10 inches. The side where the power transistors are mounted is re-enforced with a $\frac{1}{8}$-inch aluminium plate for better heatsinking.

A. Circuit Description

Transistors Q_1 and Q_2 form the input stage, a push-pull arrangement, working essentially in class *A*. The operating point is stabilized by feedback biasing (R_1 to R_4, R_6, R_7). C_2 and C_3 restrict this negative feedback to dc. Apart from the desirable push-pull features, this stage has the advantage that any dc offset, fed back to the emitters through the over-all feedback network, will not affect the operating point since, dc-wise, the bases of Q_1 and Q_2 are completely isolated from ground.

Complementary symmetry in the output amplifier permits push-pull operation without the need of transformers. However, at present, most available germanium power transistors are *p-n-p* types. But, by preconnecting a small *n-p-n* transistor (Q_3) such that it receives full negative feedback from the collector of the *p-n-p* power transistor (Q_5), a "polarity conversion" can be achieved. The combination of Q_3 and Q_5 can now be considered as a high-gain *n-p-n* power transistor.

This feedback compound connection Q_3 and Q_5 is arranged in class *B* complementary symmetry with the emitter follower compound connection Q_4 and Q_6. The resulting push-pull amplifier feeds the load in common-emitter fashion, realizing maximum power gain and requiring only moderate signal swing from the first stage. Although the two compound connections differ in input impedance, the resulting asymmetry is small enough to be reduced to negligible values by strong over-all negative feedback. The combination of these two compound connections has been used elsewhere[6] for emitter follower push-pull operation and has been referred to as quasi-complementary symmetry.

If suitable *n-p-n* power transistors are available, Q_6 may be replaced, and Q_4–Q_6 can be wired as a feedback compound connection complementary to Q_3–Q_5. This may result in improved symmetry and will eliminate the influence of the temperature sensitive emitter-base

[6] H. C. Lin, "Quasi-complementary transistor amplifier," *Electronics*, vol. 29, pp. 173–175; September, 1956.

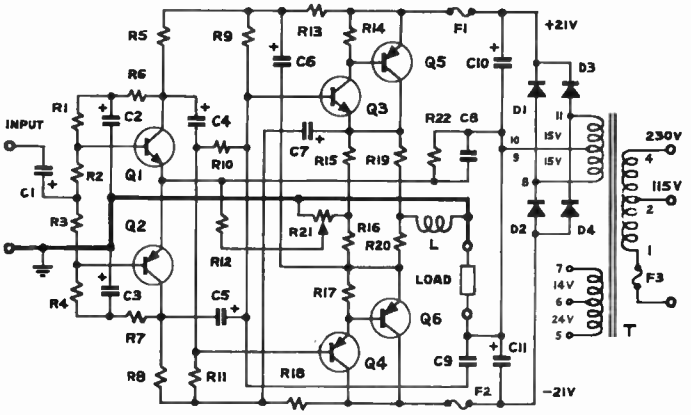

Fig. 5—Negative-impedance power-amplifier.

TABLE IV

Parts List for Negative Impedance Power Amplifier

R_1, R_4, R_5, R_8, R_9, R_{11}	6,800 ohms
R_2, R_3	470 ohms
R_6, R_7	22,000 ohms
R_{10}, R_{14}, R_{17}	220 ohms
R_{12}	33 ohms
R_{13}, R_{18}	1,000 ohms
R_{15}, R_{16}	22 ohms
R_{19}, R_{20}	2 ohms, 5 watts
R_{21}, (damping control)	100 ohms
R_{22}	330 ohms
C_1	10 μf, 25 volts
C_2, C_3	50 μf, 6 volts
C_4, C_5	25 μf, 25 volts
C_6, C_7	100 μf, 25 volts
C_8	2,200 $\mu\mu$f
C_9	1,000 $\mu\mu$f
C_{10}, C_{11}	2,000 μf, 25 volts
Q_1	*n-p-n* transistor, 2N169A, 2N1304, or similar high gain unit
Q_2	*p-n-p* transistor, 2N321, 2N1305, or similar high gain unit
Q_3	*n-p-n* transistor, 2N1312, or similar unit with sufficiently high voltage rating and current gain
Q_4	*p-n-p* transistor, 2N1373, or similar unit with sufficiently high voltage rating and current gain
Q_5, Q_6	*p-n-p* power transistors, 2N553, or equivalent
D_1, D_2, D_3, D_4	Hughes silicon rectifiers, 1N1124
T	Thordarson rectifier transformer, 23V61
L	required for negative output inductance
F_1, F_2	fuse, 1.5 amperes
F_3	fuse, 0.5 ampere

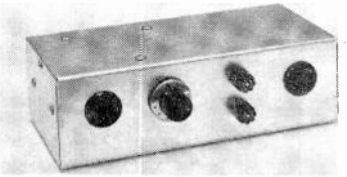

Fig. 6—Front view of amplifier.

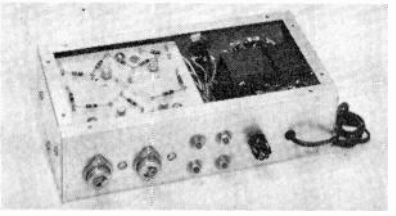

Fig. 7—Rear view with bottom plate removed.

voltage drop of Q_6 on the quiescent current of the output stage.

The positive feedback impedance Z_p (consisting of R_{19}, R_{20}, and L) is placed at the emitter side of the compound connections. The resistive part is split up into R_{19} and R_{20}. The two components of the positive feedback signal are added by R_{15} and R_{16} and fed to the emitters of the first stage through damping control R_{21}. This way it is possible to use the positive feedback resistors R_{19} and R_{20} at the same time for negative feedback to stabilize the quiescent current through the power transistors. Additional loss of power output in separate resistors for these two functions is thus prevented. L produces the negative inductance to compensate for the voice coil inductance. In some cases, the inductance of wirewound resistors R_{19} and R_{20} may be sufficient.

For stable dc symmetry, the output amplifier is designed in such a way that it behaves like an emitter-follower with respect to supply voltages, and like a common-emitter circuit for ac signals. The bases of Q_3 and Q_4 are centered by the divider R_9 and R_{11}. R_{10} (which could be made temperature dependent for additional stability) is chosen for sufficient voltage drop to produce enough quiescent current (about 50 ma) to eliminate class B crossover distortion.

The filters C_6–R_{13} and C_7–R_{18} remove ripple and output signal, which are riding on the power supply. C_6 and C_7 are connected such that all the negative feedback for the bias stabilization of the power transistors becomes restricted to dc. This reduces the swing requirements of the first stage as much as possible. As an alternative, C_6 and C_7 could be grounded, permitting some local negative feedback in the output stage.

Over-all negative voltage feedback is applied through R_{22} and C_8. The variable feedback network for the output impedance adjustment consists of potentiometer R_{21} and resistors R_{12}, R_{15}, R_{16}, and R_{22}. The amplifier being intended primarily for 8-ohm speakers, this network was chosen such that the output impedance range from plus 1 to minus 4 ohms is spread over about 80 per cent of potentiometer R_{21}, and that the negative feedback increases at first along with the positive feedback, keeping the gain approximately constant. Afterwards, the negative feedback decreases while the positive feedback increases further. This extends the range close to minus 7 ohms which may even be sufficient for 16-ohm speakers. Fig. 8 shows the output impedance vs position a of damping control R_{21}. The measured output variations are given in Fig. 9.

However, for use with 16-ohm loads, it is generally advantageous to increase the positive feedback by inserting a 1-ohm resistor in series with L. The output impedance is then twice that in Fig. 6, and the necessary values can be obtained without undue reduction of negative feedback.

The power supply has a center tap. This permits dc coupling to the load, which is necessary to keep the phase shift small enough for the required large feedback. For the same reason, the input stage was designed to permit dc coupling of the feedback signal. The center-tapped arrangement has the further advantage that no supply voltage ripple reaches the load if the bridge which is formed by the power supply and the push-pull stage is balanced.

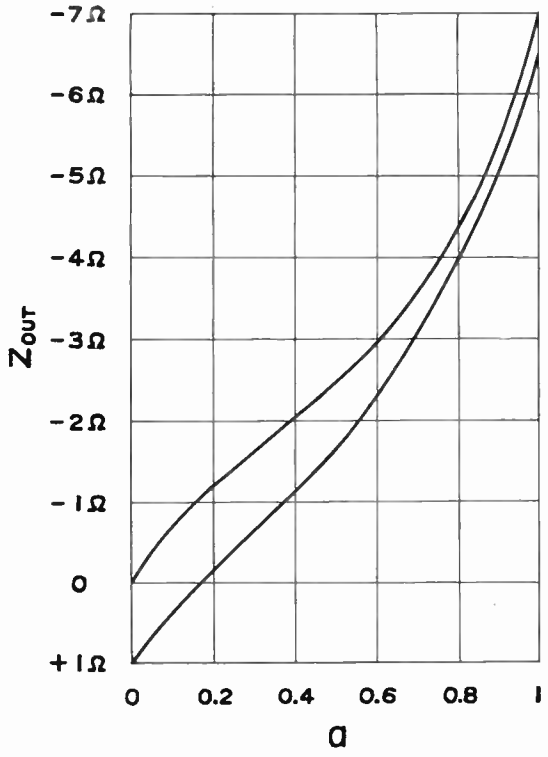

Fig. 8—Output impedance vs damping control position.

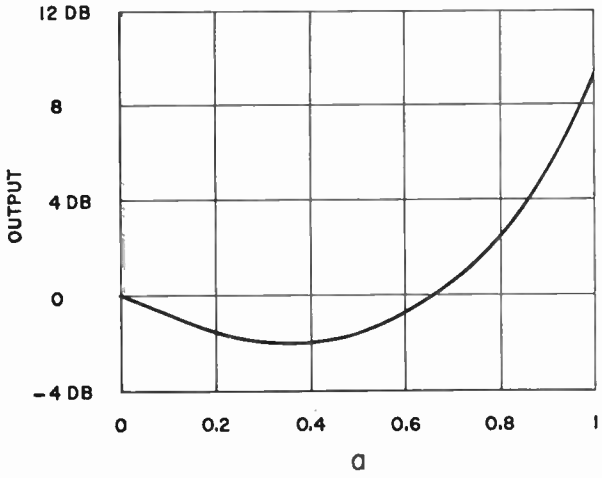

Fig. 9—Output vs damping control position.

Transformer T has a spare winding which is useful to power a preamplifier.

The whole circuit is designed for performance largely independent of transistor parameters. Normally, no bias adjustments are necessary. Matching of transistors is not required, but it is advantageous to use two units with similar current gain in each stage. High-gain

transistors are desirable; the negative feedback becomes more effective.

B. Performance Calculations

A large over-all net negative feedback is desirable for low distortion. This requires the current gain β to be as high as possible and, in turn, permits the use of Table II for calculations.

Input impedance:

$$Z_{in} = r_b = (R_1 + R_2) \| (R_3 + R_4) = 3600\ \Omega$$
$$r \cong h_{ie1} \| h_{ie2} \cong 1000\ \Omega$$
$$r_n = R_{12} + aR_{21} \| [(1 - a)R_{21} + (R_{15} + R_{19})/2]$$
$$= 33\ \Omega + a(100 - 90a)\ \Omega$$
$$r_s \cong R_{22} = 330\ \Omega$$
$$Z_p \cong R_p = R_{19} \| R_{20} = 1\ \Omega.$$

Effective Z_p:

$$Z_{p\,\text{eff}} = Z_p \frac{aR_{21}}{R_{21} + (R_{15} + R_{19})/2} = 0.9aZ_p.$$

Output impedance:

$$Z_{out} = -Z_{p\,\text{eff}}\left(\frac{1}{\sigma} - 1\right) = -0.9aZ_p r_s/r_n$$
$$= -\frac{30a}{3.3 + a(10 - 9a)}\ \Omega.$$

The upper curve in Fig. 8 represents the above expression which holds for infinite gain β. The actual measurements are given by the lower curve.

For ideal damping of an 8-ohm speaker with 4 ohms blocked voice coil impedance, we have the following conditions:

$$a \cong 0.8 \qquad \text{Effective } Z_p = 0.72 \text{ ohm}$$
$$r_e = r_n \| r_s = 47 \text{ ohms}.$$

For transistors with betas of 70 and with totally 9-db interstage transfer losses, the short-circuit current gain of the amplifier is

$$\beta = 120{,}000.$$

Assuming a 4700-ohm source resistance parallel to r_b (load resistor of a preamplifier), and with R being approximately 100 ohms, we obtain for the minimum gain necessary (Table III) for minus 4 ohms output impedance:

$$\beta_{min} = 9300.$$

The excess current gain

$$\beta/\beta_{min} \cong 22 \text{ db}$$

is available for negative feedback.

The over-all gain figures of the amplifier are in this case (Table II, $\sigma = 0.143$ and effective $\lambda = 0.9$ $a\lambda = 0.08$):

Current gain:

$$\gamma = 6300 = 76 \text{ db}.$$

Voltage gain:

$$\nu \cong 15 \cong 24 \text{ db}.$$

Power gain:

$$PG = \gamma\nu \cong 10^5 = 50 \text{ db}.$$

The sensitivity (input required for maximum output) is therefore about 0.12 mw.

C. Performance Measurements

Frequency Response: The frequency response is shown in Fig. 10 for a resistive 8 Ω load and various output impedances. Note the small difference between $a = 0$ and $a = 0.8$. The low-frequency response is primarily determined by the input capacitor. It could be extended one or two octaves if desired.

Negative Output Impedance: The output impedance vs the damping control position is plotted in Fig. 8. The dashed curve in Fig. 10 shows the wide frequency range over which the impedance is effective. In Fig. 11 the output impedance was measured at various voltage levels.

Input Impedance: The input impedance is constant from $a = 0$ to 0.8 and agrees well with the calculated value. Above this range, it starts to decrease when measured with an 8-ohm load.

Distortion: Measurements of the total harmonic distortion are shown in Fig. 12 for resistive 8- and 16-ohm loads and for various values of the negative output impedance. The curves are drawn up to the clipping points. Clipping could be delayed and the power capability increased by choice of larger supply voltage. However, driver transistors (Q_3 and Q_4) with suitably high voltage rating would have to be selected.

Transient Response: In order to measure the motional output, the moving coils of two transducers were mechanically connected. A voltage proportional to the velocity is then induced in the second coil. The resonance frequency was around 50 cps. A 10-cps square wave was applied to the amplifier input.

Fig. 13 shows the transient response with zero output impedance. For perfect reproduction, Fig. 13(b) should be the differentiation of the input square wave.

The response under conditions of perfect damping is shown in Fig. 14. The velocity [Fig. 14(b)] is without any overshoot, indicating almost perfect mechanical reproduction of the electrical square wave. The amplifier output [Fig. 14(a)], however, is now a complex waveform that adjusts itself such that the inadequate transducer characteristics are compensated for.

Noise: The measured noise was between 65 and 80 db below rated output, depending upon load and output impedance, and on how well the output stage is balanced.

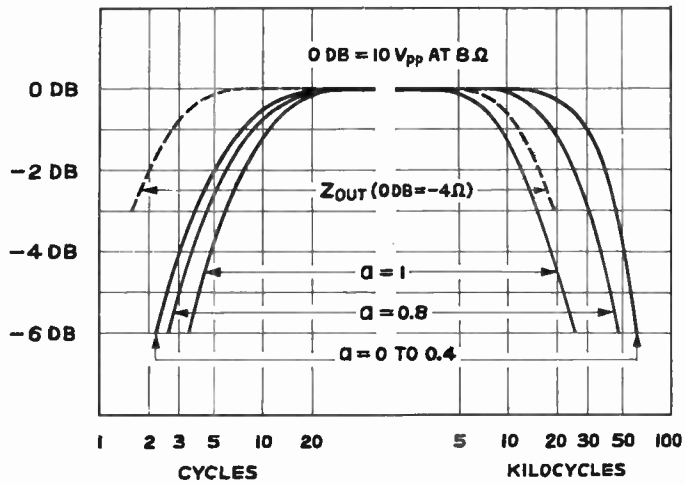

Fig. 10—Frequency response.

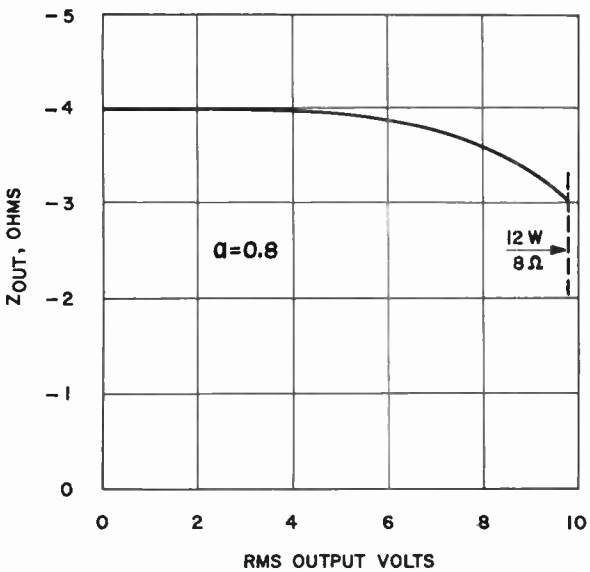

Fig. 11—Negative impedance vs output level.

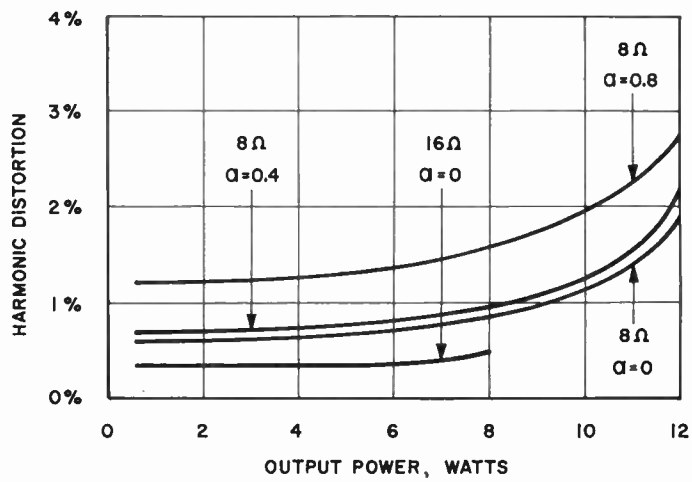

Fig. 12—Harmonic distortion.

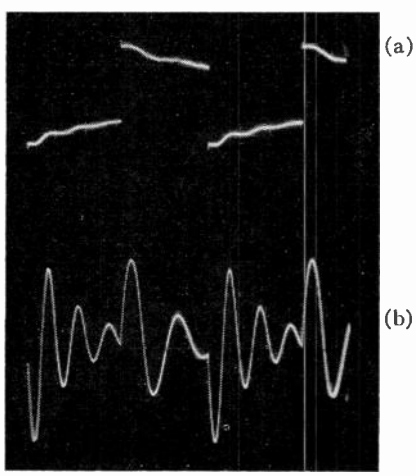

Fig. 13—Transient response with zero output impedance. (a) Amplifier output voltage. (b) Velocity of moving-coil.

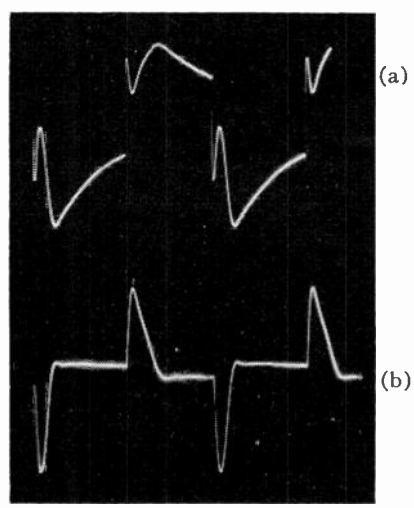

Fig. 14—Transient response with negative output impedance. (a) Amplifier output voltage. (b) Velocity of moving-coil.

A Transistor Push-Pull Amplifier Without Transformers*

J. H. CALDWELL†

Summary—A push-pull transistor amplifier has been developed using a matched pair in the output stage, with a minimum number of components and requiring no transformers.

Introduction

FOR the final power stage of audio amplifiers, the use of a pair of matched transistors in class *B* push-pull is becoming popular. Some circuits use the more conventional arrangement in which a transformer must be used to couple the symmetrical output to an asymmetric load; others use the "asymmetric push-pull" circuit shown in Fig. 1, which may be coupled directly to a suitable load without the use of an output transformer.

Although the asymmetric circuit does not require an output transformer if the load is of suitable value, it is usual to drive the output transistors by transformer coupling between the driver and output stages. This is because the "upper" unit requires its drive signal voltage to be applied between base and emitter, and in the configuration shown the emitter voltage is varying as the load and the "lower" unit collector voltage.

The circuit which has been developed overcomes this difficulty, as well as achieving the required phase inversion, by using a pair of complementary transistors in the driver stage. Previously published circuits[1,2] avoiding the use of transformers have been relatively complicated.

Development

For economy in components it was decided that, if possible, the emitter of each driver transistor should carry the same current as the base of the respective output unit. For a matched pair of *p-n-p* transistors, as in Fig. 2, this requires *p-n-p* drivers to have the driver emitter fed from the output base, or *n-p-n* drivers to have the driver collector fed from the output base.

The possible driver configurations for *p-n-p* output transistors are shown in Fig. 2.

If a *p-n-p* driver is used for the upper unit, its emitter voltage is essentially that of the upper output transistor, and therefore the signal input to the driver must be related to the output (or load) voltage. This requires either a transformer input (which is not desired) or a preceding *n-p-n* stage which will operate as in the next paragraph.

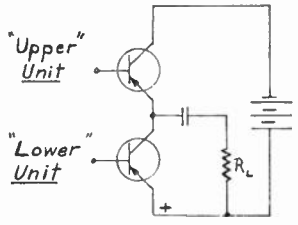

Fig. 1—An asymmetric push-pull output stage.

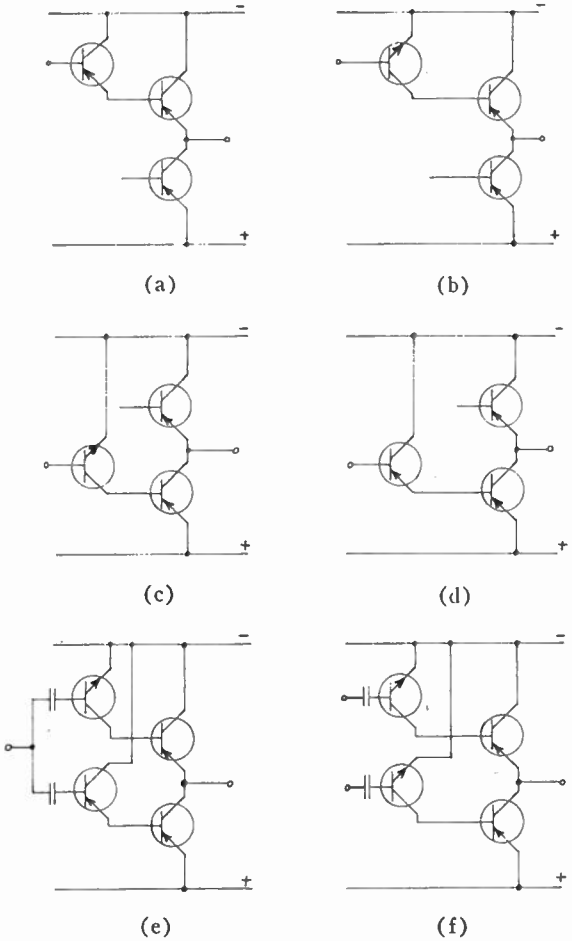

Fig. 2—Two-stage direct drive possibilities. The combination (e) gives internal phase inversion, but (f) requires external phase inversion.

* Received by the PGA, April 15, 1960.

† Hewlett Packard Co., Palo Alto, Calif.; on leave from Newcastle University College, University of New South Wales, Hamilton, N.S.W., Australia.

[1] H. C. Lin and B. H. White, "Single ended amplifiers for class B operation," *Electronics*, vol. 32, pp. 86–87; May 29, 1959.

[2] H. C. Lin, "Quasi-complementary transistor amplifier," *Electronics*, vol. 29, pp. 173–175; September, 1956.

If an *n-p-n* driver is used for the upper output unit, its emitter is at earth potential for signal voltages, and its collector current is relatively independent of the voltage at the collector. This means that the base current of the upper output transistor is to a large extent independent of the base voltage, and the emitter current of that output unit follows the voltage, with respect to earth, applied to the base of the driver.

For the lower driver, either *n-p-n* or *p-n-p* type may be used. The former type makes easier matching with the upper *n-p-n* driver, but the latter type gives a phase inversion and simple stabilization of the operating point of the output transistors, and so was the first to be investigated.

First Circuit

The type of circuit selected for first investigation is shown in Fig. 2(e).

In the first place, the output transistors used were a matched pair, type OC72, and the load was a Rola 8M speaker supplied with a voice coil of 30 ohms nominal impedance. This amplifier, with drivers and bias arrangements, is shown in Fig. 3.

To stabilize the operating point of the output transistors, it was found desirable to take the driver bias voltage dividers from the midpoint of the output transistors. Self-bias of the input transistors might be satisfactory for class *A* operation, but rectification during class *B* swings causes blocking of smaller following signals.

For the correct dc conditions, the bias resistors applied different amounts of ac feedback to the upper and lower units, and required the addition of further ac feedback to the upper unit. The circuit shown is not critical of component values.

Protection against ambient temperature variation is provided by using NTC resistors for *R2* and *R3*. Protection against thermal runaway is provided by *R1*, through *R3* to *T4* and *T2*, and then through the midpoint stabilization to *T3* and *T1*.

As *T3* is working as a grounded emitter unit loaded by an emitter follower, and *T4* is working as an emitter follower loaded by a grounded emitter unit, the input impedance of *T3* is very much less than that of *T4*. *R7* was selected experimentally[3] so that the input impedance of the amplifier as a whole was balanced at 1.0-volt rms output at 1000 cps. Fig. 4 shows the waveforms of input current, input voltage, and load voltage without and with *R7*. Fig. 4(b) gives an indication of the output distortion of the final amplifier.

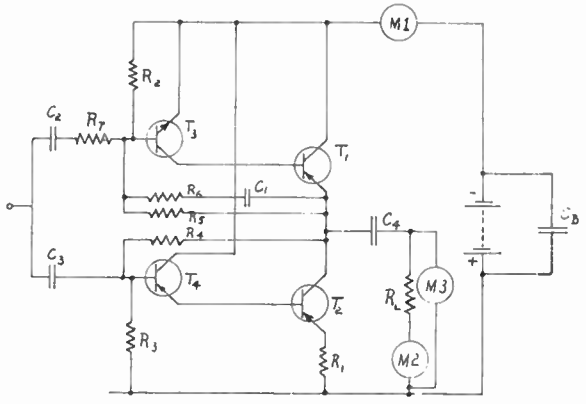

Fig. 3—The first experimental circuit.

T1, *T2*	0C72
T3	2T65
T4	0C71
R_L	33 ohms or modified 8M speaker
C_B	300 μf
C1	0.047 μf
C2, *C3*	0.27 μf
C4	100 μf
R1	1.0 ohm
R2, *R3*	6.8 kohms, NTC
R4, *R6*	68 kohms
R5	330 kohms
R7	10 kohms

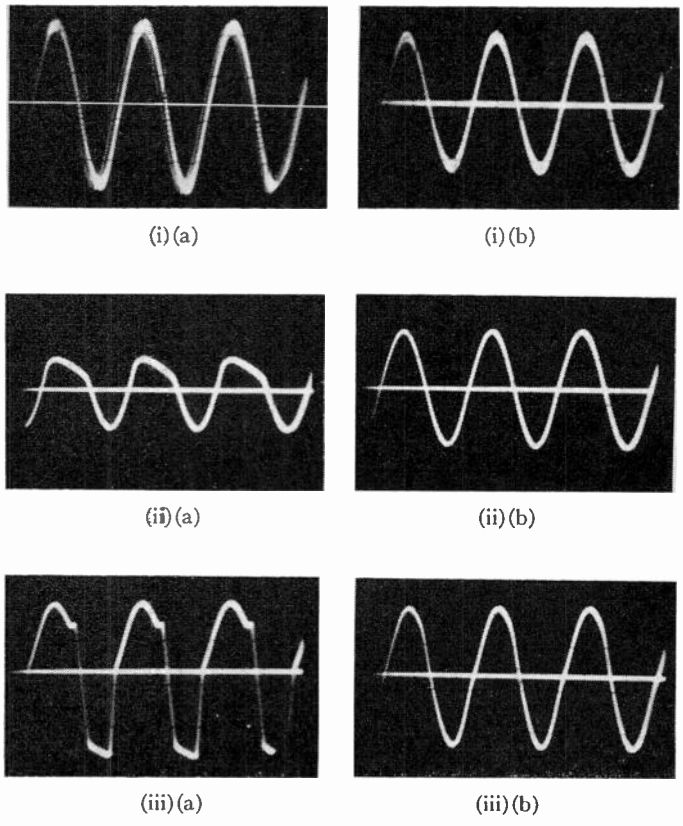

Fig. 4—Input and output waveforms of the amplifier shown in Fig.3, at 1000 cps with dc supply of 7.5 volts, for two values of *R7*. The upper halves of the oscillograms refer to conditions when the "upper" unit of the amplifier is conducting. The unbalanced input impedance evident in case (a) is reduced to almost zero in case (b). (a) *R7* = 0. (i) Input current to amplifier. (ii) Input voltage to amplifier. (iii) Amplifier output voltage, 1 V rms.

[3] (Footnote received, September 12, 1960.) Referring to Fig. 3, the author has found that an improvement in performance can be expected if a diode is inserted in the emitter circuit of *T3*. If the forward characteristic of this diode is similar to that of the base of *T2*, the input characteristics of *T3* and *T4* are better balanced, and the series input resistor *R7* can be reduced. *R5* and *R6* must also be modified.

The frequency response of the amplifier is shown in Fig. 5 for two conditions: first, in Fig. 5(a) for a load R_L of 33 ohms, resistive, and second in 5(b) for the modified 8M speaker as load. For comparison purposes, Fig. 5(c) shows the frequency characteristic of the speaker impedance. As the amplifier has essentially a constant current output, it should never be necessary to use corrective high or low boost with it.

In practice, the use of a low cut has been found desirable, in order to compensate for the low-frequency mechanical resonance of the speaker. By ear, the rise in voltage at higher frequencies at constant current seems to represent a change in power factor rather than a change in power output.

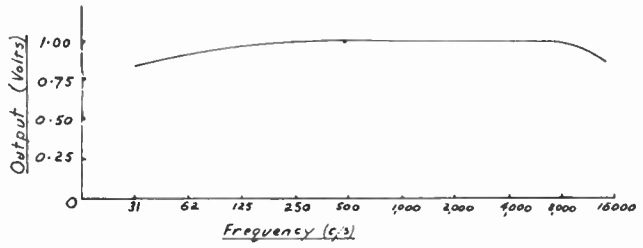

(a)

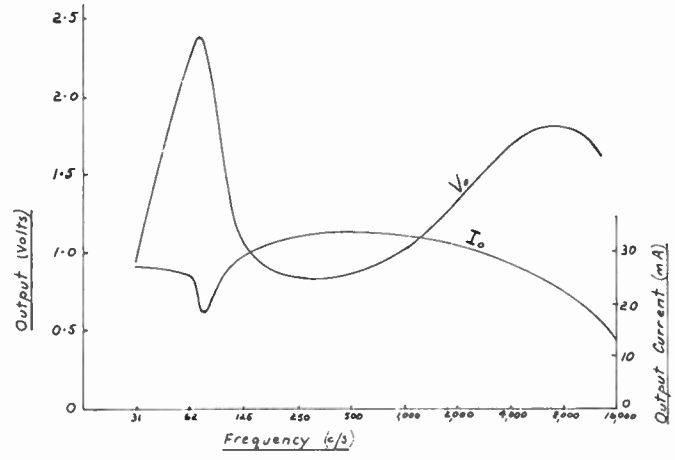

(b)

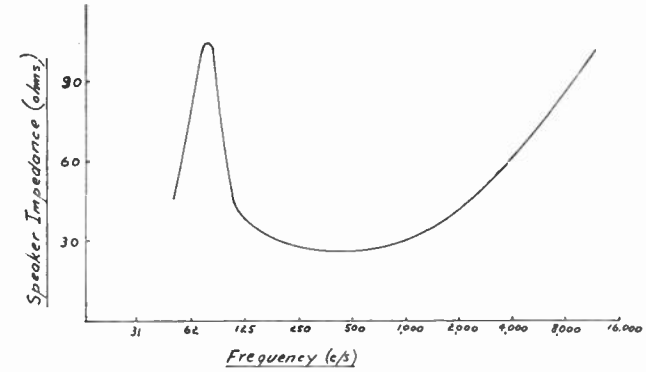

(c)

Fig. 5—General amplifier performance. DC supply 7.5 volts, input signal constant at 0.45 volt rms. (a) Output voltage with resistive load. (b) Output voltage and current with 8M speaker as load. (c) Impedance characteristic of 8M (modified) speaker.

Table I shows the limiting conditions of operation of the amplifier with various dc supply voltages, and gives an indication of amplifier performance on a failing supply. At 7.5 volts and above, the limit is imposed by peak clipping, which does not introduce severe voice distortion; but at lower voltages, with the attendant lower quiescent currents, crossover distortion becomes severe above the limits shown. In the range of supply voltage shown, the division of voltage between the output transistors is maintained almost uniformly, and on overload peak clipping of the output wave, occurs almost simultaneously on both peaks.

TABLE I

MAXIMUM* AVAILABLE OPERATING LEVELS

Supply Voltage (dc)	Quiescent Current (dc)	Maximum operating conditions at 1000 cps			
		Supply Current (dc)	Load Current (rms)	Load Voltage (rms)	Load (mva)
9.0 volts	11.0 ma	31 ma	63 ma	1.9 volts	120
7.5 volts	8.0 ma	26 ma	52 ma	1.6 volts	83
6.0 volts	4.5 ma	20 ma	41 ma	1.2 volts	49
4.5 volts	2.0 ma	14 ma	28 ma	0.86 volt	24

* Operation at levels higher than those shown results in noticeable distortion.

Practice shows that with an audience of 30 in an auditorium capable of holding 140 the output required is about 0.5 volt rms, representing about 8 mw, for public address purposes. Under these conditions, a monitoring oscillograph shows no excessive peaks or distortion.

OTHER CIRCUITS

In Fig. 6 other configurations are shown, which have the advantage of eliminating all transformers. These have not yet been experimentally checked; however, the only difficulty anticipated is in the stabilizing of the midpoint of the output transistors.

This stabilization is most easily achieved when the pair of transistors on the input side uses one *p-n-p* and one *n-p-n* type, as in Fig. 3 and also in Fig. 6(e) and 6(d). The remainder of the pairs in the amplifier may be matched pairs of similar type, and any number of stages may be built up using nothing but transistors. The only resistances used are those for bias to the input pair (and stabilization of the output midpoint at the same time) and thermal stabilization of the output stage. The only capacitors required are those coupling to load and input source. Phase inversion is obtained at the input to the amplifier, and a multistage amplifier may be made very compact, drawing very little more current than that required by the output stage.

Amplifiers of these types are at present being investigated, as well as similar amplifiers using a matched pair of *n-p-n* transistors in the output stage.

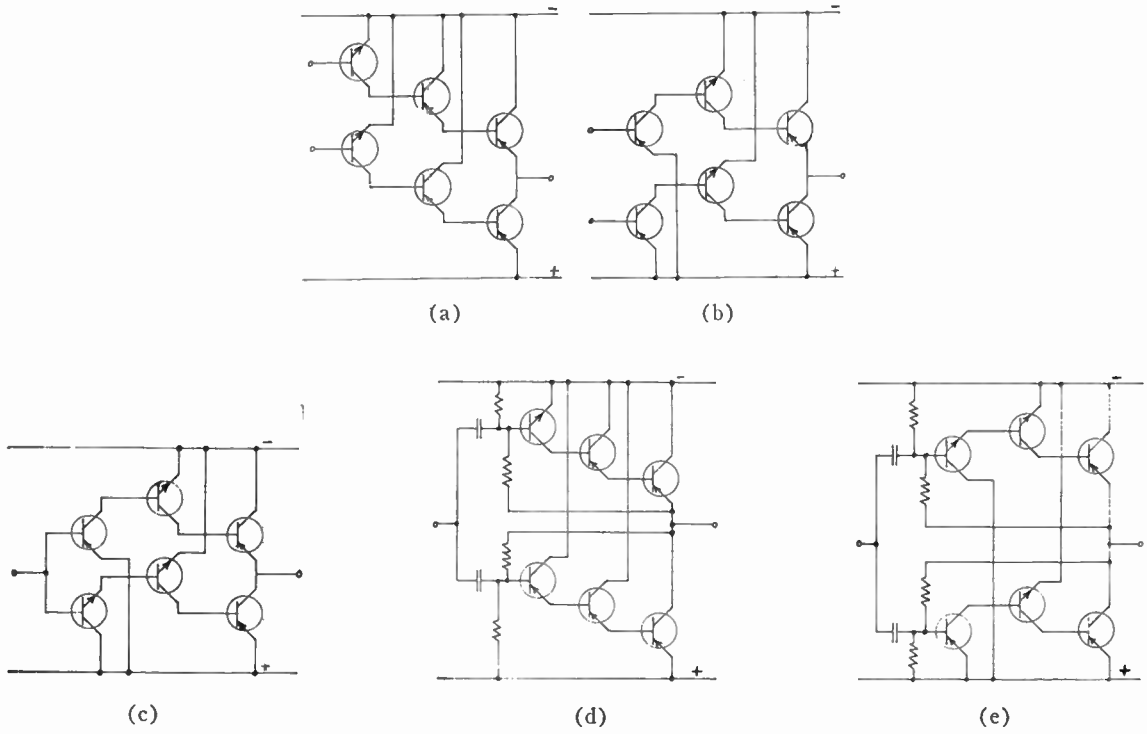

Fig. 6—(a) and (b) Two 3-stage configurations requiring external phase inversion. (c), (d) and (e) Three 3-stage configurations with internal phase inversion. Methods (d) and (e) permit simple stabilization of the output operating point.

Conclusions

It is quite practicable to operate a simple transistor asymmetric push-pull amplifier in the audio range without the use of transformers. The frequency response is limited at the upper end by the transistors used, and at the lower end by the input and output blocking capacitors.

Any number of cascade stages may be used, with only the same number of resistors and capacitors as are used by one driver and one output stage.

Acknowledgment

The author wishes to thank his colleague, R. C. Yates, for invaluable photographic assistance.

Automatic Spectral Compensation of an Audio System Operating With a Random Noise Input*

CHARLES E. MAKI†, MEMBER, IRE

Summary—A set of 80 filters is used to divide a random noise input spectrum of an audio system into 25 cps increments. An identical set operating as a spectrum analyzer provides a similar function on the system output. By means of an automatic regulating system using solid-state electronics, each of the 80 loops is closed independently, thus providing a unique control system compensating the audio system spectrum and equalizing disturbing resonance phenomena. This method has been successfully applied to the control of a vibration system spectrum where mechanical resonances at the exciter table produce high Q peaks and notches. The degree of spectral flatness reveals that adequate compensation is possible for typical resonance phenomena occurring over a wide frequency range.

Introduction

THE absolute control of the frequency response of an audio system is necessary in acoustic as well as vibration testing. A rigorously controlled test is necessary to determine the performance of apparatus subjected to a simulated environment. Ideally it should be possible to reproduce a specified environment so that the performance of future designs can be evaluated under the same known and controlled conditions.

For monosinusoidal excitation, frequency response control is achieved by using a feedback control system designed to operate with a rapid correction rate as the frequency is swept. These systems have been in use for several years and represent an approach familiar to the engineers who have designed equipment to withstand the sinusoidal environment commonly observed in military applications.

However, in high speed missile and rocket carriers it has been found that the nature of the environmental vibration is random rather than periodic. Hence, the term "random motion" caused by a "random exciting force" is used to define this type of phenomenon.

Random Vibration

In this type of environment, the acceleration force varies randomly, in which case the energy represented by the motion appears distributed over a band of frequencies. The power distribution must be defined in terms of statistical quantities common to the field of random noise. The power distribution of the vibration spectrum is defined in terms of the acceleration^2/cps and is identified as the acceleration spectral density, g^2/cps. This function is generally specified as the output of the vibration system as a function of frequency. Very often the system output requirement suggests that the acceleration specral density be flat with respect to frequency. This special case is identified as "white" random motion which is analogous to "white" noise.[1,2]

In addition to the spectral distribution of the system, it is noted that amplitude variations exist which must be evaluated using probability theory. It is generally assumed that the amplitude distribution in the vibration environment follows the Normal or Gaussian curve.

System Block Diagram

The vibration system can be thought of as a power generator (analogous to a power amplifier) producing a mechanical force (rather than an electrical current) at the output. It is desired to control the spectrum of the output acceleration and shape the system response in accordance with a given set of specifications. A block diagram of the system is shown in Fig. 1. A noise generator drives the system input with a random voltage which is transduced by an electronic power amplifier and vibration exciter into a mechanical output. It is desirable that the mechanical output spectral distribution have the characteristic defined by $G(\omega)$, where $G(\omega)$ defines the acceleration spectral density function g^2/cps in terms of frequency.

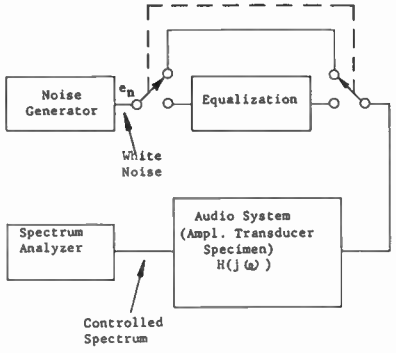

Fig. 1—Block diagram of random motion system.

* Received by the PGA, May 27, 1960. This paper was presented at the IRE International Convention, New York, N. Y., March 22, 1960.

† MB Electronics, Div. of Textron Electronics, Inc., New Haven, Conn.

[1] I. Vigness, "The fundamental nature of shock and vibration," *Elec. Mfg.*, vol. 63, pp. 89–108; June, 1959.

[2] G. Booth, "Random motion," *Prod. Engrg.*, vol. 27, pp. 169–176; November, 1956.

Assuming that the spectral response of the noise generator is "white" or that the power spectral density of e_n is flat with respect to frequency,

$$P_n(\omega) = P_0 \tag{1}$$

where $P_n(\omega)$ is the power spectral density and P_0 is a constant in volts²/cps. Since the system has a transfer function determined by the components producing the motion as well as the loading effect of the test object upon the motion generator, the output spectral density can be defined as the product of the input spectrum and the square of the absolute magnitude of the system transfer function

$$G(\omega) = P_0 \left| H(j\omega) \right|^2 \tag{2}$$

where $H(j\omega)$ is the system transfer function. If it is assumed that the transfer function of the system is linear, and that the noise generator is Gaussian, then the output of the system will also be Gaussian. Before the equalization network is inserted in series in the electrical portion of the system, it is necessary to examine the system transfer function $H(j\omega)$.

Systems with minimum phase transfer functions can be written in general form as a product of terms each with a single root. Often the roots consist of complex conjugate pairs in which case second-order terms with under-damped coefficients exist. A general transfer function can be written as

$$A(s) = K_1 s^m \frac{(s - r_1)(s - r_2) \cdots}{(s - r_a)(s - r_b) \cdots} \tag{3}$$

where

K_1 is a constant,
m any integer positive, negative or zero,
r_1, r_2 roots of the equation defined as the zeros of $A(s)$,
r_a, r_b roots of the equation defined as the poles of $A(s)$,
$s = j\omega$ the Laplacian operator.[3]

The transfer function of the vibration system has been mathematically derived and defined[4] as

$$H(s) = \frac{K_2 s}{(s^2 + 2\zeta_e \omega_e s + \omega_e^2)(s^2 + 2\zeta_a \omega_a s + \omega_a^2)} \times \prod_{h=0}^{N} \frac{s^2 + 2\zeta_{nh}\omega_{nh} s + \omega_{nh}^2}{s^2 + 2\zeta_{ph}\omega_{ph} s + \omega_{ph}^2} \tag{4}$$

where

$H(s)$ is the transfer function defined by the ratio of output acceleration to input voltage,
ω_e, ω_a, ζ_e, ζ_a are damping and frequency parameters of the vibration machine,
ζ_{nh}, ω_{nh} are damping and frequency parameters of the attached load contributing to the zeros of the transfer function,
ζ_{ph}, ω_{ph} are damping and frequency parameters of the attached load contributing to the poles of the transfer function,
N is an integer equal to the number of resonances in the load, and
Π represents the "product of."

The Laplacian operator s in (4) can be replaced by $j\omega$ and substituted into (2) to produce a complicated mathematical expression which becomes extremely difficult to treat further. Fig. 2 is included to show a typical response characteristic of the system. The vibration exciter phenomena appear as the broad characteristic at 100 cps and the sharp peak at 2000 cps. The other perturbations result from the characteristics of the load reflected into the impedance of the vibration generator.

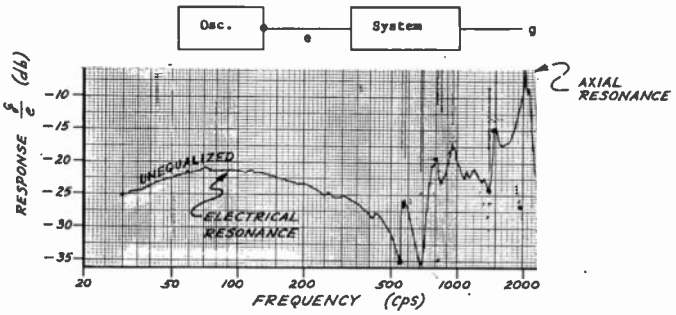

Fig. 2—Typical frequency response of vibration system.

Thus, the output spectrum is defined exclusively by the filtering action of the system. Certain frequency bands are accentuated, whereas others are rejected. Generator output impedance becomes a factor and frequency response control is necessary to provide a repeatable known power spectrum.

Classical Approaches to Equalization

Moving the switch of Fig. 1 into the lower position introduces the equalization circuitry into the system. Since the system response has been defined by (4) as a ratio of quadratic functions, it would seem that the inverse characteristic could be simulated using analog techniques. This represents the classic "peak notch" equalizer approach commonly in use.[5] Although this method represents the most accurate approach to the equalization problem, it presents several difficulties, including the tedious setup process if many resonances exist. If the system response changes during operation, it becomes difficult to correct for the shifts. Finally, the

[3] J. L. Bower and P. M. Schultheiss, "Introduction to the Design of Servomechanisms," John Wiley and Sons, Inc., New York, N. Y.; 1958.
[4] C. E. Maki, "Frequency Response Characteristics of Random Noise Systems," MB Electronics, New Haven, Conn.; 1958.
[5] C. E. Maki, "Mobility analogue technique in complex wave system equalization," in "Vibration Notebook," MB Electronics, New Haven, Conn.; 1958.

approach is an end in itself and the method cannot be adapted to automatic control.

It is recognized that instantaneous feedback will overcome difficulties due to nonlinear effects in the forward path. However, in this case this approach becomes unfeasible since the mechanical system presents nonminimum phase characteristics in the higher frequency region. Equalization to provide a stable feedback system would be more complicated and difficult to control than the original open loop system.

The typical mechanical system can contain as many as five different types of resonances.[4] Three of the five types are shown in Fig. 2. Note the wide dynamic range as well as the high Q phenomena characterized by the sharp peaks and notches. Low frequency resonances are uncommon since it is possible to design the mechanical structure with sufficient rigidity to eliminate the low frequency perturbations.

Narrow-Band Equalization

A more versatile approach divides the power spectrum into discrete finite bands which can be individually controlled. This approach can be thought of as parallel equalization since the noise generator spectrum is divided into parallel channels using narrow band-pass filters and eventually recombined. The system is shown in block diagram form in Fig. 3. Note the application

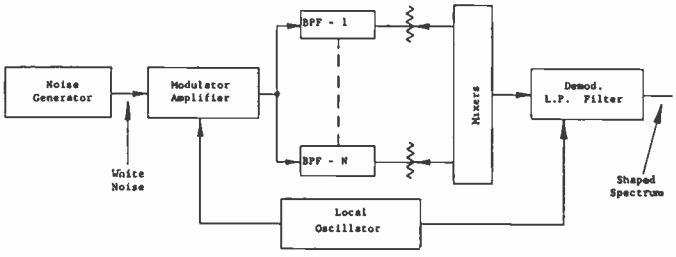

Fig. 3—Block diagram, multifilter parallel equalization.

of modulation techniques to translate the audio spectrum into the IF region to permit the use of narrow-band constant bandwidth filters. The filter output is adjusted using the potentiometer to establish the level and the signal is then applied to the mixer input. Note that only the upper sideband is used. The carrier is suppressed in the balanced modulator and the lower sideband cannot pass through the filters. Demodulation occurs after the mixer and the audio spectrum is recovered except that the spectral response has been modified according to the adjustments of the logarithmic potentiometers. The same local oscillator drives both modulator and demodulator, thus insuring that proper translation occurs in both processes.

Performance of the system depends primarily upon the characteristics of the filters. The process of modulation and mixing involves techniques well known to those in the electronics field. The quality of the electronic design eliminates effects such as harmonic and intermodulation distortion, both of which affect the dynamic range. Better performance ultimately requires more sophisticated circuitry.

Requirements of the Band-Pass Filters

A spectrum analyzer with the narrower more selective filter performs better than an alternate wider band instrument. Analogous to this is a statement that a spectrum equalizer with narrower more selective filters provides better equalization than the wide-band device. It does not follow that a flat top filter is necessary to provide the best compensation. The most desirable approach would be to have a triangular shaped filter response adjusted such that the peak intersects the desired compensation curve and the neighboring filters add to provide a linear transition between adjacent filter centers. Compensation would be accomplished by connecting adjacent filter center frequencies with a series of linear segments.

Another approach involves choosing a flat top filter with infinite slope on the skirts and producing a curve consisting of a series of steps. In any case the narrowness of the filters are significant in establishing the ultimate spectrum shape implying that the greater the number of filters, the better the equalization.

At this point it is necessary to evaluate other characteristics of filter configurations. Three important criteria must be considered. First, it is necessary that the output of all filters be summed properly. Second, since the equipment employing the filters is to be sold, the filters must be simple and economical. Finally, the performance criterion must be considered and balanced against the economic consideration.

Summing Narrow Band-Pass Filters Connected in Parallel

Consideration must be given to the summing process of band-pass filters connected in parallel. It is impossible to design and build filters which have an infinite slope at the skirts and which can be arranged adjacent to one another with infinitesimal spacing between them. Improper adding can conceivably produce peak or notch characteristics more serious than those introduced by the resonant members of the load. Thus, the ability to add the output is of prime importance.

Summation of random voltages from parallel band-pass filters is generally not considered a problem if the filter inputs are incoherent or independent of one another. Since the same random signal is introduced to all filters, coherence exists and the adding problem must be considered.[6]

A simple high Q filter such as a crystal or magnetostrictive type can be analyzed using the equivalent cir-

[6] S. Goldman, "Information Theory," Prentice-Hall, Inc., New York, N. Y.; 1953.

cuit of Fig. 4(a). The transfer function can be written[7,8]

$$G(s) = K_1 \frac{s}{s^2 + \frac{1}{Q}\omega_0 s + \omega_0^2} \tag{5}$$

$$G(j\omega) = K_2 \frac{1}{1 + Qj\left(\frac{\omega}{\omega_0} - \frac{\omega_0}{\omega}\right)} \tag{6}$$

where

K_1 and K_2 are constants,
Q is the quality factor ($Q \cong 10^4$),
ω_0 is the resonant frequency.

Since it is recognized that $(\omega - \omega_0) \ll \omega_0$, (6) can be simplified to produce

$$G(j\omega) \cong \frac{K_2}{1 + j2Q\frac{\omega - \omega_0}{\omega_0}} \cdot \tag{7}$$

Let

$$2Q\frac{\omega - \omega_0}{\omega_0} = x$$

$$G(j\omega) = \frac{K_2}{1 + jx} \cdot \tag{8}$$

The variable x is the normalized deviation from the filter center frequency in half bandwidths as plotted in Fig. 4(b).

It is possible to combine two filters together by adding their outputs out of phase to produce a composite filter having more desirable characteristics. Consider Fig. 5 showing two simple filters separated by b half bandwidths. The composite response is obtained by modifying (8) and adding the two outputs together.

$$G_2(jx) = \frac{K_2}{1 + j(x - b/2)} - \frac{K_2}{1 + j(x + b/2)} \tag{9}$$

$$G_2(jx) = \frac{K_2 jb}{\left[1 + j\left(x + \frac{b}{2}\right)\right]\left[1 + j\left(x - \frac{b}{2}\right)\right]} \cdot \tag{10}$$

$G_2(jx)$ must be resolved into the real and imaginary parts to investigate the possibility of summation. It is interesting to note that the phase relationship of the composite filter is 90° at resonance ($x = 0$) .

Eq. (10) can be resolved into the real and imaginary parts and the result given in (11).

[7] T. Usher, "Response of Narrow Band Filters Connected in Parallel," MB Electronics, unpublished memorandum, New Haven, Conn.; 1959.
[8] T. Usher, "Analyzer-Equalizer Filter Design," unpublished memorandum, MB Electronics, New Haven, Conn.; 1959.

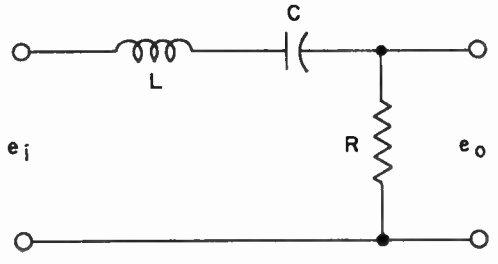

(a)

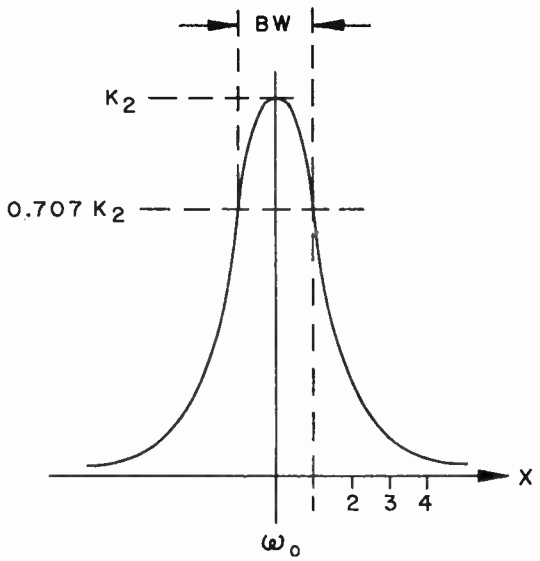

(b)

Fig. 4—(a) Equivalent filter circuit. (b) Filter response.

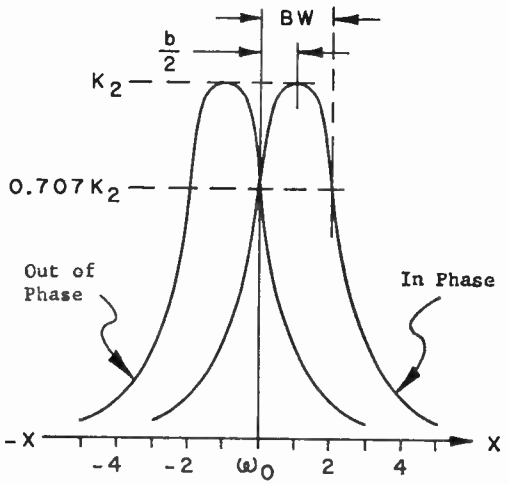

Fig. 5—Adding filters out of phase.

$$G_2(jx) = K_2\left\{\frac{2xb}{\left[1+\left(x-\frac{b}{2}\right)^2\right]\left[1+\left(x+\frac{b}{2}\right)^2\right]}\right.$$

$$\left.+\,j\frac{b\left(1+\frac{b^2}{4}-x^2\right)}{\left[1+\left(x-\frac{b}{2}\right)^2\right]\left[1+\left(x+\frac{b}{2}\right)^2\right]}\right\}. \quad (11)$$

The response given by (10) is plotted in Fig. 6 for a value of $b=2$ (individual filters separated by one bandwidth). On the same scale a single section filter would exhibit a slope of -1 whereas a 3 section composite device would have a -3 slope on the filter skirt. Note that the two-section composite filter provides considerable advantage and will be used in future analysis of the ability to add a large number of filters in parallel.

It is now necessary to determine the possibility of adding a large number of two-section composite filters in parallel and to choose the design parameters such as to minimize the amount of ripple appearing in the summed output.

Consider the magnitude of the response at the center frequency of a filter and define this as G_{tc}. The magnitude at this point will consist of the sum of all of the individual filter outputs and can be written as

$$G_{tc} = j2\left[0.5 + \sum_{m=1}^{\infty}(-1)^m \operatorname{Im}\left\{G_2(jmk)\right\}\right]. \quad (12)$$

Halfway between filters the response must be determined and can be written as

$$G_{th} = 2\sum_{m=0}^{\infty}(-1)^m \operatorname{Re}\left\{G_2\left[j(m+\tfrac{1}{2})k\right]\right\}. \quad (13)$$

It is convenient to define a parameter k which specifies the center frequency separation of the composite filter in terms of half bandwidths of the individual filters. Eqs. (12) and (13) assume that adjacent composite filters are summed out of phase.

Selection of filter parameters must be made on the basis of a criterion established from consideration of (12) and (13). In particular the summed output should have only a certain amount of ripple. Therefore, a "ripple factor" defined as the ratio of G_{tc}/G_{th} can be computed and plotted as a function of k. Intuitively, one can observe that, if the filters are separated more, the ripple factor can be expected to increase. On the other hand this condition would provide greater rejection in the center of the adjacent filter band thus permitting resonances of greater dynamic range to be equalized. The rejection at the center of the adjacent band can be defined as the "rejection factor" and plotted as a function of k. Both the ripple and rejection factors are plotted in Fig. 7 for many two-section composite filters added in parallel with adjacent filters driven "out of phase."

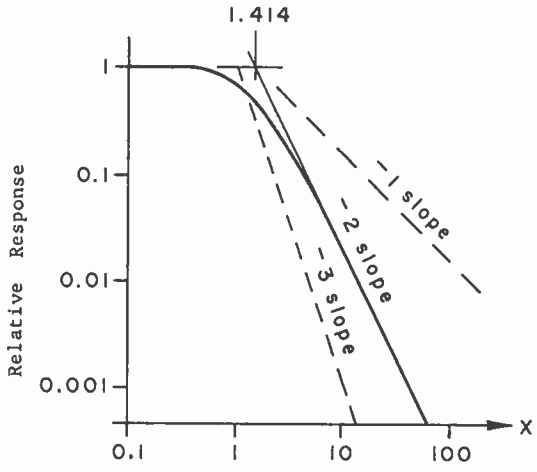

Fig. 6—Composite filter response.

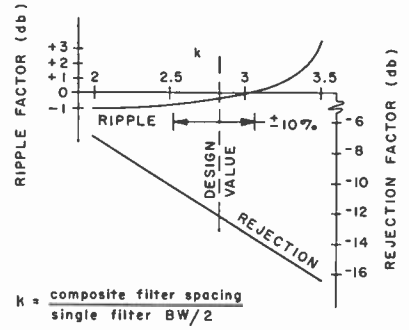

Fig. 7—Ripple and rejection factor for a two-section composite filter.

Fig. 7 reveals that the unity ripple factor occurs when k is slightly larger than 3. Note, however, that above $k=3$ the ripple factor curve increases rapidly, indicating the desirability of choosing a value of k between 2.5 and 3 to allow for normal tolerances existing in the manufacture of filters. A design value of $k=2\sqrt{2}$ appears to be a logical choice resulting in a ripple factor of ± 0.2 db and a rejection factor of 12 db.

Filter Cost

Since many filters are required, it becomes necessary to weigh the economic problem against performance. They must be simple devices, easy to build, rugged and require no maintenance. Low impedance devices are preferred since the cost of shielding for carrier frequency radiation increases with impedance.

System Performance

Performance of the system can be defined as the ability of the device to equalize a frequency spectrum within a certain flatness. The following factors must be considered

1) Number of filters
2) Narrowness of each filter
3) Steepness
4) Dynamic range
5) Stability.

The first three factors are governed by economics. This paper will be concerned with a system consisting of 80 filters each 25 cps wide and covering the frequency range from 12 cps to 2012 cps. Two-section composite filters are used and the nominal value of $k=2.818$. Dynamic range of correction should be at least 40 db and filters with 50-db rejection should be used to allow a safety margin. Stability of the filter is important since it is undesirable to have the compensation change once it has been adjusted. Frequency drifts could result in unwanted peaks or notches in the compensated response.

Results of Compensation

Magnetostrictive filters have been used in a design to perform the equalization of the audio spectrum. These devices, manufactured by Raytheon Mfg. Co., Bedford, Mass., present most of the desirable and necessary characteristics required to fulfill the compensation criterion.[9] Furthermore, they can be obtained with different bandwidths to provide performance consistent with that desired.

Frequency response tests can be performed to establish the mixing and rejection capabilities of the system. This is easily accomplished by driving the equalization system with a sinusoidal input signal and recording the output on an X-Y recorder. Fig. 8(a)–8(e) (next page) shows the results of the tests. Since the filter bandwidth is constant, 25 cps, the actual response plotted on a log frequency scale appears wider at low frequencies. Fig. 8(a) demonstrates the response for three filters, 475 cps, 975 cps, and 1975 cps. The mixing capability can be observed in Fig. 8(b) where the full output of each filter is added together. Note the absence of excessive ripple in the mixed output. Rejection is shown in Fig. 8(c) and 8(d) where one and two filters are removed respectively at several points in the spectrum. Note the existence of a 12-db rejection factor as determined by $k=2.828$. Elimination of two filters produces an extremely sharp notch since the phase characteristic produces subtraction at this point. Fig. 8(e) shows the filter capability in producing a peak-notch pair using two adjacent filters. Fig. 9 shows the system capability to compensate for an actual vibration system operating in the audio spectrum.

Automatic Compensation with Random Input

The previous section proves that the phase relationship of the system is adequate. Disturbing notch phenomena due to filter crossover is eliminated. With random noise operation the signal coherence between adjacent filter channels could introduce voids in the spectrum if an improper phase relationship existed. Confidence in the equalization eliminates the need to continuously monitor the output with a sweeping narrow band analyzer.

This confidence in the equalization also suggests the use of closed loop feedback to permit fully automatic operation with a random noise input. The basic principle involves monitoring the system output with an appropriate transducer, dividing the power spectrum with an identical filter bank, and using the spectral level of each channel to control the input level of the corresponding equalizer channel. A block diagram is shown in Fig. 10. The equalization system is similar to that considered previously except that the adjusting potentiometers are replaced by AGC amplifiers. The output of the system to be equalized is connected into a multichannel analyzer which segregates the spectrum into 80 parts each 25 cps wide.[10] A transistorized amplifier provides sufficient gain to increase the level to a desirable magnitude. Each channel has a gain set potentiometer to normalize the output before driving the final amplifier, detector, and AGC circuit. Since multiple channels exist, the control loop is transistorized to provide a saving of space as well as to add to the reliability.

Detection and Filtering

The information concerning the spectral level of the excitation appears at the output of each analyzing filter. Since the signal at the output of each filter appears as a sinusoid with randomly varying phase and amplitude, it becomes necessary to pass the signal into a detector and low-pass filter to obtain the information concerning the magnitude of the spectral density. It is interesting to observe the output of a filter driven from a random source on an oscilloscope. If the triggering level is properly adjusted, successive sweeps will appear of different amplitudes and with nearly equal frequency. Although the successive sweeps originate at the same point on each cycle and coincidence occurs at the beginning of the sweep, it will be noted that variations can exist before several cycles occur as demonstrated in Fig. 11(a). The signal in this example was passed through the 101,000-cps filter and recorded with a sweep time of 20 μsec. Thus, the observed energy is contained in the region of 101 kc.

If the sweep time is lengthened and only one sweep recorded, it appears as if a carrier frequency were modulated by a randomly varying amplitude, as shown in Fig. 11(b). In this photograph the output of the 101-kc filter with a 3-db bandwidth of 25 cps is shown. The sweep length is 1000 msec. If the filter were ideal, the modulation frequency would not exceed 25 cps.

Interesting characteristics result when a stationary random process is passed through a narrow band-pass filter. First, the envelope of the random modulation behaves according to the Rayleigh distribution. More im-

[9] "Magnetostriction Filters," Raythron Mfg. Co., Bedford, Mass.; 1957.

[10] R. Boynton, "A magnetostrictive filter random wave analyzer," 1960 IRE International Convention Record, pt. 9, pp. 217–226.

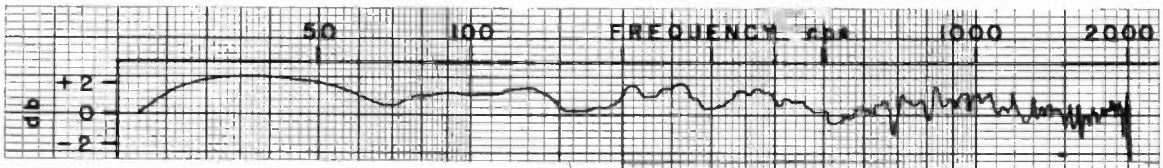

Figure 8b - Frequency Response of 80 Filters With Outputs Added in Parallel

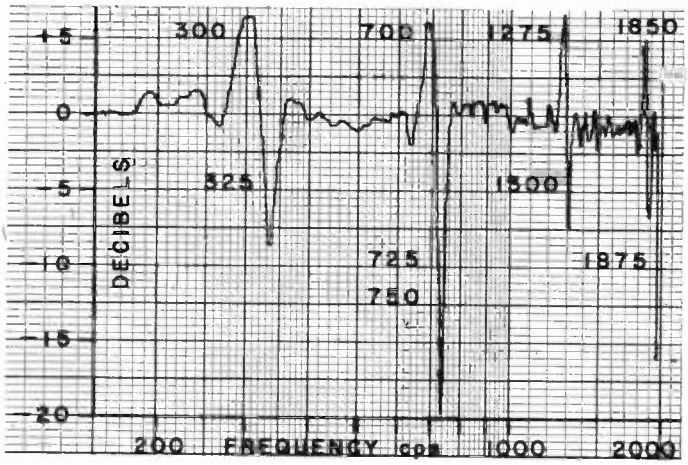

Figure 8e - Ability of System to Produce a Peak-notch Pair

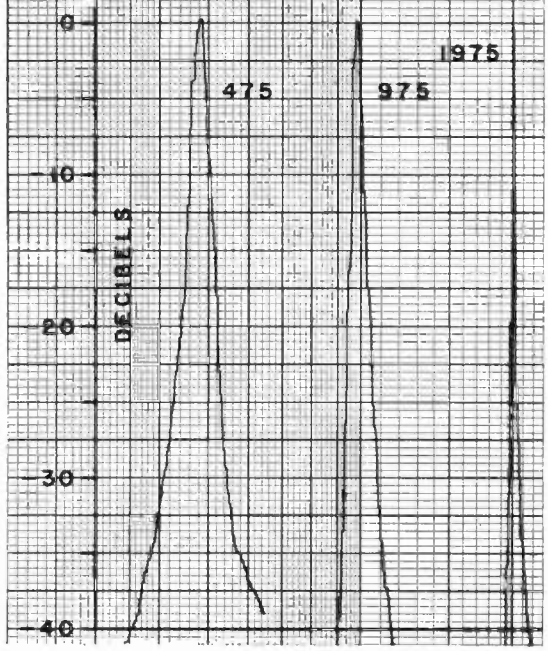

Figure 8a - Response of Three 2-Section Composite Filters

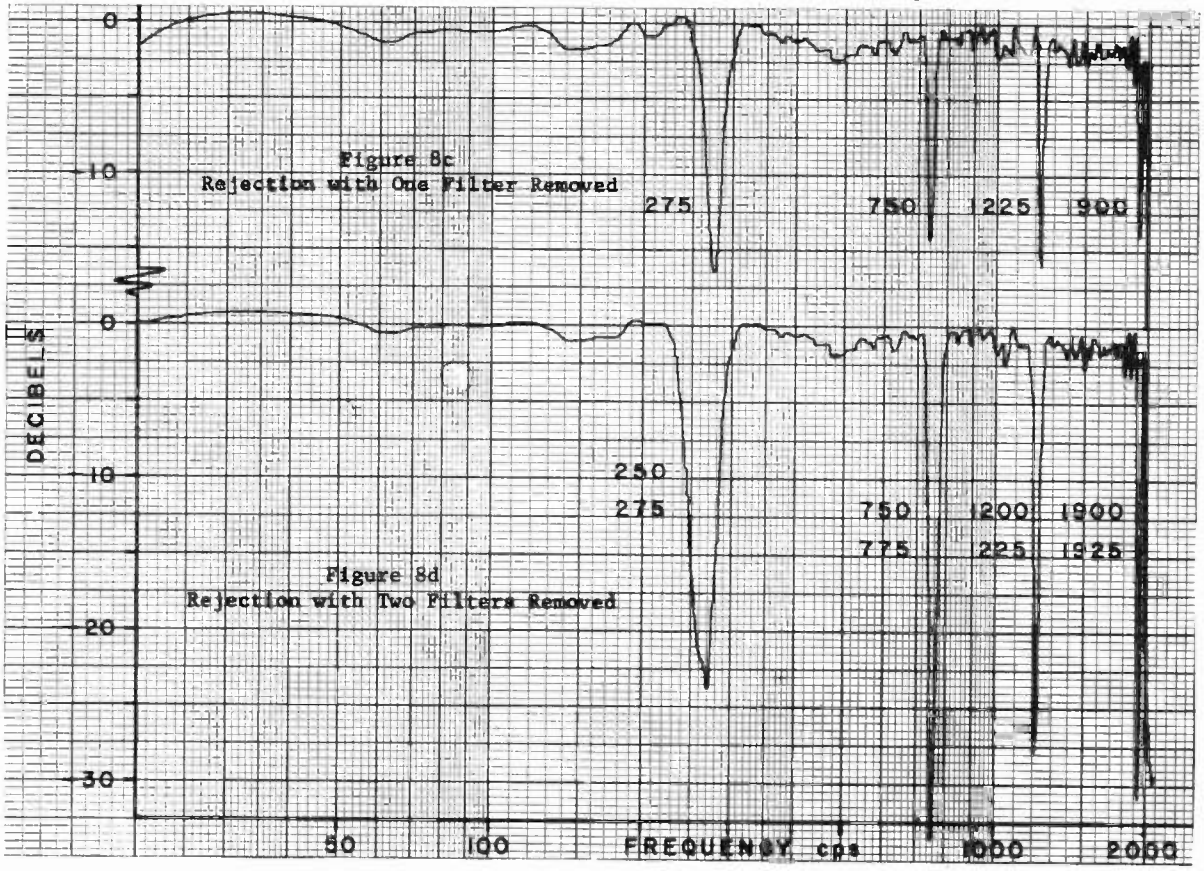

Fig. 8.

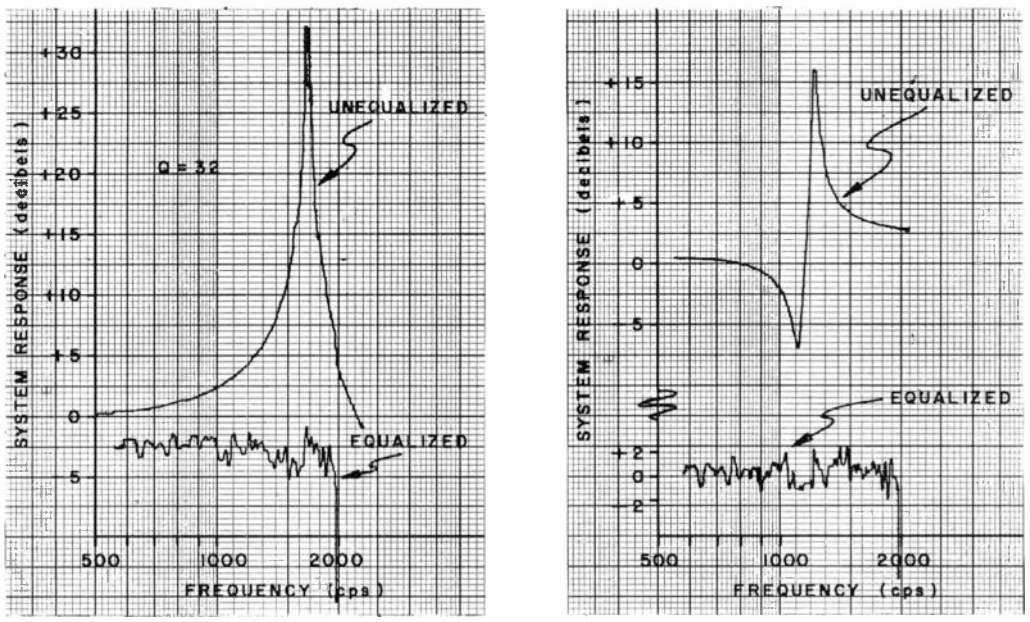

(a) (b)

Fig. 9—(a) Compensation of fixture or exciter axial resonance. (b) Compensation of peak notch specimen resonance.

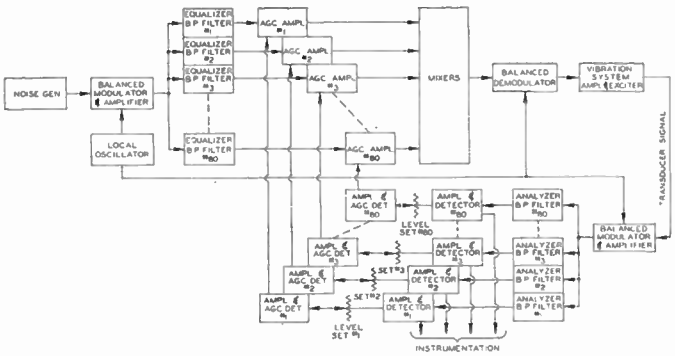

Fig. 10—Block diagram of the automatic spectrum equalizer for wide-band compensation.

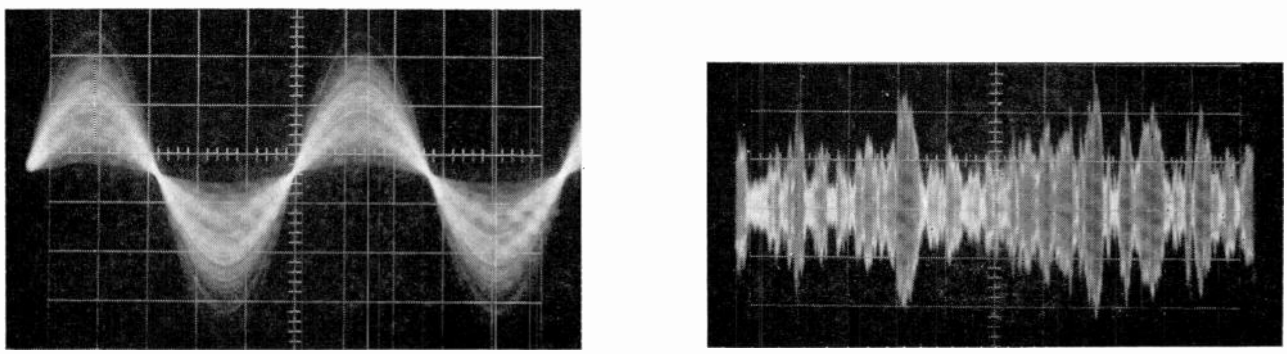

(a) (b)

Fig. 11—Output of 101-kc filter, 25 cps bandwidth. (a) Sweep time 20 μsec, exposure ⅛ second. (b) Sweep time 1 second, exposure 1 second.

portant, the instantaneous magnitude, independent of the random input distribution, will follow the Normal or Gaussian function. This fact permits the design criterion regarding the detection-filtering system to be evaluated from a different point of view. If the signal is known to follow the Normal distribution law, then the detection system can be chosen strictly on the basis of ease of filtering since the relation between all linear variables such as the mean, average, or the standard deviation, rms, are related by constants. For example, the standard deviation of a normal distribution is defined as σ, whereas the mean is 0.8σ when the signal has passed through a full wave detector.

Therefore, it may be concluded that any linear quantity can be detected and filtered since the dc output will always be directly proportional to the standard deviation, rms. Analogous to this approach is the measurement of the rms value of a sinusoidal signal with a meter containing an averaging detector. The measurement is reliable if the signal is sinusoidal, since the ratio between average and rms is always a constant factor.

Next, it is necessary to justify the aspect of power spectral control with a linear detector. This can be reasoned as follows. If the power spectrum is to be controlled, then the mean square value of the excitation must be controlled in each incremental bandwidth of 25 cps. If "white noise" is desired at the output of the audio system, then the mean squared voltage per 25 cps of bandwidth must be a constant in each filter band. However, if this is true, then the root mean squared voltage per 25 cps of bandwidth must also be constant in each band. Therefore, a linear device can be employed in the detector. Once this is established, the servo design problem can be handled on the basis of a linear control system rather than one involving a nonlinear squaring characteristic. This leads to a more simplified design, resulting in both greater economy and reliability.

Based upon the previous observation, the detector-filter combination can be chosen. For simplicity and economy the simple RC network is used to provide a dc voltage proportional to the signal in a given channel. The figure of merit for the performance of a low-pass filter operating with random input can be defined as the ratio of the mean value of the output R, to the standard deviation σ. This factor has been evaluated for several detector filter combinations including the square law full-wave, and linear half-wave types, with a simple RC filter.

The significance of the figure of merit is realized when the deviation from the true mean value of the measured process is considered. Since the input to the low-pass filter is random, the dc output voltage, which is the control for the AGC stage, will vary with the Gaussian amplitude distribution. If extreme variation exists, the compressor action of the control system will cause the AGC output to vary over wide limits, and the automatic compensation effort will fail.

Thus, it is necessary to establish the percentage variation of the observed output from the true mean value of the filter input, and express this percentage in terms of a confidence factor.[11] For example, if the output voltage is to be within p per cent, 95 per cent of the time (approximately 2σ), the filter figure of merit can be related to the percentage p by the equation[12,13]

$$0.01pR = 2\sigma$$

$$p = \frac{200}{R/\sigma} \cdot \tag{14}$$

This percentage factor is plotted on the ordinate of Fig. 12, as a function of the time constant of the low-pass filter when the bandwidth of the process is 25 cps.

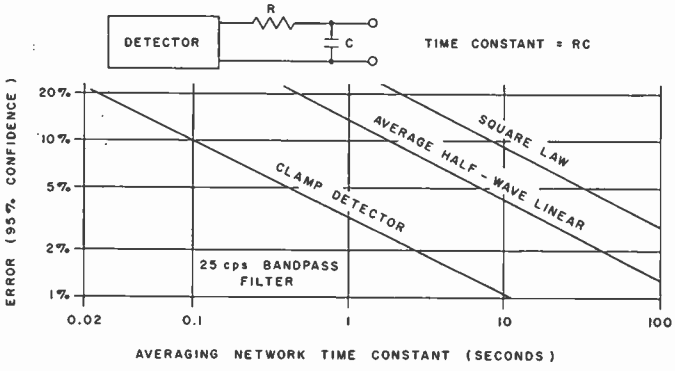

Fig. 12—Percentage error with 95 per cent confidence as a function of low-pass filter time constant for three different detectors.

Three curves are shown in Fig. 12, including calculated performance for the square law full-wave, the linear average half-wave, and measured performance of the clamp detector. These data can be interpreted by establishing a criterion regarding the tolerable percentage deviation from the true mean assuming 95 per cent confidence, and then establishing the time constant of the low-pass filter. One important observation is clearly shown in Fig. 12. For a given percentage deviation p, the linear half-wave detector requires only 1/4 of the filtering, and the clamper about 1/80 of that required for the square law type. This factor provides a significant advantage in the choice of RC filter components. The resistor in the filter must be fairly small to prevent excessive loading by the transistor circuitry, and additional filtering must be provided by increasing the capacitor size. Additional capacitors become expensive when multiplied by the number of channels, 80.

A comparison of time constants is shown in Table I.

[11] T. Usher, "Spectral Analysis," unpublished memorandum, MB Electronics, New Haven, Conn.; 1959.

[12] J. S. Bendat, "Principles and Applications of Random Noise Theory," John Wiley and Sons, Inc., New York, N. Y.; 1958.

[13] W. Davenport and W. Root, "An Introduction to the Theory of Random Signals and Noise," McGraw-Hill Book Co., Inc., New York, N. Y.; 1958.

TABLE I
COMPARISON OF TIME CONSTANTS

Detector	Process $BW = 25$ cps Accuracy = 2 Per Cent (95 Per Cent Confidence)	
	Time Constant	f_L
Square Law	210 sec.	7.5×10^{-4} cps
Average	50 sec.	3.2×10^{-3} cps
Clamper	2.5 sec.	6.25×10^{-2} cps

By choosing the clamper detector circuit, the time constant of the RC filter is reduced by orders of magnitude. This is important from the standpoint of correction time of the control system, since the filter characteristic presents the predominant lag in the response. Stated another way, a system employing the clamp detector can be 80 times faster than a system with square law detection and 20 times faster than a system with average linear detection!

Automatic Control Accuracy

Design of an automatic control system must include consideration of the control accuracy. However, before this can be considered, it is necessary, first, to estimate the accuracy performance requirement of the over-all system, and, second, to determine the expected variation in loop gain which will occur in the forward path. The first criterion can be evaluated from present specifications used in testing, the second, from experience obtained from many systems of the type being considered.

Specifications regarding system flatness vary from ± 1 db to ± 6 db, the variation generally being determined by considering the complexity of the object on the vibration exciter table. Experience obtained on many systems indicates that 30 to 35 db represents the widest dynamic range, although exceptions have been known to occur. The response of Fig. 2 indicates a dynamic range of 30 db from 20 to 2000 cps. Knowing these characteristics, one can arbitrarily state that the dynamic range of correction should be at least 40 db (100:1), and that for this variation it would be desirable to correct the system output to ± 1 db in absolute level in each 25-cps band. Those acquainted with control circuit design will recognize that this performance can be obtained with an electronic compressor. Servo motors could be used, but the expense, compared to a single transistor, makes their use impractical since the control system must be duplicated 80 times. It is true that a servo with a motor would provide integration in the loop, but this would merely attempt to reduce the error of ± 1 db which already approaches a satisfactory value.

The AGC circuit consists of a transistor capable of a gain variation of 100:1 when the base current is changed. Base current control is established by the detector-filter through appropriate networks. Thermistor compensation is applied to reduce temperature effects and satisfactory operation is obtained up to 100°F.

The characteristic of a single compressor showing the change in over-all system gain as a function of the audio system gain appears in Fig. 13. The actual performance averages approximately ± 0.75 db as shown; a tolerance of ± 0.25 db is allowed for miscellaneous changes. An adjustment normalizes each channel, thus allowing for different channel characteristics due to component and production variations. Sufficient feedback is applied around each amplifier to insure stable gain.

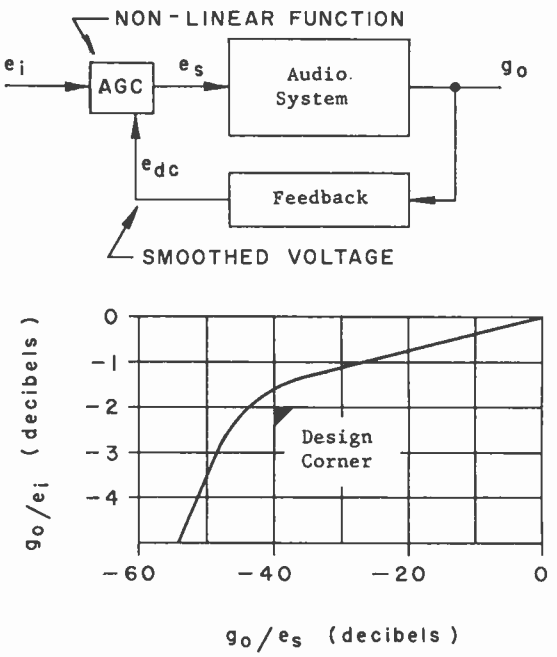

Fig. 13—Typical performance of servo, arbitrary reference on both axes.

An important observation can be made regarding harmonic distortion. Due to nonlinearity, AGC stages normally introduce even harmonic distortion. However, with the configuration shown, the AGC action occurs on the high frequency signal, 100 kc–102 kc. Harmonic distortion components will appear 200 kc and above in the frequency spectrum. Thus, in the demodulation-filtering process the harmonic components generated by the AGC circuit will be eliminated, and the audio signal introduced to the system will be free of distortion.

Control System Stability

The output of the system to be equalized consists of a voltage varying randomly according to the normal distribution law. Automatic control is being provided to maintain a given preset level within each 25-cps increment of bandwidth. Thus, the system has the characteristics of a positioning type of carrier control system. An integrator (motor) is not included in the control loop, identifying the system as a Type 0 servomecha-

nism, sometimes referred to as a regulator or a compressor. The system time constants must be considered to insure absolute stability.

Four potential lags appear in the closed loop, the most predominant one being the time constant of the low frequency smoothing-filter. A second lag exists in the narrow band-pass high frequency filter. Since a two-section composite filter is used, a second order system results. However, the roots of the system are damped since no buildup occurs at the filter corner as shown in Fig. 6. This analysis assumes two equal time constants. Resonance phenomena in the load attached to the audio system output can introduce a third lag since an inherent delay will exist during buildup of an applied excitation. It will be assumed that this characteristic will exhibit a first order effect. A transport lag exists in the high frequency magnetostrictive filters since a finite delay occurs as the energy is propagated down the length of the magnetostrictive rod. However, for the filters employed in the system this delay is less than 25 μsec and will be neglected.

Loop Gain Function

The loop gain function of each individual channel of the system can be written as shown in (15). (Note it is necessary to consider the nonlinearity of the AGC stage.)

$$A(s) = \frac{a\partial e_{s\ \mathrm{rms}}/\partial e_{\mathrm{dc|max}}}{(1+T_1 s)^2(1+T_2 s)^2(1+T_3 s)} \tag{15}$$

where

$A(s)$ is the loop gain function,
T_1 is the low pass filter time constant,
T_2 is the high frequency band pass filter time constant,
T_3 is the time constant of a resonant load connected to the audio system output, and
$a\partial e_{s\ \mathrm{rms}}/\partial e_{\mathrm{dc|max}}$ defines the maximum loop gain constant.

In 15 the $s=j\omega$ has different meaning in each of the denominator terms. The term $(1+T_1 s)$ is the low pass RC filter lag and $s=j\omega$ is the natural resonant frequency in radians/seconds. Since the band-pass filter operates at a center frequency of ω_0 between 100–102 kc the $s=j\omega$ in the $(1+T_2 s)$ term refers to the deviation of ω from ω_0. Finally, the term $(1+T_3 s)$ is concerned with the characteristics of the load, and the $s=j\omega$ in this case refers to the deviation from the audio frequency of the system.

Magnitude of the Time Constants

To establish the stability criterion, it is necessary to determine the value of K as well as the time constants T_1, T_2 and T_3. When these are determined, the Bode diagram can be drawn and the loop stability determined. $a\partial e_{s\ \mathrm{rms}}/\partial e_{\mathrm{dc}}$ can be determined by breaking the closed loop and measuring the change in AGC output as a function of audio system input using the information in Fig. 13. The critical condition occurs at maximum compression when the slope of the $\partial e_{s\ \mathrm{rms}}/\partial e_{\mathrm{dc}}$ curve reaches the greatest negative value. The minimum negative slope occurs for minimum compression. For this system

$$(-1000) < a\frac{\partial e_{s\ \mathrm{rms}}}{\partial e_{\mathrm{dc}}} < (-2). \tag{16}$$

T_2 can be computed from the half bandwidth of the high frequency band-pass filter. Assuming that f_2 (half bandwidth) is equal to 12.5 cps,

$$T_2 = \frac{1}{\omega_2} = \frac{1}{2\pi f_2} = \frac{1}{78.5} = 0.0127 \text{ sec} \tag{17}$$

and the corner frequency ω_2 is fixed.

T_3 depends upon the load. The most undesirable situation occurs when a resonance appears in the low frequency range. Although this rarely occurs, it must be considered. If a mass resonates at 25 cps (lowest filter frequency) and exhibits a Q of 25, the one-half bandwidth is

$$\frac{BW}{2} = \frac{f_a}{2Q} = \frac{25}{50} = 0.5 \text{ cps} \tag{18}$$

and

$$T_3 = \frac{1}{\omega_3} = \frac{1}{\pi BW} = \frac{1}{1.57} = 0.637 \text{ sec.} \tag{19}$$

The time constant T_3 depends upon the resonant frequency. For example, if f_a, the resonant frequency, appears at 250 cps, $T_3 = 0.0637$.

Finally, T_1 depends upon the RC time constant of the low-pass filter. This factor can be as low as 2 seconds. However, it must be selected to insure absolute stability as well as the fastest possible response time. A value of $T_1 = 25$ seconds will be arbitrarily chosen.

Eq. 15 can be rewritten:

$$A(s) = \frac{1000}{(1+25s)\left(1+\frac{s}{78.5}\right)^2\left(1+\frac{s}{1.57}\right)} \tag{20}$$

and the Bode diagram drawn as shown in Fig. 14.

Although instability is not indicated in Fig. 14, the worst situation does show that the phase margin is only about 15°. The time constants of the lower frequency loops are compensated to allow for this factor.

Evaluation of the Bode diagram points out some important results. For a system with a fast correction time it is desirable to have a wide band-pass filter with minimum slope. Unfortunately, this precludes good equalization. However, it should be noted that the carrier frequency filter in the system does provide an excellent characteristic when stability criterion is considered. With a 25-cps filter, the break frequency occurs well under the unity gain axis. Furthermore, when the

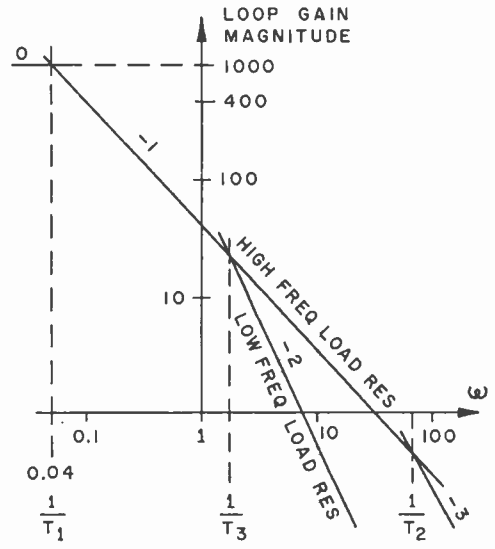

Fig. 14—Bode diagram showing loop gain function of a single control loop.

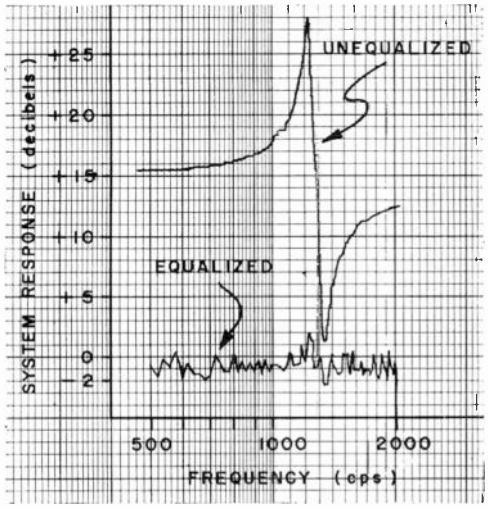

(a)

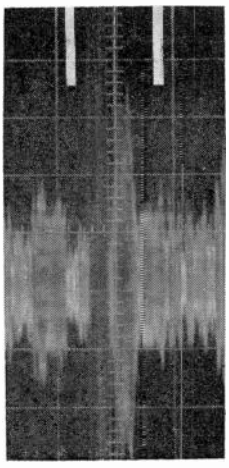

(b)

Fig. 15—(a) Results of automatic compensation with wide-band input. Analyzer BW: 10 cps. (b) Response time of a single channel with 10:1 step change in system gain. Smoothing filter t_c: 10 seconds; sweep: 0.4 sec/cm; correction time: 0.6 second.

control system employs the clamp detector, the system correction time is under 3 seconds for all loops.

Results of Automatic Compensation

Closed loop performance is shown in Fig. 15. One response shows the characteristic of the uncompensated audio system as plotted on an X-Y recorder; the other shows the results of compensation. The equipment was adjusted to produce a flat response. A narrow-band sweeping analyzer incapable of driving an X-Y recorder was used to measure the compensated response, thus, this result is plotted on a point basis.

Physical Equipment

A typical system employing a vibration machine with 10,000 pounds of rms force is shown in Fig. 16. The vibration exciter and power amplifier are clearly shown. Fig. 17 is a photograph of the automatic control system. Fig. 18 shows a typical filter bank and some of the printed circuit transistorized electronics. Approximately 500 transistors are included in the system.

Conclusions

In vibration work a need exists for rapid spectral compensation of an audio system operating with a random noise input. Fulfillment of this need will result in more rapid environmental testing of missile components and systems with simulated random motion.

Compensation using multiple narrow band-pass filters in parallel can be used to control the spectrum provided the filter characteristics are satisfactory. The quality of equalization is dependent upon the narrowness and slope of the filter; the ability to sum the output of all filters is dependent upon the use of a filter with certain characteristics. Proper summation eliminates the problem of signal coherence.

Automatic control provides a means of eliminating setup time completely. This is achieved by simultaneously closing 80 control loops, one for each 25 cps of bandwidth. Performance of the automatic control system depends upon the response time, accuracy, stability, distortion, and ability to measure the filter output.

Use of a clamp detector permits the fastest response time with the lowest RC product. Furthermore, the output of the filter can be measured accurately with components of reasonable size.

Accuracies of ± 1 db with 100:1 variation in system gain is possible using a single transistor compressor circuit.

Distortion generated in the AGC system is eliminated by demodulation and filtering.

Stability depends primarily upon three factors, but with a time constant of less than 25 seconds in the low-

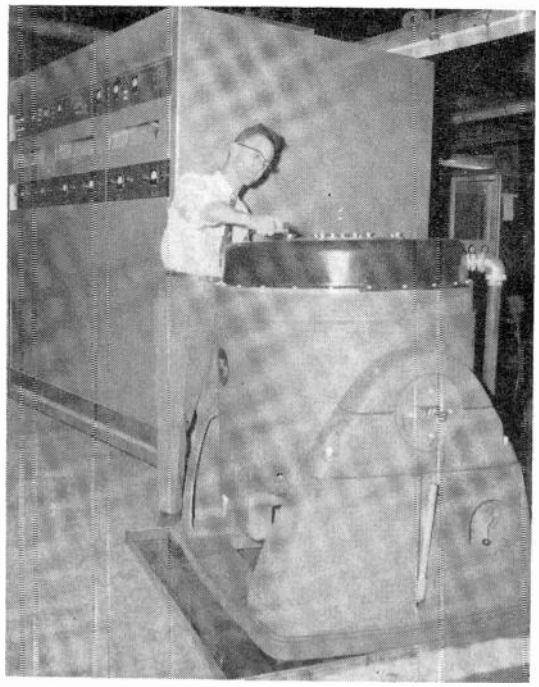

Fig. 16—Audio system consisting of 50 kva power amplifier and 10,000 pounds force vibration exciter.

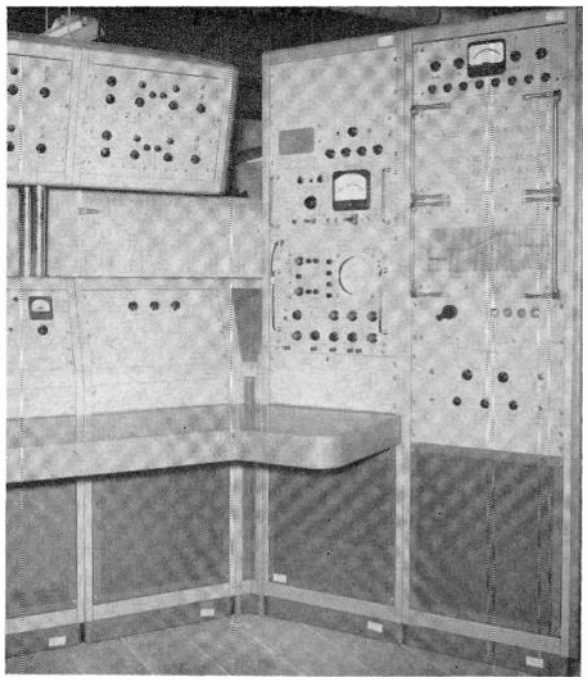

Fig. 17—Section of control console showing operator's controls for shaping the spectrum. The automatic electronic controls are contained within the cabinet.

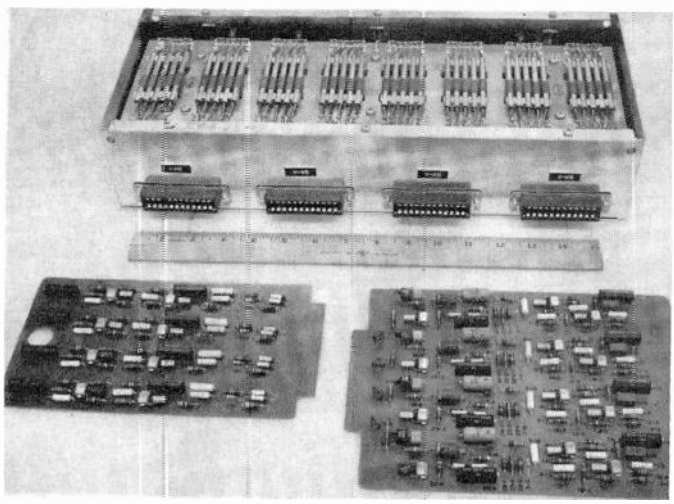

Fig. 18—Components of the control system showing the magnetostrictive filter bank, a 4-channel AGC assembly, and a 4-channel amplifier.

pass filter, the system is stable under all conditions.

Results show that rapid compensation is possible over the range of 20 cps to 2 kc, and that the principle can be extended over the entire audio range to 20 kc.

Preliminary studies show that filters with one-half the present bandwidth will improve the equalization by at least a factor of two. This will enable low frequency resonances in the range of 200 cps to be compensated adequately, thus providing complete frequency coverage. Resonances below 200 cps appear only as a notch if a low impedance power amplifier is used to drive the mechanical transducer. On the other hand, since low frequency resonances are rare, classical peak notch equalizers can be employed to provide additional compensation in those special cases.

Acknowledgment

The author wishes to acknowledge the efforts of Dr. Theron Usher, Assistant Professor of Electrical Engineering, Yale University, New Haven, Conn., who did some of the analysis work in the early stages of the development program. The efforts of the Misses Margaret Mittwollen and Eleanor Melnicsak in the preparation of the manuscript is greatly appreciated.

A New Cardioid-Line Microphone*

ROBERT C. RAMSEY†, MEMBER, IRE

Summary—A new microphone, the Electro-Voice Model 642, is described. Designed particularly for television and motion picture applications where the usable microphone working distance must be a maximum, the model 642 has improved directivity and high sensitivity. The improved directivity is achieved by functioning as a first-order gradient microphone at bass frequencies and as a line microphone at higher frequencies. A detailed description of the directional characteristics is included.

IN television and motion picture applications the distance that a microphone can be used from a sound source is an important limitation on microphone technique. This distance limitation is controlled, in part, by two important characteristics of the microphone being used: directivity and sensitivity.

Assuming a constant sound-pressure source, an increase in microphone working distance normally requires the use of higher gain in the associated amplifying equipment. This higher gain has two undesirable consequences: 1) the ratio of signal-to-system electrical noise deteriorates, and 2) acoustic noise, such as room reverberation, becomes more prominent. At some maximum working distance, either or both of these effects reach an objectionable level. The distance limitation imposed by system electrical noise can be reduced by increasing the sensitivity of the microphone. Distance limitations arising from acoustic noise can be lessened by sharpening the directivity pattern of the microphone. Therefore, to expand the scope of microphone technique by increasing maximum working distance, a microphone of high sensitivity and sharp directivity is required. The Electro-Voice Model 642 Cardiline Microphone, to be described in this paper, possesses these attributes.

Directivity

In applications requiring good directional characteristics, particularly in boom applications, the most popular microphones have been gradient microphones with cardioid or bidirectional polar responses. The polar response of these two types is shown in Fig. 1.

In addition to this plot of polar response, the directional characteristics of these microphones can be described by a ratio called the directivity index. The directivity index of a microphone is the ratio of the energy output from the microphone in a sound field which arrives at the microphone with equal intensity from all directions to the energy output of a nondirectional microphone (with equal axial sensitivity) in the same sound field. The directivity index is a measure of nonaxial response; the lower the directivity index ratio, the narrower the polar response. The directivity index is useful in describing directional characteristics which change with frequency. For example, the directivity index for microphones with bidirectional and cardioid polar response is $\frac{1}{3}$; however, because of baffle effect, the polar response will become narrow at higher frequencies. The plot of directivity index vs frequency for a $1\frac{1}{2}$-inch diameter dynamic gradient microphone with a cardioid polar response is shown in Fig. 2.

A plot of the directivity index for the Electro-Voice Model 642 is also shown in Fig. 2, illustrating the

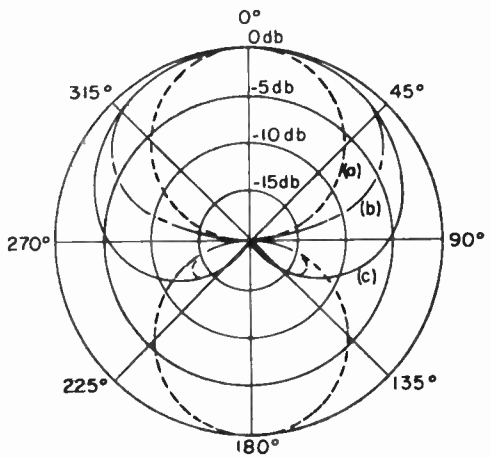

Fig. 1—Polar response of (a) bidirectional response, (b) line microphone at $L=\lambda$, (c) cardioid response.

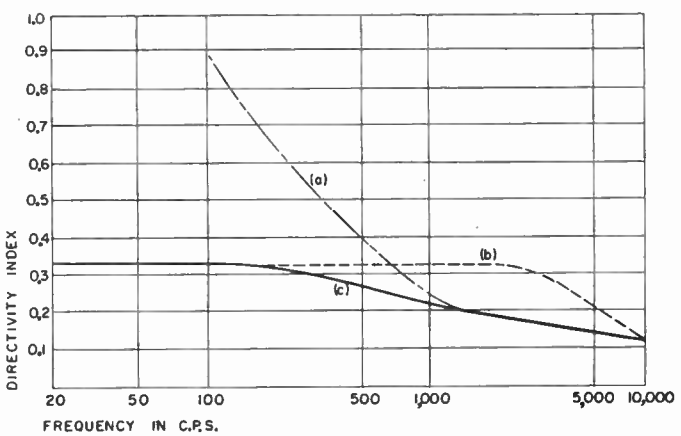

Fig. 2—Plot of directivity index for (a) 11-inch line microphone, (b) gradient microphone, $1\frac{1}{2}$ inches in diameter, with cardioid polar response, (c) Model 642 Cardiline microphone.

* Received by the PGA, February 2, 1960. This paper was presented at the Audio Engineering Society Convention, New York, October, 1959, and is reprinted with permission of the AES.

† Electro-Voice, Inc., Buchanan, Mich.

improved directional characteristic of the microphone. To achieve this improved directivity the Model 642 microphone was designed to function as a line microphone over a substantial portion of its frequency response range.

A schematic drawing of the microphone is shown in Fig. 3. The front opening of the microphone extends along the straight line A, B. All points along this line are equally sensitive; *i.e.*, equal sound pressure at points along this line will cause equal voltages to be produced by the transducer element C. In addition, the points along this line are acoustically connected to the transducer by a common tube D, thereby introducing an acoustic delay between the points on the line and the transducer element.

This equally sensitive line, with variable delay, when placed in a plane-wave sound field will produce wave interference at a common cavity in the transducer element, the amount of interference depending upon the angle (θ) between the plane wave and the axis of the line A, B. The theory and operation of this type of microphone is described by Olson[1] and the equation relating voltage output with θ is

$$R_\theta = \frac{\sin \frac{\pi}{\lambda}(L - L\cos\theta)}{\frac{\pi}{\lambda}(L - L\cos\theta)}, \qquad (1)$$

where R_θ = absolute value of the ratio of the microphone response at the angle θ to the response for $\theta = 0$, L = length of the line, and λ = wavelength. The polar response of a line microphone at $L = \lambda$ is shown in Fig. 1.

As (1) demonstrates, the directivity of a line microphone is a function of frequency. The lower the frequency, the broader the polar pattern. Fig. 2 shows the plot of directivity index vs frequency for a microphone having a line of 11 inches as in the case of the Model 642. This variation in directivity index represents an extreme variation in the response to sounds off the axis. To overcome this objection the Model 642 is designed to function as a first-order gradient microphone at the bass frequencies, and is adjusted to have a cardioid polar pattern at these frequencies. By doing this, the directivity index is limited to a maximum value of $\frac{1}{3}$ (see Fig. 2). A comparison of the directivity of the Model 642 to that of a microphone with cardioid or bidirectional polar response shows that the Model 642 does have improved directivity.

Sensitivity

As mentioned above, the electrical signal-to-noise ratio becomes lower as the distance of the microphone from a sound source is increased. For this reason, microphones used at comparatively large distances from a sound source should have high sensitivity.

To achieve high sensitivity, a large magnetic structure, using an Indox V magnet, was designed for the Model 642. The magnet used is over $2\frac{1}{2}$ inches in diameter and weighs 8 ounces. It was possible to use this large magnet because no baffle effect occurs, the directivity at higher frequencies being controlled by the front opening only. The comparatively large diameter of the magnetic structure permitted the use of a $1\frac{1}{4}$-inch diameter diaphragm and a $\frac{3}{4}$-inch voice coil. These factors combine to give a level of -48 db (reference 0.001 watt, 10 dynes). This is an increase in sensitivity of approximately 7 db over directional microphones in general use today.

Conclusions

In addition to improved directivity and high sensitivity, other features have been incorporated into the Model 642 microphone. To permit the reduction of low-frequency noise and reverberation a two step bass rolloff filter has been included in the design. By means of an external screwdriver adjustment a three-position switch changes the low frequency response of the microphone. Attenuations of 0, 5 or 10 db at 100 cps may be selected. Other features, such as external adjustment of impedance, low hum-pickup sensitivity, and an accessory for shock isolation have been included.

Field tests with the Electro-Voice Model 642 microphone shown in Fig. 4 indicate that the characteristics described here do result in improved performance, including increased microphone working distances and increased separation of sound sources.

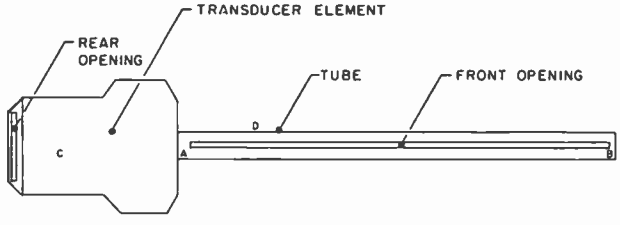

Fig. 3—Schematic drawing of Electro-Voice Model 642 Cardiline microphone.

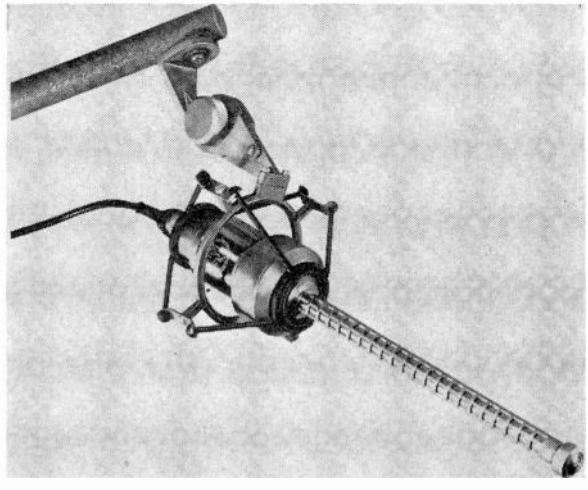

Fig. 4—Electro-Voice Model 642 Cardiline microphone mounted in the Model 356 shock mount.

[1] H. F. Olson, "Elements of Acoustical Engineering," D. Van Nostrand Co., Inc., New York, N. Y.; 1947.

Choice of Base Signals in Speech Signal Analysis*

LADISLAV DOLANSKÝ†, SENIOR MEMBER, IRE

Summary—Fourier series is generally considered to be one of the most basic mathematical tools of the communications engineers; when experimental support is sought for the theoretical conclusions obtained, it has the advantage of having readily available source equipment in the form of sine-wave generators. In many cases, however, due to the characteristics of the signals under study, the analysis into other base functions would result in a reduction of expression complexity and a better insight into the problem. This is demonstrated on a specific example, in which the damped-oscillatory voiced speech sounds are expressed by means of complex-exponential base functions. The method of measuring the pertinent coefficients is given; the nature of the analyzing equipment, which is also used for synthesis, is described briefly, and experimental results, including synthetically obtained approximations of the original signals, are presented.

While speech signals are used to illustrate the method, the latter is applicable to other signals as well.

Introduction

RECENT history shows that in speech signal analysis considerable progress has been made without the benefit of precise mathematical expressions for the speech wave forms. More recently, computers are helping to solve certain quantitative aspects of speech analysis. Nevertheless, in order to make better use of the more theoretical tools of mathematics which are available, it would be desirable to have at least an approximate mathematical expression for speech waveforms under study.

The Problem

The problem considered in this paper is to obtain relatively simple expressions for the waveforms of voiced speech sounds in terms of damped oscillatory base functions. While the base functions form an orthonormal set and their shape is fixed for all sounds, the pertinent multipying factors are to be obtained by a simple measurement.

Theoretical Considerations

Damped Oscillatory Base Functions

In view of the quasi-periodic waveform of voiced sounds, the question arises why some standard method of analysis, such as Fourier expansion, should not be used. There are at least three reasons which make the use of undamped sinusoids for base functions undesirable in the case of voiced-sound waveforms. First, while successive pitch periods resemble each other to a considerable degree, the duration of this quasi-periodic function is limited, and thus, Fourier analysis in terms of the fundamental pitch frequency and its harmonics is not strictly applicable (Fig. 1). Second, because of variation of pitch and volume, successive pitch periods seldom have exactly the same waveform. Finally, from the mechanism of generation of voiced sounds, it is known that a pulse-like excitation, originated by the action of the vocal cords, excites the various resonant cavities of the vocal tract and thus starts a combination of decaying oscillatory functions. Thus, an approximation of these decaying functions by ordinary sinusoids does not appear to be too efficient. This is also indicated by the values of the correlation coefficients in certain typical cases. For instance, the correlation coefficient between two damped exponentials $\exp(s_j t)$ and $\exp(s_k t)$ is equal to [3]

$$r_{jk} = \frac{\int_0^\infty \exp(s_j t)\cdot\exp(\bar{s}_k t)\,dt}{\left\{\int_0^\infty \exp[(s_j+\bar{s}_j)t]\,dt\cdot\int_0^\infty \exp[(s_k+\bar{s}_k)t]\,dt\right\}^{1/2}} \quad (1)$$

$$= \frac{[(s_j+\bar{s}_j)(s_k+\bar{s}_k)]^{1/2}}{s_j+\bar{s}_k}$$

where

$$s_j = -\alpha_j - j\beta_j = \text{complex frequency},$$

$$\bar{s}_j = -\alpha_j + j\beta_j$$

and

$$\alpha_j \geqq 0.$$

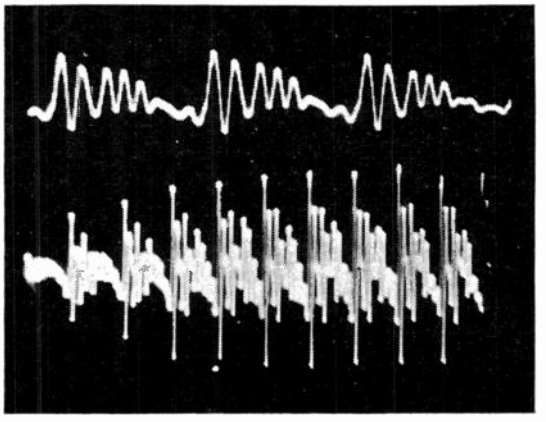

Fig. 1—Waveform of sound *a*. (a) Expanded waveform of the center part. (b) Initial part of the sound.

* Received by the PGA, May 31, 1960. The research reported in this paper has been sponsored by the Geophysics Research Directorate of the Air Force Cambridge Research Center, Air Res. and Dev. Command under Contract No. AF 19(604)-4979.

† Harvard University, Gordon McKay Lab., Cambridge, Mass.

For a sinusoid, $\alpha_j = 0$. Thus, if it is attempted to approximate a damped oscillation by an undamped oscillation, (1) indicates that $r_{jk} = 0$. On the other hand, if a damped oscillation is approximated by another damped oscillation, $\alpha_j > 0$, and $r_{jk} \neq 0$, which indicates that a better approximation may be expected in the latter case.

Using damped oscillatory base functions, the approximation $f_a(t)$ to the given function $f(t)$ becomes

$$f_a(t) = \sum_{i=1}^{n} A_i \exp(s_i t). \tag{2}$$

Other kinds of base functions have been mentioned in the literature. For instance Laguerre functions, which have poles at real values of the complex frequency, have been suggested by Wiener [6]. However, as pointed out by Kautz [4], many problems may be solved more easily with complex poles, because of the greater versatility of damped sinusoids over mere damped real exponentials. This is particularly true in our case because of the nature of the phenomenon considered.

Orthonormality

It has been stated by Huggins [3] that the use of not uncorrelated base functions results in mathematical equations whose solutions are excessively sensitive to slight numerical errors, and that the corresponding instrumentation suffers from the physical counterparts of these same effects. It is therefore most desirable to select base functions which, besides being generated by a process similar to the one which generates the function under study, also form an orthonormal set.

A set of functions which is originally not orthonormal, can be orthonormalized by forming weighted sums of the given functions by adding one of the given functions for each successive base function, $g_i(t)$, and imposing the condition [1]

$$\int_0^\infty g_i(t)\bar{g}_k(t)dt = e_{ik} \tag{3}$$

where

$$e_{ik} = \begin{cases} 1, & i = j \\ 0, & i \neq j \end{cases}.$$

In practice, the use of (3) results in considerable algebra. Therefore, Kautz [4] advanced another method of obtaining the orthonormal base functions, based on the complex convolution theorem of the Laplace transform theory. The method uses the fact that orthonormality can also be stated in the complex-frequency domain and is given by the relation

$$\frac{1}{2\pi j}\int_{-j\infty}^{j\infty} G_i(s)\overline{G}_k(-s)ds = e_{ik}, \tag{4}$$

where $G_i(s)$, $G_k(s)$ are the Laplace transforms of the orthonormal base functions $g_i(t)$, $g_k(t)$. For the case of complex poles, the Kautz method leads to (5) and (6) which define the set of orthonormal functions in the complex frequency domain [5].

$$G_{2n-1}(s) = \sqrt{2\alpha_n}\,\frac{s + |\alpha_n + j\beta_n|}{(s+\alpha_n)^2 + \beta_n^2} \cdot \prod_{j=1}^{n-1} \frac{(s-\alpha_j)^2 + \beta_j^2}{(s+\alpha_j)^2 + \beta_j^2} \tag{5}$$

$$G_{2n}(s) = \sqrt{2\alpha_n}\,\frac{s - |\alpha_n + j\beta_n|}{(s+\alpha_n)^2 + \beta_n^2} \cdot \prod_{j=1}^{n-1} \frac{(s-\alpha_j)^2 + \beta_j^2}{(s+\alpha_j)^2 + \beta_j^2}. \tag{6}$$

That is, networks which have transfer functions of (5) and (6) will produce a set of orthonormal time functions at their output terminals when a unit impulse is connected to their input terminals. For simplicity of design, the critical frequencies of (5) and (6) have been chosen according to (7).

$$s_i = -\alpha_i \mp j\beta_i = i(-\alpha_1 \mp j\beta_1), \quad i = 1, 2, 3, 4, 5, 6, 7. \tag{7}$$

Base functions corresponding to $i \geq 8$ have been omitted in view of the fact that with a choice of $\beta_1/2\pi = 400$ cps, the most important frequency range for voiced speech sounds is reasonably well represented by the set of critical frequencies identified by (7). In view of certain preliminary investigations of speech wave forms,[1] the ratio β_i/α_i was chosen to be

$$\beta_i/\alpha_i = 20. \tag{8}$$

Transformation of the Base Functions into the Time Domain

The expressions of (5) and (6) can be transformed into the corresponding time functions by decomposing the multiple product of fractions into a partial fraction expansion and finding inverse Laplace transforms for the individual fractions which can be obtained readily by standard methods. If $\beta_1/2\pi$ is chosen to be equal to 400 cps and $\beta_1/\alpha_1 = 20$, the first two base functions become

$$g_1(t) = 22e^{-125.7t}\sin(2512t + 0.811) \tag{9}$$

$$g_2(t) = 22.95e^{-125.7t}\sin(2512t + 2.381) \tag{10}$$

where t is the time in seconds. The rest of the orthonormal functions contain these functions as well as similar functions having

$$\alpha_i = i\alpha_1 \tag{11}$$

and

$$\beta_i = i\beta_1 \tag{12}$$

[1] Dolanský [2], p. 17.

with an appropriate multiplying factor for each term. These factors follow from the partial fraction expansion of (5) and (6).[2]

Evaluation of Base Function Factors for a Particular Speech Wave

In order to obtain an approximate expression $f_a(t)$ for a particular speech wave $f(t)$,[3] it is necessary to form an appropriate weighted sum of the base functions

$$f(t) \approx f_a(t)$$

$$= \sum_{i=1}^{n} c_i g_i(t). \tag{13}$$

In other words, it is necessary to find the particular multiplying factor c_i for each base function, which gives the best approximation $f_a(t)$ to $f(t)$. It remains to be shown how these factors can be obtained by measurement.

For orthonormal functions [4], the coefficients of the base functions can be evaluated by means of the relation

$$c_k = \int_0^\infty f_a(t) g_k(t) dt. \tag{14}$$

Now suppose that the signal that we want to approximate is one pitch period of a voiced sound, *i.e.*, let

$$f_a(t) = h(t) \tag{15}$$

where $h(t)$ is the approximate unit-impulse response of the vocal tract, shaped for a particular voiced sound, and can be expressed in terms of the base functions as indicated in (13). Then

$$c_k = \int_0^\infty h(t) g_k(t) dt. \tag{16}$$

Assume that we have a set of filters whose unit impulse responses are the orthonormal, damped oscillatory base functions, and consider the convolution integral

$$v_k(t) = \int_0^\infty e_i(t - u) g_k(u) du \tag{17}$$

where

$v_k(t)$ = output signal of the kth filter at time t,
$g_k(u)$ = unit impulse response of the kth filter,
$e_i(t-u)$ = input signal at time $(t-u)$.

Eq. (17) can be interpreted in physical terms as giving the instantaneous value of the output voltage v_k of the kth filter network which is caused by a continuously varying voltage e_i, connected to the input terminals of the same filter. A partial contribution to the output voltage at time t, caused by a certain value of the input voltage e_i, occurring u seconds earlier, is equal to

$$e_i(t - u) g_k(u) du \tag{18}$$

and if the effects of all past values of e_i are added, the relationship expressed by (17) is obtained.

Now assume that $e_i(t)$ is a particular time function, namely the unit-impulse response of the vocal tract, which has been reversed in time,[4] *i.e.*,

$$e_i(t) = h(-t). \tag{19}$$

Under these conditions,

$$v_k(t) = \int_0^\infty h(u - t) g_k(u) du \tag{20}$$

and

$$v_k(0) = \int_0^\infty h(u) g_k(u) du. \tag{21}$$

It is seen that, except for the variable of integration, (21) is identical to (16), from which the following procedure for measuring the coefficients of the base functions g_k is obtained (see Fig. 2):

1) the transient signal under study (in our case one pitch period of a voiced sound) is recorded;
2) the signal is reversed with respect to time and reproduced;
3) the time-reversed signal is fed into the orthonormal filter set;
4) the voltages at the output terminals of the orthonormal filter at the instant when the time-reversed input signal suddenly ceases[5] are proportional to the desired coefficients.

It should be noticed that, theoretically, $e_i(t)$ must start at $t = -\infty$. However, since $e_i(t)$ is for physical

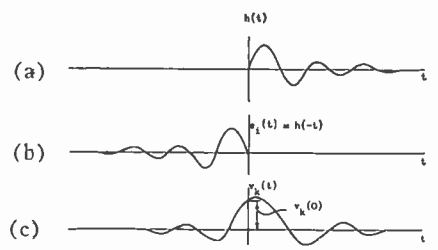

Fig. 2—Transient signal and output of the kth filter. (a) Original transient signal under study (*e.g.*, impulse response of the vocal tract). (b) Same, but reversed in time. (c) Output signal of the kth filter. Note: The instant at which the original transient starts is chosen to be the origin of the time scale t.

[2] A complete list of the fourteen orthonormal base functions thus obtained is given in Dolanský [2], Appendix B, while the pole-zero patterns of the Laplace transforms of (5) and (6) are given in Appendix A.

[3] *E.g.*, for one pitch-period of a particular sound.

[4] *E.g.*, by reversing the direction of a tape recording during playback.

[5] This instant corresponds to the sudden start of the original forward-time transient.

reasons usually negligible for large negative values of t, it is only necessary to choose the beginning of the input at such time t that will make the effect of earlier contributions of $e_i(t)$ to $v_k(0)$ negligible. In practice, the instantaneous voltages $v_k(0)$ were found by measuring the physical size of the instantaneous deflection of one trace of a dual-beam oscilloscope while the other trace of the oscilloscope, displaying $e_i(t)$, was used to identify the instant at which the deflection of the first trace should be read.

Experimental Apparatus

In the preceding section, a four-step procedure for the evaluation of the coefficients of the orthonormal base functions by measurement has been outlined. The apparatus used to perform this procedure will now be described.

Signal Slides

In order to obtain a time-reversed signal of a pitch period of a voiced sound, the microphone signal is first amplified and added to a 500-kc sine wave of suitable magnitude.[6] A Polaroid transparency of such a signal is shown in Fig. 3. This silhouette pattern is then photographically copied onto a high-contrast film. The film copy is used for the reproduction of the original signal in a photoformer.

Photoformer

The block diagram of the photoformer is shown in Fig. 4. The photocell signal, which is the result of the light generated by the oscilloscope beam, is amplified in the vertical amplifiers of both oscilloscopes and deflects the image[7] of the electron beam of the Tektronix oscilloscope toward the edge of the shadow mask. When the edge of the shadow mask is reached, further deflection of the beam is impossible, since the photocell would no longer obtain the light which causes the deflection. The beam therefore stays in a position which causes its image to fall at the edge of the shadow mask. If the beam is deflected in the horizontal direction at the proper speed, a replica of the original signal appears on the faces of both oscilloscopes, and the signal is also reproduced electrically at A (see Fig. 4). If the pattern is reversed, the reproduced signal appears reversed in time. Incidentally, the same oscilloscope camera is used both for the production of the original slide and for the reproduction of the electrical signal from the slide.

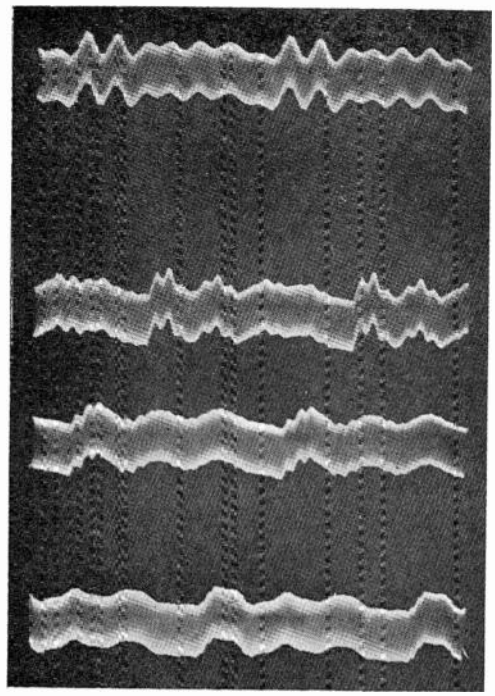

Fig. 3—Photoformer slide.

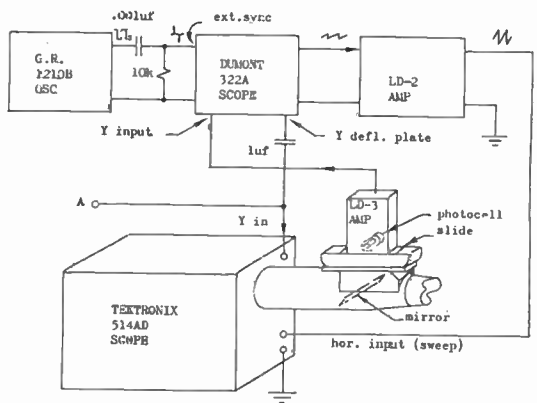

Fig. 4—Photoformer.

In order to establish to what extent the finite size of the electron-beam light spot in the (photographic) recording process affects the frequency response of the photoformer, the latter was measured in two different ways, keeping the sweep time the same in all cases. In Fig. 5, curve a was obtained by recording an even number of periods of a sinusoid of a certain frequency, but using only one half of the total length of the trace during playback. Thus, for a certain *reproduced* frequency f, the recording frequency must be $2f$. Curve b was obtained by recording the frequency which was desired in reproduction but, before reproduction, the size of the film record was photographically reduced 2:1. During reproduction, the length of the trace, the sweep time and the number of sinusoidal periods per sweep are the same in both cases, resulting in the same *reproduced* frequency, but in case b the finite spot of the recording

[6] The exact frequency used here is not critical, but should always be very much higher than the highest frequency component of the speech signal under study. The high-frequency sine wave is added to the signal in order to obtain a shadow pattern in which the dividing line between the illuminated areas is of the same shape as the original signal, while the area on one side of this dividing line is illuminated because of the presence of the high-frequency sine wave.

[7] The image is formed in the plane of the slide. Alternatively, the slide could be placed directly onto the face of the picture tube, but this results in poorer high-frequency reproduction due to the fact that the slide and the phosphor surface are separated by a glass layer of considerable thickness. Thus, even if the illuminated point is directly behind an opaque point, some light may reach the photocell; this results in a poorer high-frequency response.

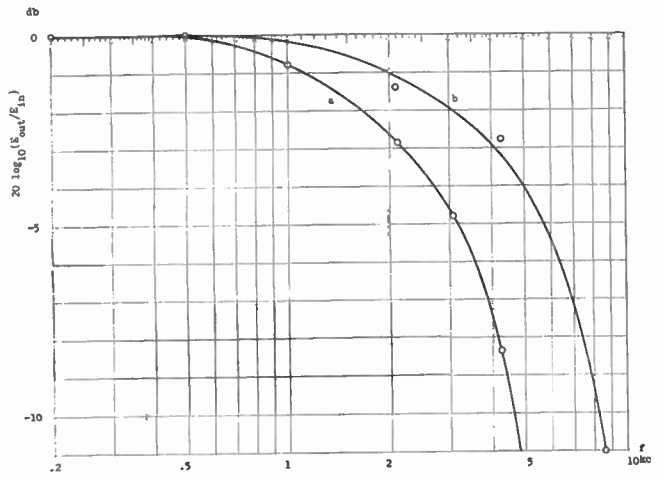

Fig. 5—Photoformer response as a function of the *reproduced* frequency f, (a) when the recorded frequency is divided by two in the playback by sweeping only over one half of the pattern, (b) when the same playback frequency is obtained by reducing a recorded signal photographically by a factor of two.

electron beam is photographically reduced 2:1. Therefore, if the recording spot size is the limiting factor, curve *b* should have a cutoff frequency about twice as high as curve *a*. This is indeed confirmed by the curves of Fig. 5.

By a separate measurement it was established that the phosphor persistence[8] of the CRT screen is not a serious limiting factor in our problem. The measurement simply consisted of increasing the sweep rate of the oscilloscope until the reproduced sinusoidal signal decreased to 70.7 per cent of its original value. For the conditions of curve *a* in Fig. 5, the half-power point was reached at a frequency $f_{co} \approx 12$ kc, and for curve *b*, $f_{co} \approx 24$ kc was obtained.[9]

Orthonormal Filters

Based on the theoretical considerations outlined above, a set of filters, capable of generating the first seven functions defined by (5) and the first seven functions defined by (6) has been constructed. According to (7), seven pairs of critical frequencies s_n, $\bar{s}_n$ are involved. Thus, in the scheme developed, all component filters occur seven times, with the response-controlling elements appropriately scaled according to the critical frequency of the particular filter considered.

The construction of the orthonormal filter set used is indicated in Fig. 6. Three basic blocks, I, II and III are used, together with the gain factors M_{2n-1}, M_{2n}, to obtain the desired response. The circuit diagram of the filters I, II, III for one pair of critical frequencies s_n, $\bar{s}_n$ is given in Fig. 7.[10] The computed phase and amplitude response and the experimentally measured points are shown in Figs. 8–11. The amplitude responses of

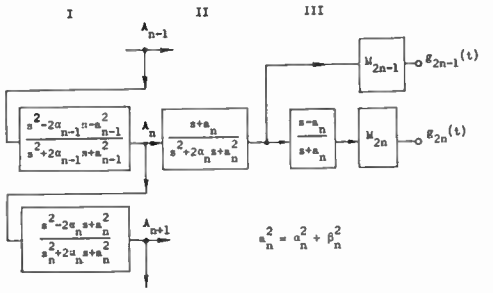

Fig. 6—Orthonormal filter set.

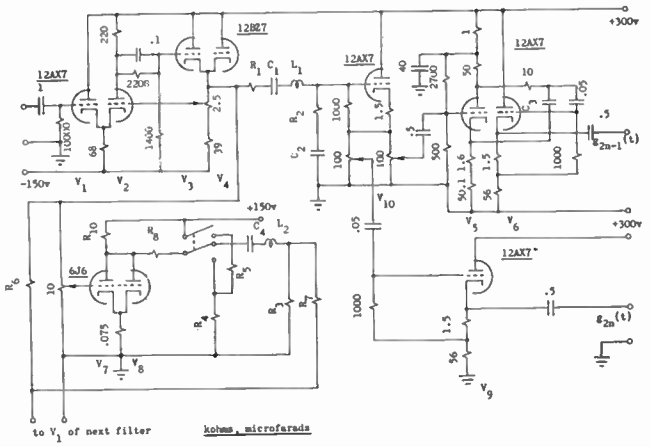

Fig. 7—Circuit diagram for orthonormal filters.

type I and type III filters are not given, since they do not vary with frequency and the deviation of experimental points is only slight. The magnitude response of type II filters deviates somewhat at higher frequencies; this is considered to be unimportant because, in these frequency regions, the relative response of the filters is rather low.

The experimentally obtained impulses are shown in Figs. 12 and 13. It is perhaps somewhat surprising that the sum of the various decaying oscillations gives short trains of sine waves of constant magnitude which suddenly change to a smaller level at regular steps, the spacing between adjacent steps being one period of the lowest-order orthonormal function.

Adding Circuit

While the orthonormal filter set can be used to either generate the orthonormal base functions or to measure the appropriate multipliers of these functions for a particular transient signal under study, some adding circuit capable of forming a weighted sum of the fourteen base functions must be used, if it is desired to reconstruct the original transient signal from the fourteen measured coefficients. The performance of the circuit should be such that the adjustment of one of the coefficients does not affect the remaining coefficients.

The principle of operation of the circuit constructed for this purpose can be explained by means of the basic diagram shown in Fig. 14.

[8] P11 phosphor has been used.

[9] A description of additional experimental equipment used in the photoformer is given in Dolanský [2], ch. V, sec. 1.

[10] More detailed information about the filter circuits can be found in Dolanský [2], ch. V, sec. 3 and Appendix C.

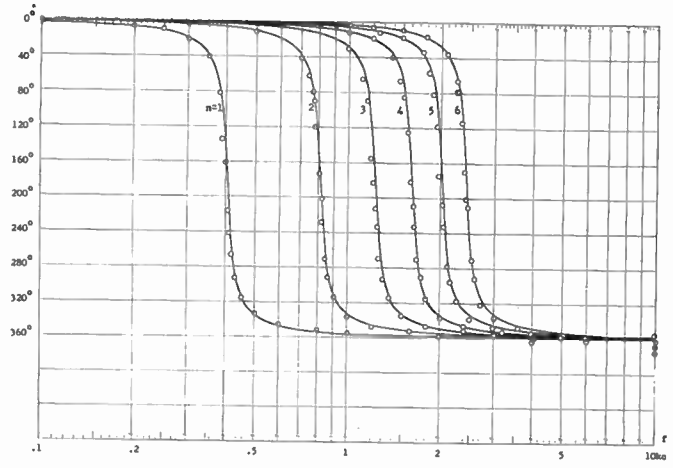

Fig. 8—Phase response of type-I filters.

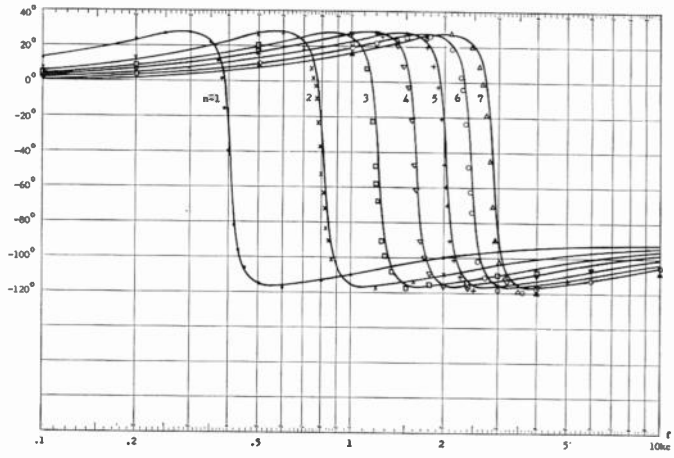

Fig. 9—Phase response of type-II filters.

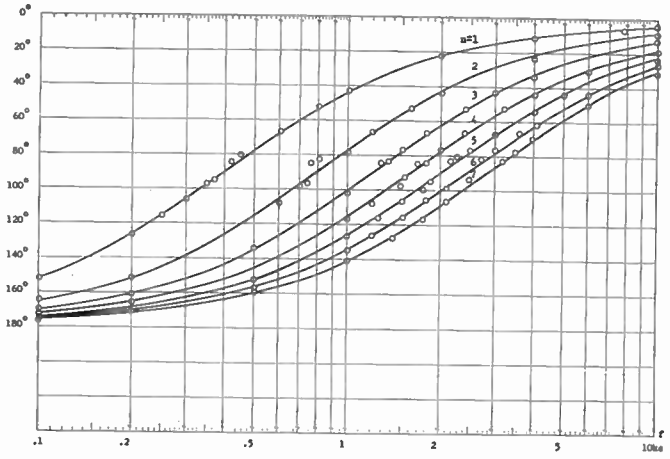

Fig. 10—Phase response of type-III filters.

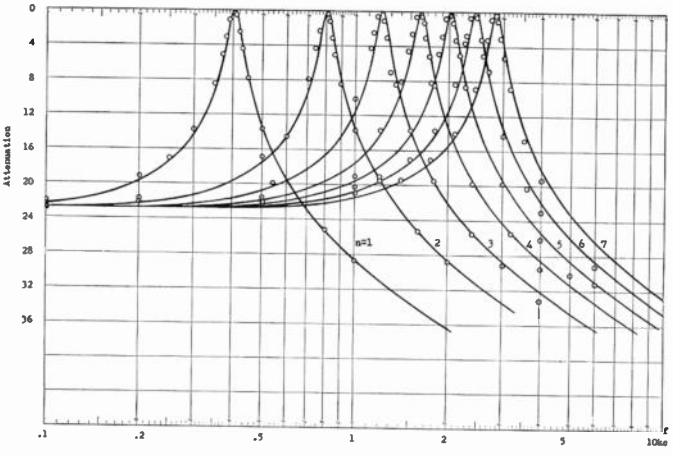

Fig. 11—Magnitude response of type-II filters.

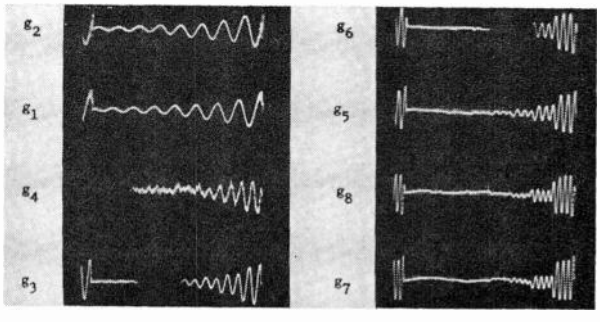

Fig. 12—Unit impulse response of orthonormal filters: $g_1(t)$ to $g_8(t)$. Time increases from right to left. Repetition period 20 msec.

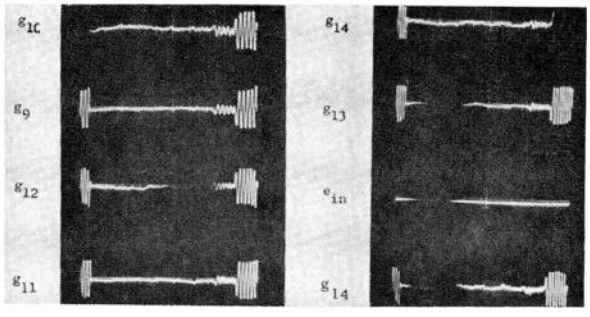

Fig. 13—Unit impulse response of orthonormal filters: $g_9(t)$ to $g_{14}(t)$ and input signal e_{in}. Time increases from right to left. Repetition period 20 msec.

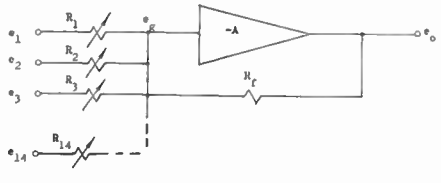

Fig. 14—Basic scheme of adding circuit.

Applying Kirchhoff's current law for the node at the amplifier input, one obtains

$$\sum_{i=1}^{n} \frac{e_i - e_g}{R_i} + \frac{e_o - e_g}{R_f} = 0. \tag{22}$$

Using the relationship between the grid voltage e_g and the output voltage e_o of the amplifier,

$$e_o = - A e_g, \tag{23}$$

(22) can be simplified, for a large gain A, to the relation

$$e_o \approx - R_f \cdot \sum_{i=1}^{n} (e_i/R_i). \tag{24}$$

From (24) it is seen that under these conditions a variation in a particular controlling resistor will affect only the contribution due to the corresponding input voltage e_i, while the effect upon other source voltages will be negligible.

Since each of the constants may have either a positive of a negative sign, two separate adding circuits have been constructed, as shown in Fig. 15. In a particular example, all base functions having multipliers of one sign are added in the same adder. Subsequently, the difference between the positive and negative terms is obtained by means of a difference amplifier. In Fig. 15, V_1 and V_2 represent a cascode amplifier, for which V_3 and V_4 represent a plate load of several megohms. More conventional ways of obtaining the necessary high gain[11] resulted in excessive phase shift which transformed the negative feedback of the circuit into a positive one, thus causing instability.

The degree of the residual mutual dependence of the magnitude-controlling input resistors is indicated by the curves of Fig. 16. Curve *a* represents the output of the adder with the input signal control set for maximum input, while all other inputs are disconnected by means of the switches shown in Fig. 15. Curve *b* indicates the output signal magnitudes obtained for the same input signal as in case *a*, but with all other inputs short-circuited to ground and their control resistors adjusted to their minimum value of 10 kilohms. It is seen that for $0.1 < f < 5$ kc, which includes the range of greatest interest, the signal difference for the two extreme settings is only 0.2 db. Since it is very unlikely that such extreme cases would be encountered, a second resetting of the magnitude controls, after the entire set of them has been adjusted once, should be unnecessary. This has indeed been found to be the case in the practical use of the circuit.

Experimental Analysis and Synthesis of Speech Signals

In order to demonstrate the performance of the orthonormal filters on actual speech signals, a limited

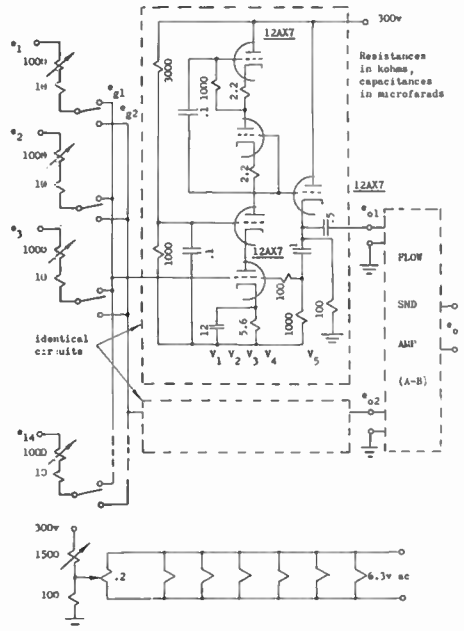

Fig. 15—Adding circuit for orthonormal functions.

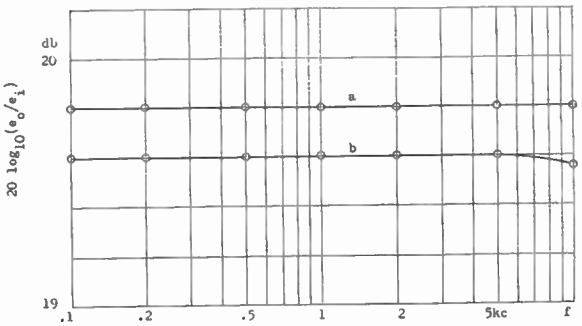

Fig. 16—Response curves of the adding circuit. (a) No loading of grid circuit by other input connections. (b) Maximum loading by other input connections.

number of voiced-phoneme signals was analyzed by means of the filter set.

Coefficient Matrices

As indicated previously (13), the transient under study[12] is approximated by a weighted sum of damped-oscillatory base functions, which are fixed by the choice of the particular elements in the filters. The same base functions are used to approximate the waveform of any voiced phoneme and the various phonemes differ only in the values of the coefficients of the individual base functions. Thus, the essential information identifying phoneme resides in these coefficients alone, and can be expressed, for example, as a row matrix

$$M(i) = [c_1, c_2, \cdots c_{14}], \tag{25}$$

which can also be regarded as a vector in a 14-dimensional signal space.

[11] A gain of about 5000 was considered desirable.

[12] *I.e.*, one pitch period of a voiced phoneme.

Analysis of Speech Sounds

Following the procedure outlined under theoretical considerations, the coefficients c_i of (25) were measured for 25 phoneme samples. These samples consisted of one pitch period of the sounds *i*, ε, *a*, ɔ, *u* as pronounced by five different male speakers. The pitch frequency was held constant at 100 cps. The normalized values of the constants c_i thus obtained were used in the synthesis of speech-sound waveforms described below.

Synthesis of Speech Sounds

In order to show how closely the individual waveforms can be approximated by means of the given base functions, the adding circuit has been used to obtain a weighted sum of these functions. The gain controls for the individual base functions were set to provide multipliers proportional to the constants c_i, obtained in the analysis of the preceding section. The original signal, as obtained from the photoformer, and the signal synthetized from the base functions $g_i(t)$ and from the coefficients c_i are shown in the double oscilloscope traces of Fig. 17. Traces of the same row represent five different sounds pronounced by the same speaker, while all traces of the same column represent the same sound, pronounced by five different speakers. It is seen that for many samples, particularly for all samples of sound *a*, and some samples of sound *i*, ε, and *u*, the synthetic waveform is a very good approximation to the original one. In some other cases, especially for the sound ɔ, the agreement is not quite as good. In the case of these poorer approximations, it was usually difficult to determine the exact location of the beginning of the pitch period, which is essential for the measurement of the constants c_i. It is very likely that with a more accurate determination of the exact beginning of the pitch period, better waveform approximation could be obtained in these cases, too. In the case of the phoneme ɔ, the most prominent oscillation seems to be in the vicinity of 600 cps. Since the closest components of the base functions are 400 cps and 800 cps, this sound may be harder to approximate than other sounds which have a prominent component at either 400 or 800 cps. However, as can be seen from trace *a*, AAP (see Fig. 17), a waveform resembling seven cycles in 10 msec can be obtained using the same base functions.

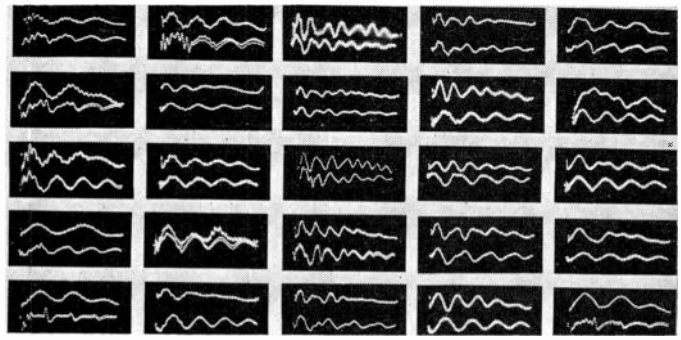

Fig. 17—Original waveforms (upper traces) and reconstructed waveforms (lower traces) of five vowel sounds, spoken by five speakers. Speech sounds (left to right): *i*, ε, *a*, ɔ, *u*. Voices (top to bottom): DWB, JGB, LD, AAP, AZ.

Conclusions and Limitations

In view of the research reported in this paper, the following conclusions and limitations can be stated:

1) Waveforms of voiced speech sounds can be analyzed and synthetized in terms of a small number of orthonormal, damped-oscillatory base functions, multiplied by appropriate coefficients.
2) These coefficients can be obtained by simple measurement.
3) The result of this analysis-synthesis procedure is a simple mathematical expression in closed form, which can be manipulated by standard mathematical procedures available, in contrast to the original microphone signal or oscillograph display to which these powerful methods cannot be applied.
4) The method of analyzing signals in terms of suitable base functions is not limited to speech waveforms. However, in order to obtain a simple result, the base functions should be carefully selected. Frequently, a study of the process which generates the functions may reveal which functions are more suitable than others in a particular problem under study.
5) Only male voices have been used. Because of the shorter pitch period, more residual signal due to the preceding pitch period may perhaps be expected for female voices, although if the attenuation is approximately constant per cycle, comparable conditions to the case of male voices may be obtained.
6) Turbulent components of voiced sounds are neglected. They would probably be entirely eliminated in a reproduced signal.
7) Although the method is in principle applicable also to waveforms of sounds having only turbulent excitation, in practice it would be difficult to a) establish the exact time of each individual random excitation and b) eliminate interference of residual signals due to recent previous excitations, because of the rapid succession of such excitations.
8) In its present form, the method requires a time reversal of the signal and therefore a recording of the signal which results in a delay. While powerful for basic studies of the characteristics of speech, the method in its present form would not be suitable for a continuous processing of speech in a live transmission link.
9) Frequency normalization with respect to some significant frequency parameter has not been carried out. This may be desirable, particularly if the studies are extended to voices of women and children.

ACKNOWLEDGMENT

The author wishes to express his thanks to Dr. D. W. Batteau, who supervised this research, for his continued support during the entire duration of this work. The scientific advice of Professors P. E. LeCorbeiller and W. P. Raney of Harvard University, Cambridge, Mass., was also very much appreciated.

BIBLIOGRAPHY

[1] R. Courant and D. Hilbert, "Methoden der Mathematischen Physik," Springer Verlag, Berlin, Germany, vol. 1, 1924; Interscience Publishers, New York, N. Y., p. 40, 1943.
[2] L. O. Dolanský, "A Novel Method of Speech-Sound Analysis and Synthesis," Ph.D. dissertation, Harvard University, Cambridge, Mass.; January, 1959.
[3] W. H. Huggins, "Representation and Analysis of Signals, Part 1; The Use of Orthogonalized Exponentials," The Johns Hopkins University, Baltimore, Md., Rept. No. AF 19(604)-1941, AFCRC TR-57-357, ASTIA Doc. No. AD 133741, pp. 7 and 15; September, 1957.
[4] W. H. Kautz, "Network Synthesis for Specified Transient Response," Res. Lab. Electronics, Mass. Inst. Tech., Cambridge, Mass., pp. 6, 16 and 21, Tech. Rept. No. 209; April, 1952.
[5] W. H. Kautz, "Transient synthesis in the time domain," IRE TRANS. ON CIRCUIT THEORY, vol. CT-1, pp. 29–39; September, 1954. See p. 31.
[6] N. Wiener, "Extrapolation, Interpolation and Smoothing of Stationary Time Series," John Wiley and Sons, Inc., New York, N. Y., p. 35; 1950.

The Use of Pole-Zero Concepts in Loudspeaker Feedback Compensation*

WILLIAM H. PIERCE†, STUDENT MEMBER, IRE

Summary—**Pole-zero concepts, with the associated techniques of signal flow graphs and root locus plots, are introduced and used in the analysis and synthesis of integrated loudspeaker-amplifier systems in the lower-frequency region. The case of the infinite baffle system is treated in detail, and formulas are developed for general voltage and current feedback. This is then simplified into a design method using only RC elements, and the compensation of the high-efficiency woofer in an undersized enclosure illustrates the method.**

INTRODUCTION

POLE-ZERO concepts are a very powerful synthesis tool for linear systems, and are so powerful for systems that are of the lumped-constant linear type that the design engineer can synthesize a system from specifications in a straightforward analytical procedure.[1] This paper will show how pole-zero concepts can be applied to loudspeaker systems in the lower frequency range where they may be approximated by lumped, linear elements. In addition to the features that make pole-zero concepts so useful in lumped system synthesis, several topics peculiar to loudspeakers will be discussed. The most fundamental is that in the usual loudspeaker system, there is no electrical voltage or current that is proportional to the sound output, and thus there can be no direct feedback of the acoustic output. Other topics will be analytical procedures for handling voltage and current feedback in terms of pole-zero positions, and a simple way of accounting for variable radiation resistance in calculations of frequency response.

Consider a parallel RLC circuit. The differential equation is

$$i = C\frac{de}{dt} + \frac{1}{R}e + \frac{1}{L}\int_{-\infty}^{t} e(\tau)d\tau.$$

In engineering, this is customarily treated as

$$Y = j\omega C + \frac{1}{R} + \frac{1}{j\omega L}$$

or

$$Y = Cs + \frac{1}{R} + \frac{1}{Ls},$$

where s can be considered to be equal to $j\omega$, or to the operator d/dt, or to the complex frequency in e^{st}, or to

* Received by the PGA, February 3, 1960; revised manuscript received, October 17, 1960.
† 14380 Manuella Ave., Los Altos, Calif.
[1] J. G. Truxal, "Automatic Feedback Control System Synthesis," McGraw-Hill Book Co., Inc., New York, N. Y.; 1955.

the variable in the Laplace transform.

$$Z = \frac{1}{Y} = \frac{\frac{1}{C}s}{s^2 + \frac{1}{RC}s + \frac{1}{LC}},$$

$$Z = \frac{\frac{1}{C}s}{\left[s + \frac{1}{2RC} + \sqrt{\frac{1}{(2RC)^2} - \frac{1}{LC}}\right]\left[s + \frac{1}{2RC} - \sqrt{\frac{1}{(2RC)^2} - \frac{1}{LC}}\right]}.$$

When Z is written in its factored form, it is clear that for certain values of complex s, Z approaches infinity in magnitude. These values are called poles, and occur where the denominator goes to zero and the numerator does not. Where the numerator is zero and the denominator is not, Z goes to zero in magnitude, and is said to have a zero. The same terminology is used for all frequency functions, whether they are impedances, admittances, or ratios of quantities at one point to quantities at another point, such as output divided by input. Poles are in fact the natural resonant frequencies of the system.

The frequency response for any complex frequency can be either calculated algebraically or measured graphically when the poles and zeros are known. Fig. 1

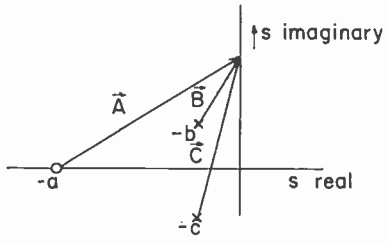

Fig. 1—Vector representation and evaluation in the complex s plane of a rational function in s in terms of poles and zeros.

shows a calculation at frequency s. The response for

$$\frac{s + a}{(s + b)(s + c)}$$

is the vector

$$\frac{A}{BC},$$

which is

$$\frac{|A|}{|B|\,|C|}\,\underline{/A - /B - /C}.$$

Thus, a quick graphical method of evaluating frequency response not only facilitates computation, but gives the designer an intuitive feel for the effects of changing pole and zero locations.

Objectives of Pole-Zero Synthesis

The objective of any synthesis, regardless of method, is to produce a system that is as "good" as possible, or perhaps as "good" as possible using certain elements, powers, or cost. The design engineer interprets this into what will be expected in frequency response, transient response, and power inputs and outputs. With quantitative knowledge of these factors, a desired pole-zero position is chosen, which in general will be a compromise between a desired low-frequency response (which requires poles near the origin), and the need to keep in the linear region of the speaker (which for any fixed power level, requires poles to be away from the origin).

In choosing the pole positions for a simple system of two poles, such as an infinite baffle speaker system, there are two quantities which are chosen. In polar coordinates, they are the distance of the poles from the origin and the angle from the $-s$ axis. In rectangular coordinates, they are the oscillatory frequency (the projection on the imaginary axis) and the decay constant (the projection on the negative s axis). The polar form is often more useful, because the root locus of a simple oscillatory system stays on a circle of constant radius from the origin as the damping is varied from none to critical.

The simplest parameter to adjust electrically is the damping, which will be called zeta, and defined as the cosine of the angle from the $-s$ axis to the poles. Proper damping avoids the extremes of too much, resulting in unnecessarily reduced low-frequency response, and too little, resulting in boominess and other undesirable effects of excessive cone excursion. Looking at the moving cone as a motor-generator whose "back voltage" is proportional to velocity, avoiding excessive damping resistances has the effect of having the current flow in the coil controlled by the cone velocity. This has the additional bonus of bringing nonlinear distortion more under control. For a simple source of R_s,

$$E_m \text{ (mechanical velocity)} = \frac{E_s}{1 + \frac{R_s}{R_m}}.$$

Clearly, low R_s reduces nonlinear effects from R_m.

The amplifier output impedance and the speaker voice coil impedance add in series to form the damping resistance for Z_m, the mechanical circuit. For high flux speakers, the amplifier impedance may be the rated speaker impedance, and optimum damping is still achieved. Low flux speakers would need zero or negative amplifier impedance to produce optimum damping. The use of negative current feedback to achieve the negative output impedance suggests the possibility of using the available magnetic flux for a larger linear region at the expense of flux density. For damping less than critical, changing the value of voice coil plus amplifier resistance keeps the poles on a circle of constant radius at a changing angle.

The radius of the poles of the oscillating system is more difficult to adjust. In the first place the output, the cone velocity, is not available as an electrical quantity. The current flowing in the speaker coil, however, has been "worked over" by the mechanical impedance, and therefore may be used for feedback purposes because it is a function of Z_m. The next section develops formulas and techniques for changing the radius of the poles, which is often (but not exclusively) called the "resonant frequency." For frequencies at which the cone is smaller than a quarter wavelength, the sound power falls off as s^2, where s is the complex frequency.[2] In an amplitude plot, this would be proportional to s, or a single zero at the origin. Thus in the lower-frequency range, the infinite baffle speaker has an output pressure pole-zero position of complex conjugate poles at the speaker resonant frequency and a double zero at the origin (one from the mechanical circuit and one from the unloading of the air). Thus, the pole-zero plot shows the well known fact[3] that flat response is obtainable in a region whose lower bound is at or near the speaker resonant frequency, depending upon the damping, and whose upper bound is determined by the frequency where the cone no longer moves as a unit. The pole-zero plot also gives the design engineer a convenient means to interpret sinusoidal frequency response in terms of pole positions, and also, perhaps more important, to interpret pole positions in terms of desired frequency response. But even while being able to concentrate on sinusoidal frequency response, the complete s-plane pole-zero locations give simultaneous control over transient responses.

In the simple infinite baffle, the designer's only problem is to either change the location of the control poles or to add pairs of poles and zeros. The purpose of this paper is to show how these two alternatives may be employed to avoid the necessity of requiring the mechanical system to be designed so as to achieve the desired pole positions without compensation. Possible advantages of electrical compensation over straight mechanical design are:

1) Adjustability. Speaker resonance and damping could be adjusted to suit the user's room acoustics and tastes, and even power levels.
2) Use of standard high-efficiency speakers in small cabinets.
3) Reapportionment of gap flux. Amplifiers with negative output impedances could dampen speakers with weak magnetic flux, thus enabling the size of the linear flux gap to be increased.

Considerations in the choice of pole-zero positions are those of any loudspeaker design. Power handling capacity and the lowness of resonance must be chosen in a mutual compromise. The damping factor, zeta, defined previously, will generally vary from 0.7 to 0.5. A ratio of 0.7 would have a step response overshoot of 5 per cent, while 0.5 would have 18 per cent. The ratio of 0.5 would produce an approximately level frequency response down to the resonant frequency, and then fall off at 12 db per octave.

Pole-Zero Synthesis Procedure

Pole-zero synthesis begins with the development of a formula for the cone velocity divided by electrical input to the amplifier. Consider a system which has a preamplifier with transfer function P, a power amplifier with transfer function G, an amplifier output impedance Z_a, voltage feedback beta, current feedback alpha, and a loudspeaker load. This is shown in Fig. 2. Any transfer quantity such as P, beta, etc., may actually be a ratio of polynomials in s. The signal flow graph of this is shown in Fig. 3.

Standard procedures for obtaining transfer functions give

$$\frac{E}{E_1} = \frac{PG}{1 + G\left[-\beta - \frac{\alpha}{Z_m} - \frac{\beta Z_v}{Z_m}\right] + \frac{Z_a}{Z_m} + \frac{Z_v}{Z_m}}.$$

This formula gives the piston velocity in terms of input voltage, and with proper choice of the constants any transfer function could be realized. However, the formula gives too much freedom to be immediately useful. We may redraw the graph as shown in Fig. 4(a). Let the transfer function of the part inside the dotted box be G', where

$$G' = \frac{G}{1 - G\beta}.$$

Thus, Fig. 4(b) shows the simplified amplifier-speaker combination as it is normally considered.

One form of the general equation for E, the output

[2] H. Olson, "Acoustical Engineering," D. Van Nostrand, Co., Inc., Princeton, N. J., p. 92; 1957.
[3] *Ibid.*, p. 149.

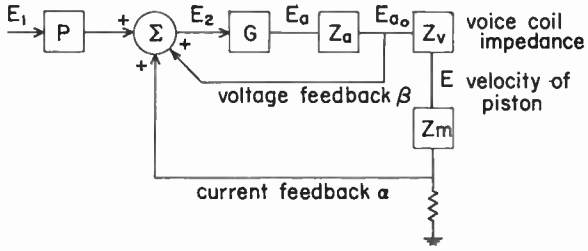

Fig. 2—Diagram of amplifier and speaker.

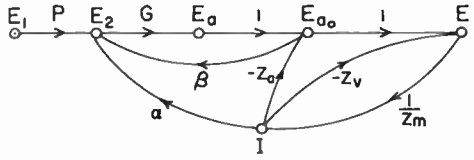

Fig. 3—Signal flow graph for Fig. 2.

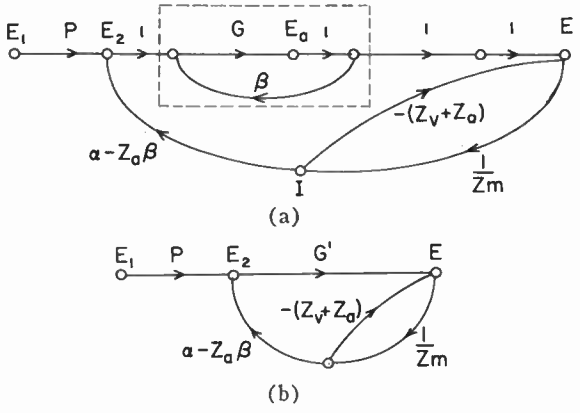

Fig. 4—Simplification of the signal flow graph.

cone velocity, is

$$E = E_1PG' \frac{Z_m}{Z_m + Z_v + Z_a(1 + G'\beta) - G'\alpha}.$$

This form of the equation suggests a voltage generator of E_1PG' and impedance $Z_v+Z_a(1+G'\beta)-G'\alpha$ driving the load Z_m. Now we restrict the analysis to an infinite baffle. Then, the output pressure would have an additional factor proportional to s due to unloading at the frequencies where the cone diameter is less than a quarter wavelength.

The formula for the output velocity has now been put in a form showing the source impedance that the mechanical circuit sees. If this source impedance is purely resistive, then it is simply adjusted to give optimum damping. If it includes reactance, however, it must be put in a form so that the relation of the source impedance to the output function—in terms of poles and zeros—can be controlled by the designer. The form to be used is simply the form of a root locus diagram for a unity feedback system, that is,

$$\frac{Ap_1(s)}{p_2(s) + Ap_1(s)},$$

where $p_1(s)$ and $p_2(s)$ are polynomials in s. Let

$$Z_m = K_1 \frac{n_1}{d_1}$$

$$Z_v + Z_a(1 + G'\beta) - \alpha G' = K_2 \frac{n_2}{d_2}$$

where n_1, n_2, d_1, d_2 are polynomials. Then

$$E = [PG'E_1]\left[\frac{\left(\frac{K_1}{K_2}\right) n_1 d_2}{n_2 d_1 + \left(\frac{K_1}{K_2}\right) n_1 d_2}\right].$$

This is a second form of the output velocity formula, but now it is in the form of two factors, the first being the feed forward term, and the second showing the impedance dividing effect. It should be noted that the formula is completely general within the lumped element category, and that the second term is in the exact form required for root locus analysis.

Now that a general formula has been developed in useable form, it may be inquired whether any special cases may prove useful. Since resistance-capacitance circuits are usually the most practical, we are led to investigate the simplest such circuit, namely of one of the form

$$\frac{n_2}{d_2} = \frac{s + s_1}{s + s_2}.$$

Evaluating Z_m from a simple electromechanical equivalent circuit[4] we have

$$Z_m = K_1 \frac{n_1}{d_1} = \frac{L_m s}{C_m L_m s^2 + G_m L_m s + 1}.$$

Now for convenience, normalize to unit angular frequency and change other variables as follows:

$$s^2 L_m C_m = \frac{s^2}{\omega_0^2} = p^2$$

$$K = \frac{L_m \omega_0}{K_2} \qquad \frac{n_2}{d_2} = \frac{p + a}{p + b}$$

$$L_m \omega_0 G_m = 2\zeta_0.$$

We then get

$$\frac{E}{E_1PG'} = \frac{Kp(p + b)}{(p + a)(p^2 + 2\zeta_0 p + 1) + Kp(p + b)}.$$

This formula is suggested for use in a design procedure in which the parameters K, a, and b are chosen to move the control poles to the desired position. Various values of a and b would be chosen, and then the root

[4] L. Beranek, "Acoustics," McGraw-Hill Book Co., Inc., New York, N. Y., ch. 3; 1954. The Z_m used here is that seen by the electrical circuit, namely the type in which mechanical force is analogous to electrical current and referred to the electrical terminals. In Beranek's terms, this is the mobility analogy.

locus plotted as a function of K. However, note that this process introduces a zero at $-b$, and a pole which originated at $-a$ but moved down the $-s$ axis because of the "feedback" K. The unwanted pole and zero can easily be cancelled by a simple RC bass boost circuit in P. A further simplification occurs when the speaker mechanical damping is much less than the electrical damping, when ζ_0 can be considered to be zero.

Synthesis Example

The speaker to be compensated is a Jensen P-12 NL 12-inch woofer, with a $1\frac{3}{4}$-pound permanent magnet. This woofer was furnished by the Jensen Company, and the author is grateful to the Jensen Company for their assistance. The speaker is of the high-efficiency type, intended for use in a large enclosure. It was mounted in a closed, padded box with an internal volume of about 2.2 cubic feet. The equivalent circuit for the mounted speaker was measured as indicated in Fig. 5.

In this case, the object is to select current feedback in order to reduce the resonant frequency of the speaker from 84.5 cps to about 50 to 55 cps with a zeta of about 0.5. This is an equivalent requirement to the conventional statement of flat frequency response to 50 cps. In order to bring the poles in toward the origin, the value of b will be less than the value of a. Neglecting the slight damping already present, and normalizing to

$$p = \frac{s}{2\pi(84.5)},$$

we select

$$\frac{n_2}{d_2} = \frac{p + \frac{1}{2}}{p + 1}$$

as a trial. The root locus of

$$G = \frac{Kp(p + \frac{1}{2})}{(p + 1)(p^2 + 1)}$$

is plotted in Fig. 6. A value $K = 2.17$ is seen to give a zeta of 0.53, and ω_n of 0.632, which is 53.4 cps unnormalized. (In construction of a third order root locus, it is convenient to assume a particular value for the root that is known to be on the real axis, thus in effect assuming an exact factor. Dividing by this exact factor gives a simple equation for K which comes from forcing the remainder to be zero. It also gives, of course, a quadratic for the other two roots.)

This point on the root locus is a satisfactory one, in that the complex poles have been moved to their desired position, but at the expense of inserting an unwanted zero at $p = -\frac{1}{2}$ (*i.e.*, $s = -265$) and an unwanted pole, which has moved to $p = -2\frac{1}{2}$ (*i.e.*, $s = -1330$). These will be eliminated by making

$$P = (\text{constant})\frac{s + 1330}{s + 265}.$$

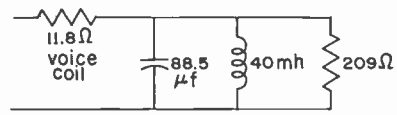

Fig. 5—Equivalent circuit, referred to electrical terminals, of woofer mounted in 2.2 cubic foot sealed enclosure.

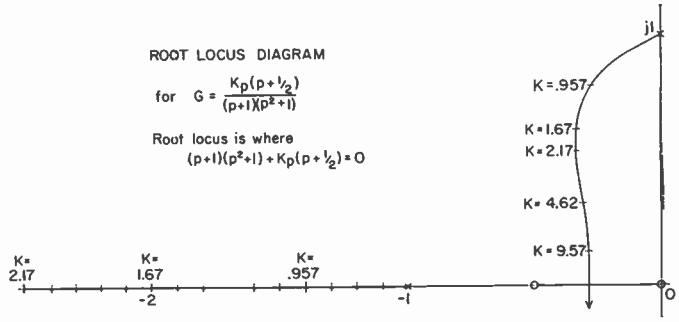

Fig. 6—Root locus diagram used in example.

The current feedback is found as follows: From the root locus of

$$\frac{E}{E_1PG'} = \frac{Kp(p + b)}{(p + a)(p^2 + 1) + Kp(p + b)},$$

the values were selected for a, b, K.

$$a = 1$$

$$b = \tfrac{1}{2}$$

$$K = 2.17$$

$$K = 2.17 = \frac{L_m\omega_0}{K_2} = \frac{40 \times 10^{-3} \times 2\pi(84.5)}{K_2}$$

$$K_2\frac{n_2}{d_2} = 9.80\frac{s + 531}{s + 265} = Z_v + Z_a(1 + G'\beta) - \alpha G'.$$

$$Z_v + Z_a(1 + G'\beta)$$

is the impedance of the voice coil plus the impedance of the amplifier after voltage feedback, and is taken to be 13 ohms.

$$\alpha G' = 13 - 9.80\frac{(s + 531)}{s + 265}$$

$$\alpha G' = 3.20\frac{(s - 550)}{s + 265}.$$

This current feedback could be achieved in a circuit such as shown in Fig. 7.

In the example chosen, the amplifier closed-loop gain is 25.3, and the calculated values are $R_1 = 0.15\ \Omega$, $R_2 = 0.24\ \Omega$, $R_3 = 37.6\ \Omega$, $C = 100\ \mu$f. The amplifier was compensated with the above current feedback, and as noted, the necessary RC compensation was added before the feedback loop. Subjective evaluation of the compensated system was made difficult by excessive reverberations in the author's apartment. The improvement seemed quite noticeable but not really

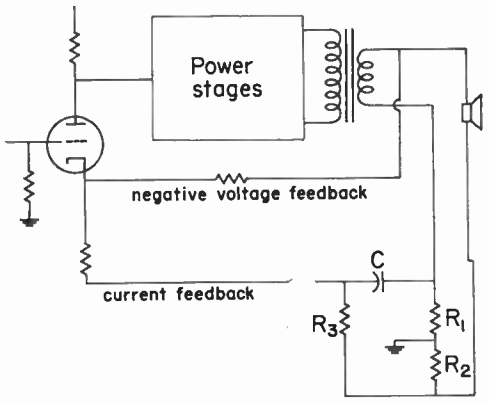

Fig. 7—Arrangement for current feedback in example in the text.

radical. Theoretically, it would correspond to using a truly infinite baffle and amplifier damping such as to give zeta of 0.5.

The actual output sound pressure was deduced from voltages measured across the speaker by the following procedure. Refer again to Fig. 2 and note that the cone velocity E is related to the voltage across the speaker terminals E_{a_0} by

$$\frac{E}{E_{a_0}} = \frac{Z_m}{Z_m + Z_v}.$$

As previously noted for infinite baffles, the sound pressure amplitude is proportional to $1/s$ times the cone velocity in the low frequency region, so that

$$\frac{\text{sound pressure output}}{\text{voltage across speaker terminals}} = (\text{constant})\,\frac{Z_m}{s(Z_m + Z_v)}.$$

Using the vector method of Fig. 1, the above formula was used to determine the necessary relative voltage as a function of frequency for flat response from the woofer. The function calculated is the dashed line shown in Fig. 8. For comparison, the relative voltage actually obtained across the speaker terminals from the compensated amplifier is also shown in Fig. 8. This voltage function indicates that rather precise compensation has in fact been achieved.

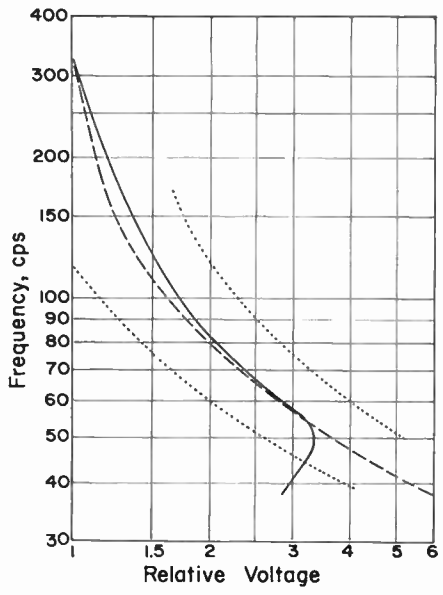

Fig. 8—Relative voltages at speaker terminals. Dashed line: voltage for flat response calculated from equivalent circuit. Solid line: measured voltage from compensated amplifier. Dotted lines: ±3 db points from dashed line.

General Remarks and Conclusions

The importance of the pole-zero method of design lies primarily in the simplicity in which quantitative control is obtained in design while simultaneously enhancing an intuitive feel for what the equations mean. By using pole-zero concepts, current feedback was introduced naturally and analytically in this paper, and by using this theoretical tool, results were predicted and obtained with simple RC circuits which match the results obtained by previous workers using RLC circuits empirically[5] or using impedance concepts and *a priori* knowledge of the impedance desired.[6] Besides getting current feedback into an analytical status, it is hoped that this paper will stimulate further applications in which the speaker and amplifier form an integrated system.

There is really no need for the cabinet size to necessarily stop at 2.2 or 1.7 cubic feet for high-quality bass. If current feedback can reduce the cabinet size to 2.2 cubic feet, and if high mechanical compliance can do the same, what could be done with the two together? And with power transistors available and relatively immune to mechanical vibration, why not put the amplifier in the speaker cabinet? There is another topic suggested but not fully answered by this paper, namely the use of current feedback to help control distortion.

This paper has only been an introduction, for it treats only the infinite baffle, which we saw involved a total of three poles if its resonant frequency was to be changed. A bass reflex could be similarily treated, but its own four poles plus the compensating poles would involve considerable rather complex analysis. However, the success of the bass reflex enclosure indicates that the results may be well worth the analysis.

At present, integration of the speaker and amplifier is not very extensive, with control of the damping being the only widespread example. But the cost, size, weight, and flexibility of electronic elements make it possible that not too far in the future the design engineer may be faced by such decisions as whether to add another stage of amplification, or whether instead to make the speaker enclosure one cubic foot larger.

[5] H. D. Zink and L. R. Sanford, "A new look at positive current feedback," *Radio and TV News*, vol. 58, p. 56; November, 1957.

[6] R. E. Werner, "Loudspeakers and negative impedances," IRE Trans. on Audio, vol. AU-6, pp. 83–89; July–August, 1958.

Correspondence

Amplitude Limitations in Nonlinear Distortion Correction*

Waldhauer, in a recent note,[1] has shown that it is possible to achieve perfect distortion correction, provided that the two amplifiers of his Fig. 2 have zero and infiinte output impedances. Pritchard and Macdonald have pointed out[2] that in practice, amplifiers cannot be designed to have zero and infinite output impedances, and hence conclude that "perfect nonlinear distortion correction over an indefinitely large input amplitude range is impossible." It would appear, however, that it is theoretically possible to achieve perfect nonlinear distortion correction over amplitude ranges which are limited only by the considerations outlined below.

Consider Fig. 1, in which B is the amplifier to be corrected and A is the correcting network. The input voltage is e_0 and the output voltage is e_2.

If the transfer characteristic of B is given by

$$e_2 = \sum_{n=1}^{\infty} b_n e_1^n,$$

then, in order to make the system linear, a predistortion network having the transfer characteristic

$$e_0 = \sum_{n=1}^{\infty} a_n e_1^n$$

must be used. The ratio of the output voltage to the input voltage is then given by

$$\frac{e_2}{e_0} = \frac{\sum_{n=1}^{\infty} b_n e_1^n}{\sum_{n=1}^{\infty} a_n e_1^n}.$$

* Received by the PGA, September 16, 1960.

[1] F. D. Waldhauer, "Comments on 'Nonlinear distortion reduction by complementary distortion'" (Correspondence), IRE TRANS. ON AUDIO, vol. AU-8, p. 103; May–June, 1960.

[2] J. R. Macdonald, "Reply to comments on 'Nonlinear distortion reduction by complementary distortion'" (Correspondence), IRE TRANS. ON AUDIO, vol. AU-8, pp. 104–105; May–June, 1960.

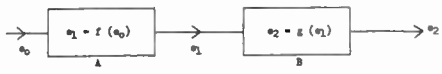

Fig. 1.

Fig. 2.

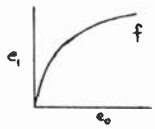

Fig. 3.

For linear amplification, the a coefficients must be equal to a constant times the b coefficients where the reciprocal of the constant is the voltage gain of the system shown in Fig. 1. If the voltage gain is k[1] and $a_n = kb_n$, then it follows that:

$$\frac{e_2}{e_0} = \frac{\sum_{n=1}^{\infty} b_n e_1^n}{k \sum_{n=1}^{\infty} b_n e_1^n} = \frac{1}{k} = k^1$$

and hence linear amplification results.

To see that this is possible practically, consider an amplifier B, possessing only second harmonic distortion as shown in Fig. 2. To achieve linear amplification, a predistortion network of the form $e_0 = k(b_1 e_1 + b_2 e_1^2)$ must be used. If $k = 1$, then $e_0 = b_1 e_1 + b_2 e_1^2$ (see Fig. 3). The system is now linear with a voltage gain of 1.

Note that f is the inverse function of g. Thus, if the transfer function g of an amplifier is known, then the required correcting transfer function f is merely the inverse of g. The problem that remains is one of synthesizing the required transfer function f over the signal range desired.

One possible solution to this problem lies in the use of three-terminal varistor-resistor networks[3] as interstage coupling devices.

The amplitude range over which an amplifier may be corrected by the use of passive nonlinear networks is limited by the following factors:

1) The maximum ratings of the amplifier and the associated nonlinear networks from the point of view of temperature rise.
2) The minimum permissible gain of the corrected amplifier. Thus if an attempt is made to correct a vacuum tube stage for amplitude ranges approaching cutoff, by means of passive nonlinear devices, the resultant corrected amplifier may well provide an intolerably low value of gain.
3) The onset of a discontinuity in the transfer characteristic of the uncorrected amplifier such as grid current in a vacuum-tube amplifier or collector bottoming in a transistor amplifier. Such discontinuities cannot be readily corrected by reasonably simple varistor-resistor combinations.

G. W. HOLBROOK
E. P. TODOSIEV
Dept. of Elec. Engrg.
Royal Military College of Canada
Kingston, Ont., Canada

[3] G. W. Holbrook, "Reducing amplifier distortion," *Electronic Tech.*, vol. 37, pp. 13–20; January, 1960.

Contributors

John H. Caldwell was born on February 26, 1924, in Sydney, New South Wales, Australia. He received the B.S. degree in 1950 and the B.E.E. degree with honors in 1952, both from Sydney University, Sydney.

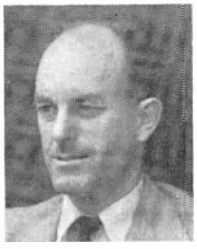

J. H. CALDWELL

In 1942 he joined the Royal Australian Air Force. After completing his academic studies, he rejoined the Air Force in 1950 as a technical officer. In November, 1954, he became lecturer in electrical engineering at the Newcastle University College of the University of New South Wales, Hamilton. His present research interests are in transistor applications.

Mr. Caldwell is an associate member of the IEE.

❖

Ladislav Dolanský (SM'53) was born in Vienna, Austria on May 6, 1919. In 1946, he received the Ing. degree in electrical engineering from the Institute of High Technical Learning in Prague, Czechoslovakia. In 1949, he received the M.S. degree and in 1952, the E.E. degree in electrical communications, both from the Massachusetts Institute of Technology, Cambridge, Mass. In 1959, he received the Ph.D. degree in applied physics at Harvard University, Cambridge, Mass.

L. DOLANSKÝ

From 1942 to 1945, he worked with Radiotechna, a.s. (a subsidiary of Siemens u. Halske, A.G.) in Přelouč, Czechoslovakia. In 1945, he joined the teaching staff of the Institute of High Technical Learning in Prague. He was associated with the Research Laboratory of Electronics at the Massachusetts Institute of Technology from 1947 to 1952, working on research problems in magnetic tape recording, pulse code modulation, frequency modulation and television.

Since 1952, he has been working with the Electronics Research Project at Northeastern University on problems related to visual message presentation, speech analysis, and more recently, on mathematical techniques for complex systems. From 1958 to 1960 he was also associated with the Gordon McKay Laboratory, Harvard University, Cambridge, Mass.

Dr. Dolanský is a member of the Acoustical Society of America, AIEE, Eta Kappa Nu, Tau Beta Pi and Sigma Xi.

❖

Charles E. Maki (S'50–A'52–M'53) was born in Virginia, Minn., on January 28, 1928. He received the B.S.E.E. degree in 1951 from the Massachusetts Institute of Technology, Cambridge.

C. E. MAKI

From 1951 to 1954 he was with the Sandia Corporation, Albuquerque, N. M. In 1954 he joined MB Electronics in New Haven, Conn., and also studied at Yale University, New Haven, receiving the M.E.E. degree in 1959. At present he is chief development engineer at MB responsible for the development of accessories and systems.

Mr. Maki is a member of the Acoustical Society of America, Tau Beta Pi and Sigma Xi.

❖

William H. Pierce (S'59) was born in Washington, D. C., on July 10, 1933. He received the B.A. degree in physics from Harvard University, Cambridge, Mass., in 1955.

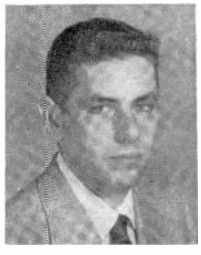

W. H. PIERCE

From 1955 to 1958 he served as an officer in the Atlantic Fleet destroyer force. Since 1958 he has been a student in the Electrical Engineering Department at Stanford University, Stanford, Calif., where he received the M.S. degree in 1959. Although primarily interested in systems theory, he is also interested in audio collaterally with an interest in music.

Mr. Pierce is currently a National Science Foundation fellow studying for the doctorate degree, with a thesis topic on redundancy in digital systems.

❖

Robert Ramsey (S'49–A'50–M'55) was born in Cedar Rapids, Iowa, on August 31, 1924. In 1949 he received the B.S. degree from Iowa State College, Ames, Iowa.

R. C. RAMSEY

From 1949 to 1954, Mr. Ramsey worked for television station WOC-TV in Davenport, Iowa. Since 1954, he has been employed at Electro-Voice, Inc., Buchanan, Michigan, as a design engineer in loudspeakers and microphones. Currently, he is Chief Microphone Engineer.

Mr. Ramsey is a member of ASA, Tau Beta Pi and Eta Kappa Nu.

❖

Werner Steiger (M'58–SM'60) was born in Zurich, Switzerland, on August 2, 1926. He received the Dipl.Ing. degree in electrical engineering from the Swiss Federal Institute of Technology, Zurich, in 1949.

W. STEIGER

From 1950 to 1951, he was with Mullard Ltd., Mitcham, England, engaged in work on television receivers. From 1951 to 1956, he worked for Schindler Ltd., St. Gallen, Switzerland, in the Department for Industrial Electronics, where he was responsible for research and development. He was with International Harvester Company, Fort Wayne, Ind., designing transistorized test equipment, from 1956 to 1957. From 1957 to 1958, at the Applied Science Corporation, Princeton, N. J., he designed telemeter transistor circuitry. Since 1958, he has been with Hughes Semiconductor Division, Newport Beach, Calif., where he heads the Advanced Applications Section, dealing with semiconductor circuit design and analysis.

Mr. Steiger is a graduate member of the IEE.

Index
to
IRE Transactions
on
Audio
Volume Au-8, 1960

IRE Professional Group on Audio Combined Index for 1960

Compiled by D. W. Martin

Classification of Subjects

1. IRE-PGA
   - 1.1 General
   - 1.2 Constitution and By-Laws
   - 1.3 National and Regional Meetings
   - 1.4 Chapters
   - 1.5 Membership
   - 1.6 Transactions
   - 1.7 People
2. Bibliographies, Reviews, Standards, Tapescripts
   - 2.1 Bibliographies
   - 2.2 Reviews
   - 2.3 Standards
   - 2.4 Tapescripts
3. Sound Systems
   - 3.1 General
   - 3.2 Stereophonic, Binaural, and Spatial Effects
   - 3.3 Military
4. Microphones
   - 4.1 General
   - 4.2 Condenser
   - 4.3 Magnetic
   - 4.4 Crystal
   - 4.5 Moving-Coil
   - 4.6 Ribbon
   - 4.9 Special Microphones
5. Amplifiers
   - 5.1 General
   - 5.2 Preamplifiers and Voltage Amplifiers
   - 5.3 Power Amplifiers
   - 5.4 Frequency-Range Dividing Networks
   - 5.5 Transistorized Amplifiers
   - 5.6 Filters
   - 5.9 Special Amplifiers
6. Loudspeakers
   - 6.1 General
   - 6.2 Direct-Radiator Units
   - 6.3 Horn-Driver Units
   - 6.4 Horns, Enclosures, Baffles
   - 6.9 Special Types
7. Disk Recording and Reproduction
   - 7.1 General
   - 7.2 Disks
   - 7.3 Recording
   - 7.4 Pickups and Tone Arms
   - 7.5 Pre-Emphasis and Postequalization
   - 7.9 Special Mechanical Recorders
8. Magnetic Recording and Reproduction
   - 8.1 General
   - 8.2 Tape and Wire
   - 8.3 Recording and Erasing
   - 8.4 Playback
   - 8.5 Pre-Emphasis and Postequalization
   - 8.9 Special Magnetic Recorders
9. Acoustics
   - 9.1 General
   - 9.2 Room Acoustics
   - 9.3 Sound Waves and Vibrations
   - 9.4 Speech
   - 9.5 Music
   - 9.6 Hearing
   - 9.7 Psychoacoustics
10. Broadcast Audio
11. Audio Measuring Equipment and Techniques
12. Electronic Musical Instruments

TRANSACTIONS OF THE IRE CONTENTS

January–February, 1960

AU-8-1

March–April, 1960

AU-8-2

May–June, 1960

AU-8-3

July–August, 1960

AU-8-4

September–October, 1960

AU-8-5

November–December, 1960

AU-8-6

AUTHOR INDEX FOR 1960 IRE TRANSACTIONS ON AUDIO

B

ANALYTIC SUBJECT INDEX FOR 1960 IRE TRANSACTIONS ON AUDIO

INSTITUTIONAL LISTINGS

The IRE Professional Group on Audio is grateful for the assistance given by the firms listed below, and invites application for Institutional Listing from other firms interested in Audio Technology.

JAMES B. LANSING SOUND, INC., 3249 Casitas Ave., Los Angeles 39, California
Loudspeakers and Transducers of All Types

JENSEN MANUFACTURING CO., Div. of the Muter Co., 6601 S. Laramie Ave., Chicago 38, Ill.
Loudspeakers, Reproducer Systems, Enclosures

KNOWLES ELECTRONICS, INC., 10545 Anderson Place, Franklin Park, Ill.
Miniature Magnetic Microphones and Receivers

UNITED TRANSFORMER COMPANY, 150 Varick St., New York, New York
Manufacturers of Transformers, Filters, Chokes, Reactors

Charge for listing in six consecutive issues of the TRANSACTIONS—$75.00. Application for listing may be made to the Technical Secretary, Institute of Radio Engineers, Inc., 1 East 79th Street, New York 21, N.Y.